

AD-A103 726

TEXAS UNIV AT AUSTIN APPLIED RESEARCH LABS

F/G 8/10

ACOUSTICAL PROPERTIES OF SEDIMENTS.(U)

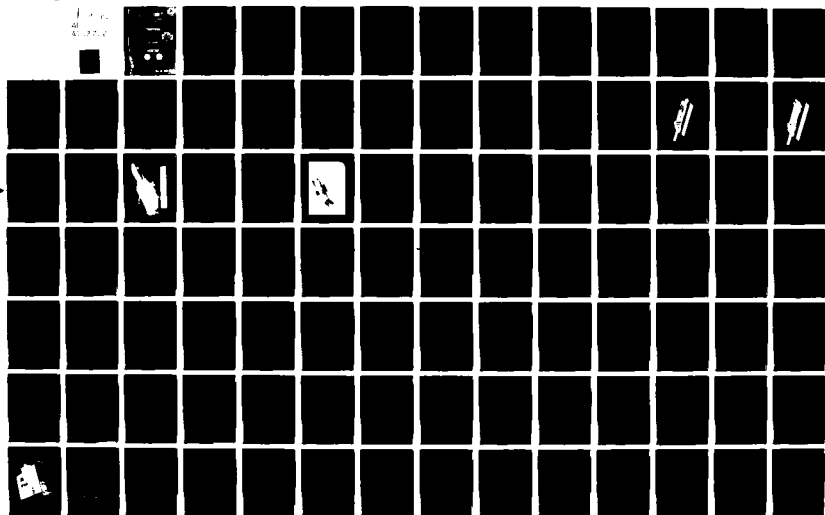
MAY 81 D J SHIRLEY

N00014-76-C-0117

UNCLASSIFIED

ARL-TR-81-20

NL



AD A103726

UNCLASSIFIED

SECURITY CLASSIFICATION OF THIS PAGE (When Data Entered)

REPORT DOCUMENTATION PAGE		READ INSTRUCTIONS BEFORE COMPLETING FORM	
1. REPORT NUMBER	2. GOVT ACCESSION NO.	3. RECIPIENT'S CATALOG NUMBER	
	AD-A103	726	
4. TITLE (and Subtitle)	(9)	5. TYPE OF REPORT & PERIOD COVERED	
ACOUSTICAL PROPERTIES OF SEDIMENTS.		annual report	
	(14)	1 January - 31 December 1980	
7. AUTHOR(s)	(15)	6. PERFORMING ORG. REPORT NUMBER	
Donald J. Shirley		ARL-TR-81-20	
		8. CONTRACT OR GRANT NUMBER(s)	
		N00014-76-C-0117	
9. PERFORMING ORGANIZATION NAME AND ADDRESS		10. PROGRAM ELEMENT PROJECT, TASK AREA & WORK UNIT NUMBERS	
Applied Research Laboratories The University of Texas at Austin Austin, Texas 78712			
11. CONTROLLING OFFICE NAME AND ADDRESS	(11)	12. REPORT DATE	
Office of Naval Research Department of the Navy Arlington, Virginia 22217		11 May 1981	
14. MONITORING AGENCY NAME & ADDRESS (if different from Controlling Office)		13. NUMBER OF PAGES	
(12) 147		160	
		15. SECURITY CLASS. (of this report)	
		UNCLASSIFIED	
		15a. DECLASSIFICATION DOWNGRADING SCHEDULE	
16. DISTRIBUTION STATEMENT (of this Report)			
Approved for public release; distribution unlimited.			
17. DISTRIBUTION STATEMENT (of the abstract entered in Block 20, if different from Report)			
18. SUPPLEMENTARY NOTES			
19. KEY WORDS (Continue on reverse side if necessary and identify by block number)			
in situ shear wave acoustics acoustic impedance sediments compressional wave			
20. ABSTRACT (Continue on reverse side if necessary and identify by block number)			
During the period 1 January - 31 December 1980, work under Contract N00014-76-C-0117, consisted of (1) final development of the ARL:UT profilometer recorder and transducer to enable the in situ measurement of compressional wave, shear wave, acoustic impedance, and static shear strength of ocean bottom sediments during geophysical coring, and (2) laboratory acoustical measurements on artificial sediments to test predictions of the Hovem model when the pore fluid viscosity is varied. The new profilometer recorder and			

404434

UNCLASSIFIED

SECURITY CLASSIFICATION OF THIS PAGE(When Data Entered)

20. (Cont'd)

transducer are described in detail as well as the microcomputer band playback system. Data obtained from the laboratory measurements are displayed.

UNCLASSIFIED

SECURITY CLASSIFICATION OF THIS PAGE(When Data Entered)

TABLE OF CONTENTS

	<u>Page</u>
I. INTRODUCTION	1
II. IN SITU MEASUREMENTS	5
A. Introduction	5
B. Profilometer Development	6
C. Transducer Development	13
D. Laboratory Tests	25
III. LABORATORY MEASUREMENTS	33
A. Introduction	33
B. Background	34
C. Experimental Results	36
IV. SUMMARY	53
REFERENCES	55
APPENDIX A	57
APPENDIX B	79
APPENDIX C	87
APPENDIX D	149

Accession For	
NTIS GRA&I	<input checked="" type="checkbox"/>
DTIC TAB	<input type="checkbox"/>
Unannounced	<input type="checkbox"/>
Justification	
By _____	
Distribution/	
Availability Codes	
Dist	Avail and/or Special
A	

LIST OF FIGURES

<u>Figure</u>	<u>Title</u>	<u>Page</u>
1	Block Diagram of the Profilometer Recording Unit with Magnetic Tape Recorder Data Storage	8
2	Block Diagram of the Profilometer Recording Unit with Solid State Digital Data Storage	9
3	Block Diagram of the Profilometer Playback System Using Magnetic Tape	14
4	Schematic Drawing of the Profilometer Dual Compressional Wave Transducer Set Showing Relative Positions of Transducer Elements	17
5	Two-Channel Compressional Wave Profilometer Transducer	18
6	Schematic Drawing of the Profilometer Compressional Wave/Shear Wave Transducer Set Showing Relative Positions of Transducer Elements	19
7	Shear Wave/Compressional Wave Profilometer Transducer	20
8	Schematic Drawing of the Profilometer Transducer Set To Measure Compressional Wave Speed, Acoustic Impedance, and Shear Strength	21
9	Compressional Wave/Acoustic Impedance Profilometer Transducer	23
10	Cross Section of Acoustic Impedance Transducer	24
11	Compressional Wave/Shear Strength Profilometer Transducer	26
12	Compressional Wave Velocity Profiles in a Sediment Test Tank	28
13	Compressional and Shear Wave Velocity Profiles in a Sediment Test Tank	29

<u>Figure</u>	<u>Title</u>	<u>Page</u>
14	Compressional Wave Velocity and Acoustic Impedance Profiles in a Sediment Test Tank	31
15	Compressional Wave Velocity and Shear Strength Profiles in a Sediment Test Tank	32
16	Behavior of Viscosity as a Function of Concentration for Aqueous Solutions of Ethyl Alcohol and Glycerin	37
17	Compressional Wave Velocity as a Function of Glycerin Concentration in an Aqueous Solution	38
18	Compressional Wave Velocity of an Aqueous Solution of Glycerin as a Function of Viscosity	39
19	Bulk Modulus as a Function of Glycerin Concentration in an Aqueous Solution	41
20	Bulk Modulus of an Aqueous Solution of Glycerin as a Function of Viscosity	42
21	Compressional Wave Velocity in a Glass Bead Sediment as a Function of Glycerin Concentration in the Pore Fluid	45
22	Shear Wave Velocity in a Glass Bead Sediment as a Function of Glycerin Concentration in the Pore Fluid	46
23	Compressional Wave Attenuation as a Function of Glycerin Concentration in a Glass Bead Sediment	48
24	Shear Wave Attenuation as a Function of Glycerin Concentration in a Glass Bead Sediment	49
25	Compressional Wave Attenuation versus Viscosity in a Glass Bead Sediment Saturated with Water-Glycerin Mixture	50
26	Shear Wave Attenuation versus Viscosity in a Glass Bead Sediment Saturated with Water-Glycerin Mixture	51
27	Pulse Generator Schematic	60
28	Schematic Diagram of the Acoustic Impedance Measuring Circuit	63

<u>Figure</u>	<u>Title</u>	<u>Page</u>
29	Schematic Diagram of the Acoustic Impedance Transducer Circuit	64
30	Schematic Diagram of the Shear Strength Measuring Circuit	65
31	Schematic Diagram of the Digital Memory Control Circuit	67
32	Timing Diagram for the Digital Memory Control Circuits	68
33	Schematic Diagram of the Digital Memory Board	73
34	Memory Power Supply Schematic Diagram	75
35	Microcomputer to Memory Interface Board Schematic Diagram	77
36	Profilometer Playback Microcomputer Unit	82
37	Schematic Diagram of Microcomputer Memory Board	83
38	Schematic Diagram of the Microcomputer Input-Output Board	85

I. INTRODUCTION

Applied Research Laboratories, The University of Texas at Austin (ARL:UT), has for the past nine years been heavily involved in the field of low frequency acoustic propagation in the ocean. As part of the overall program of acoustic propagation studies, ARL:UT has had a program funded by ONR (Code 480) directed toward development of techniques and equipment to measure acoustic parameters of ocean sediments directly in situ. The initial goal of the program was to develop a method of measuring in situ compressional wave velocity and attenuation that would be both relatively cheap and easy, but one that would also produce accurate data. Methods available were (1) in situ measurements from platforms of various configurations, deployed either by cable from ships or by submersible, and (2) laboratory measurements on cores or other samples removed from the bottom. The first of these methods suffers from the fact that such measurements require additional ship time and specialized handling equipment and are slow and costly. The second method is, by comparison, easier and cheaper since cores are made on a routine basis, but the method can provide only inaccurate data since the process of sampling and retrieval causes physical disturbance to the samples as well as changes to the ambient temperature and pressure of the sample so that corrections based on assumed temperature and pressure in situ have to be made to the data.

With the above considerations in mind, ARL:UT developed a system to combine the best features of both methods. An instrument was developed to make acoustic measurements in situ in the bottom by attachment to a geophysical corer. The instrument requires only minor modification to the cutting edge of the corer and adds little in the way of cost or time to a normal coring operation.

Initially, only compressional wave velocity was measured by the apparatus, but as the program developed, other measurements were examined as additional features to be added to the measurement capabilities of the instrument. During the period covered by this report, the instrument was restructured to record six data channels to encompass a larger range of measurements. Included in the capability of the instrument are compressional wave velocity, shear wave velocity, acoustic impedance, static shear strength, and corer deceleration. Pulse amplitude data for both compressional and shear waves are also available. The deceleration is integrated by the system to provide a depth axis against which the other data are plotted. The deceleration data are also being examined to provide a measurement of the static shear strength of the cored sediment.¹ For this reason a transducer to independently measure static shear strength was included in the instrumentation.

This report discusses the new instrumentation and provides initial laboratory test data. The updated electronic circuits are provided in Appendices A and B, while the software required for the microprocessor playback unit is provided in Appendix C.

A program of laboratory measurement and computer modeling of acoustical propagation in sediments evolved from the in situ studies, due mostly to a requirement for these type data to enable the in situ data to be interpreted properly. It was realized early in the program that new transducers being developed for the in situ measurement tasks offered a unique opportunity to study acoustic processes in the laboratory. Analytical models based on the work of Biot² and Stoll³ have been developed to augment the measurements and to develop an understanding of the fundamental processes in sediment acoustical propagation.

During 1980, the program was divided into two major parts.

1. Modification of the in situ measuring equipment to enable at least six data channels to be processed and recorded and final development of transducers for those measurements.

2. Laboratory measurements and model development to include artificial sediments with a variation in pore fluid viscosity.

A bibliography of publications under the sediment acoustics program is included as Appendix D. Since the program was started, 14 technical reports have been published, 13 papers have been presented at technical meetings, 7 papers have been published in scientific journals, 3 papers have been included in books, and 2 invention disclosures have been submitted for patent. Of these, 1 technical report and 1 invention disclosure were submitted during 1980.^{4,5}

II. IN SITU MEASUREMENTS

A. Introduction

Field tests aboard R/V IDA GREEN in August 1979 showed that the shear wave transducer design being tested would operate and provide a shear wave velocity profile of ocean sediments.⁴ The next step was to modify the in situ recording instrument so that more data channels could be accommodated to allow shear wave and compressional wave parameters to be recorded concurrently. Previous designs⁶ were structured so that three data channels plus one reference channel were recorded on a 4-channel FM magnetic tape. The three data channels were (1) velocity (either compressional wave or shear wave), (2) amplitude (either compressional wave or shear wave as appropriate), and (3) acceleration. On playback, the output of the reference track was subtracted from the data track outputs to reduce noise associated with tape movement (wow and flutter) and to compensate for long term differences in the tape speed between record and playback. Approximately 10 sec of data were recorded on each tape. After noise compensation, the data were converted from analog to digital signals in the playback system and stored in digital memory. The acceleration data were then integrated by computer and the resultant depth data used as the x axis to plot velocity and amplitude as a function of depth on an x-y plotter.

To increase the number of data channels available in the system, it became necessary to multiplex two data channels on each of the recorder channels, which in turn required an increase in the bandwidth of the record-playback system. The increased bandwidth required faster tape speeds and increased power requirements for the tape drives which, coupled with the mechanical problems that had been encountered in the past with the tape drives, led to a decision to eliminate

the tape recording system altogether and instead go to a system to digitize the analog signals internally and store the digital data in a high density digital memory. The resulting design change has resulted in an instrument with increased bandwidth, lower power requirements, higher reliability, and increased data handling capacity. The new design will record six channels of analog data for 10 sec with a sample rate for each channel of 200 samples/sec. The total memory size is 12 kilobytes of digital data (2 kilobytes per channel) with a word size of 8 bits.

Concurrent with the redesign of the profilometer recording system, new transducers were designed to interface to the system to utilize the added capabilities. The new transducer arrangements include:

1. a set of compressional wave transducers to measure compressional wave velocity inside and outside the core cutter,
2. a set of transducers to measure compressional wave and shear wave velocity concurrently, and
3. a set of transducers to measure compressional wave velocity, acoustic impedance, and static shear strength.

The new design of the recording instrument is explained in Section B while a detailed explanation of the new transducer arrangements is presented in Section C. Laboratory tests were made of the new circuits and transducers and the results of these tests are presented in Section D.

B. Profilometer Development

The new profilometer recorder design is basically the same as the previous design.^{1,6} The previous design for the mechanical layout of the system had allowed space for the addition of more printed circuit cards to allow shear wave measurements to be made in conjunction with the compressional wave measurements. The electronic circuitry is the same for both types of measurements with only changes in component values to allow for the differences in frequency and velocity between shear wave

and compressional wave measurements. The circuits have been described previously¹ and the description will not be repeated.

The point of departure between the old and new design is the recording of the analog voltages representative of the various measured parameters. Figure 1 shows a block diagram of the previous recorder design incorporating the magnetic tape unit. The dotted line separates the measurement part of the circuits from the recording part of the circuits. The circuit design has remained the same above the dotted line with the addition of identical circuits to measure the additional acoustical parameters. The FM modulators, reference frequency generator, and magnetic tape transport shown below the dotted line have been replaced by the new digital recording circuits.

Figure 2 shows a block diagram of the new profilometer recording system. The new additions to the circuitry include the measurement channels for shear wave velocity and amplitude, acoustic impedance, and shear strength, along with the analog-to-digital converter, the solid state memory, and control circuits for the digitizer and memory. General operations of each of the circuits will be described below, with a detailed circuit diagram and circuit description for only the new circuits included in Appendix A. The shear strength channel is shown connected to the digitizing circuit in Fig. 2 by a dotted line since it is not a permanent part of the measurement package, but will be implemented temporarily. When implemented, the shear strength measurement will replace the shear wave measurement since only six data channels are available in the recorder. Changes to the data channels are made by simple wiring changes on the connectors inside the instrument and require only a few minutes to alter the measurement capability of the instrument.

The compressional wave measuring circuits are identical to those reported previously¹ for the existing profilometer design with the exception that the timing of the pulse generator is synchronized to the digital recorder. As in the previous design, the pulse generator

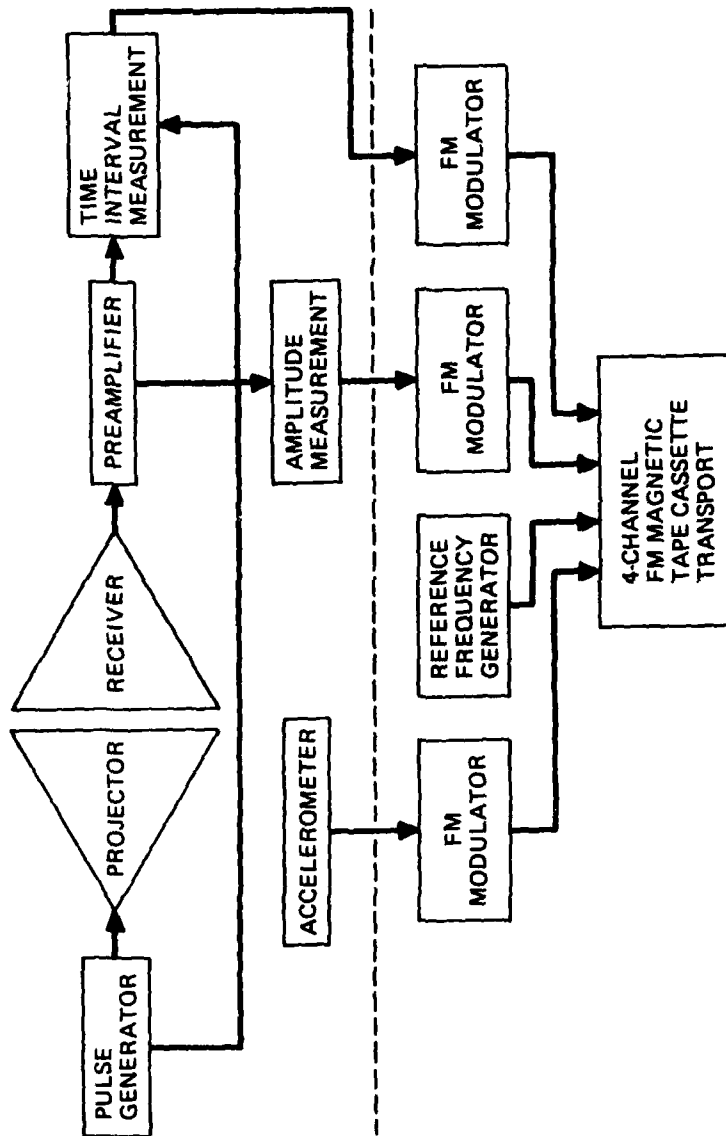


FIGURE 1
 BLOCK DIAGRAM OF THE PROFILOMETER RECORDING UNIT
 WITH MAGNETIC TAPE RECORDER DATA STORAGE

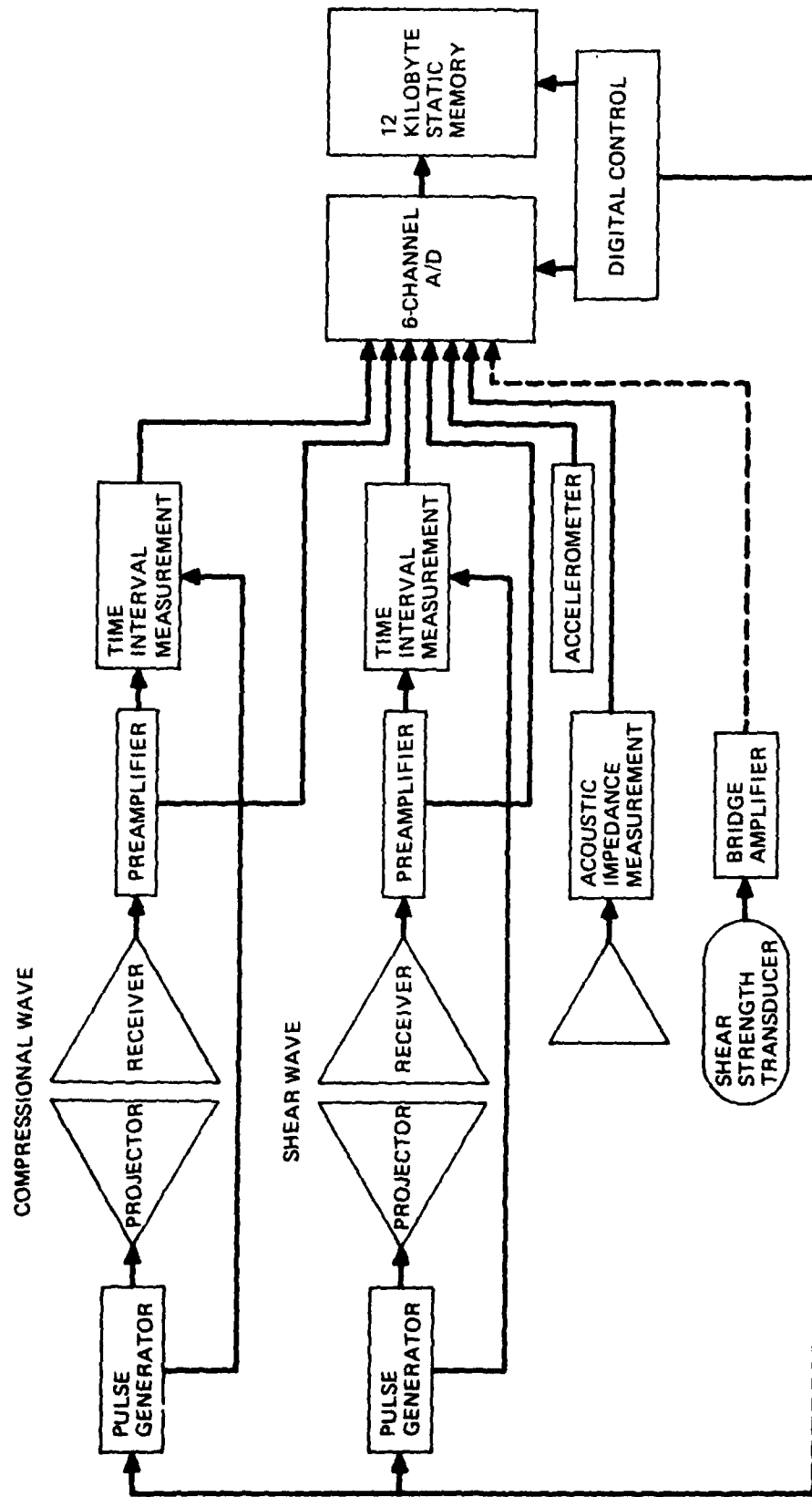


FIGURE 2
 BLOCK DIAGRAM OF THE PROFILOMETER RECORDING UNIT
 WITH SOLID STATE DIGITAL DATA STORAGE

ARL:UT
 AS-81-416
 DJS - GA
 4-18-81

provides a series of 2.5 μ sec pulses to the compressional wave projecting element mounted in the cutter of the corer. The pulses are at an amplitude of 10 V and a repetition rate of 200 pulses per second. A pulse of compressional wave acoustic energy is emitted by the projector and travels through the sediment across the inside diameter of the corer. A receiving element detects the acoustic pulse and generates an electrical pulse which is amplified and filtered by the preamplifier circuit. The amplitude of the pulse is also detected and an analog voltage proportional to the pulse amplitude is provided to one channel of the digitizer. The amplified and filtered pulse is then converted to a train of square pulses by a zero crossing detector and the time interval between the time a pulse is emitted by the pulse generator and the time of arrival of the first pulse in the received pulse train is converted to an analog voltage and provided to another channel of the digitizer.

The shear wave channel is identical to the compressional wave channel with the exception that component values in the circuits are selected to accommodate a lower frequency and a slower velocity for the shear wave. In fact, the shear wave channel can be used for a second channel of compressional wave measurement by the use of appropriate circuit cards in the shear wave positions. Table I shows the required characteristics for the two types of measurements.

Due to the possibility that electrical feedover in the cables from the electronic circuits to the transducer could cause interference between the two measurement channels, synchronization by the digital control circuit is such that the generation of the shear wave pulse is delayed 1.5 msec after the compressional wave pulse to allow the compressional wave measurements to be completed before the shear wave measurement is initiated. The shear wave measurement is then completed before another compressional wave measurement is again started.

The accelerometer measures the deceleration of the corer. The circuit has not been changed and is identical to that used in the previous design.¹ The accelerometer consists of a cantilever mounted

TABLE I

PARAMETERS FOR THE COMPRESSSIONAL WAVE AND SHEAR WAVE MEASUREMENT CHANNELS

	<u>Compresssional Wave</u>	<u>Shear Wave</u>
Frequency	200 kHz	2 kHz
Velocity Range	1400-1900 m/sec	25-300 m/sec
Filter Bandwidth (3 dB)	150-250 kHz	1-10 kHz
Generator Pulse Length	2.5 μ sec	250 μ sec
Repetition Rate	200 pps	200 pps

ceramic bender element with a small mass mounted on the free end. A charge amplifier circuit amplifies the signals resulting from changes in acceleration and provides them to one channel of the digitizer.

The acoustic impedance measurement is similar to that described for laboratory measurements.⁷ The acoustic impedance circuit provides a cw signal to the transducer element mounted on the core cutter. Frequency of the signal is 400 kHz and is maintained at a constant 5 Vpp level. The electrical current amplitude is detected by a resistor in series with the acoustical element and is rectified to provide an analog voltage that is proportional to the electrical impedance of the acoustical element. The electrical impedance of the element is proportional to the acoustic impedance of the sediment in contact with the element. For simplicity in the electronic circuits, no attempt is made to maintain the driving frequency at the resonance frequency of the element; the resonance frequency changes as the acoustic impedance changes and results in phase differences between the voltage and current waveforms. Instead, the frequency is set at resonance with the element in water and is maintained constant. The result is that the analog output is not a linear function of acoustic impedance. However, calibration can be done so that the output as a function of acoustic impedance is known.

The static shear strength measuring transducer consists of a small penetrometer body attached to one of the acoustic transducer housings. A strain gauge is attached to the penetrometer and connected to the electronic circuits of the instrument. Changes in strain gauge resistance in response to varying load on the penetrometer body are detected and amplified by a bridge amplifier and provided to one channel of the solid state recorder.

The solid state recorder consists of a 6-channel multiplexer, a sample-and-hold amplifier, an analog-to-digital converter, a 98,304 bit static memory organized as 12,288 x 8-bit bytes, and a digital control circuit to initiate recording, to synchronize pulse generation of the measuring circuits and the multiplexing of data channels, and to supply

appropriate addresses and chip select signals to the static memory. Detailed descriptions of the circuits are provided in Appendix A. Each data channel thus occupies 2 kilobytes in the memory and at a repetition rate of 200 pps will provide 10 sec of recording time. The recording of data is initiated by the tripping of a switch when the corer is triggered at the ocean bottom and starts to free-fall. Free-fall and penetration of the corer usually occur in 3 to 8 sec, depending on the length of core barrel and stiffness of the bottom sediments.

Once data have been recorded and the instrument recovered aboard ship, it is necessary to process the data and reduce it to a usable form. Figure 3 shows a block diagram of the playback system used with the previous profilometer design. The system consists of a tape transport and demodulator unit to convert the FM data recorded on tape to analog voltages. The unit has three data outputs which are provided to the microcomputer unit in which the three data channels are digitized and the accelerometer data integrated twice to provide depth data. The microcomputer output is input to an x-y plotter where the three data channels are plotted as a function of depth.

The new design eliminates the tape transport and demodulator unit and instead an interface cable from the microcomputer plugs directly into the sockets in the recorder unit normally occupied by the digitizer and digital control cards. The microcomputer addresses the recorder's static memory and transfers all the data from recorder memory to memory located internal to the microcomputer. Once inside the microcomputer, the data are manipulated and plotted in the same manner as before.

C. Transducer Development

In order to utilize the increased recording capacity of the new profilometer recording instrument, three sets of transducers have been developed and constructed. Each of the three transducer designs was developed to address a particular problem in the area of in situ

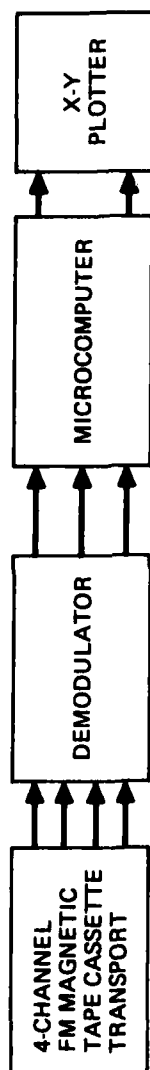


FIGURE 3
BLOCK DIAGRAM OF THE PROFILOMETER
PLAYBACK SYSTEM USING MAGNETIC TAPE

acoustical measurement. One problem was to measure the amount of disturbance to the sediment that occurs before the in situ measurement is made. The profilometer transducers are mounted such that the transducer elements are about 5 cm back from the cutting edge of the core cutter to maintain the strength and structural integrity of the cutter assembly.⁶ Even this short distance could introduce a measurable amount of disturbance to the sediment and affect the acoustical measurement. A solution to the question of disturbance is to place another set of transducer elements in a position out in front of the cutting edge so that a comparison can be made between the two positions. The front transducer, of course, will also disturb the sediment to some degree, but a measurement of the difference can be made and an estimate of the amount of disturbance developed from the data. A bonus to the above measurement is that the travel paths for the two transducer sets can be made different so that a measurement of attenuation can be obtained. The reason that attenuation measurements cannot be obtained from the pulse amplitude data that are presently recorded by the profilometer equipment is that the amplitude is dependent not only on attenuation of compressional waves in the sediment, but also on the variation of the coupling between the transducer element and the sediment. With two sets of identical transducer elements operating over two different path lengths, the changes to signal amplitude due to variation in coupling can be eliminated so that the attenuation can be calculated.

The second problem to be addressed by transducer design was the concurrent measurement of shear wave and compressional wave parameters that has been the ultimate goal of the in situ measurement program for the past several years. A successful shear wave transducer design was demonstrated in FY 79 and the composite shear wave/compressional wave transducer is based on that previous design.

A third transducer design addresses the problem of an acoustic impedance transducer capable of operating at high ambient pressures. Such a design has been proposed and tested in the laboratory¹ and the

third transducer set incorporates this design along with a set of compressional wave elements operating to measure compressional wave velocity in the usual way.

This same transducer set also addresses another problem, which is the measurement of shear strength of a sediment in situ. Preliminary work on adapting the accelerometer data from the profilometer to calculate shear strength has been done,¹ but there are so many unknown factors associated with the calculations that it was desired to have an independent measurement of shear strength for comparison. For this reason a penetrometer measurement was added to the third transducer set.

Figures 4, 6, and 8 show schematic cross-sections of the three transducer designs as they would be mounted on a cutter and illustrate the relative positions that the acoustical elements occupy. In all three designs, a pair of compressional wave elements occupy the same relative position as in the previous profilometer compressional wave transducer design, and thus the new transducer design can be used on the same modified cutters as previously without further modification.

From Fig. 4, the difference in separation between the set of elements inside the cutter and those outside the cutter is 2.3 cm. Since the expected attenuation range for compressional waves at 200 kHz in ocean sediment is from 10 to 100 dB/m,⁸ the above difference in separation should yield a difference in recorded signal levels of from 0.23 to 2.3 dB between the two channels. Such a difference should be easily observable on the output from the instruments. Thus a directly measured attenuation profile of ocean bottom sediment would be obtained for the first time in situ. A photograph of the dual compressional wave transducer is shown in Fig. 5.

Figure 6 shows the relative positions of the shear wave and compressional wave transducer elements on the composite transducer set. Again the shear wave elements are positioned outside and ahead of the

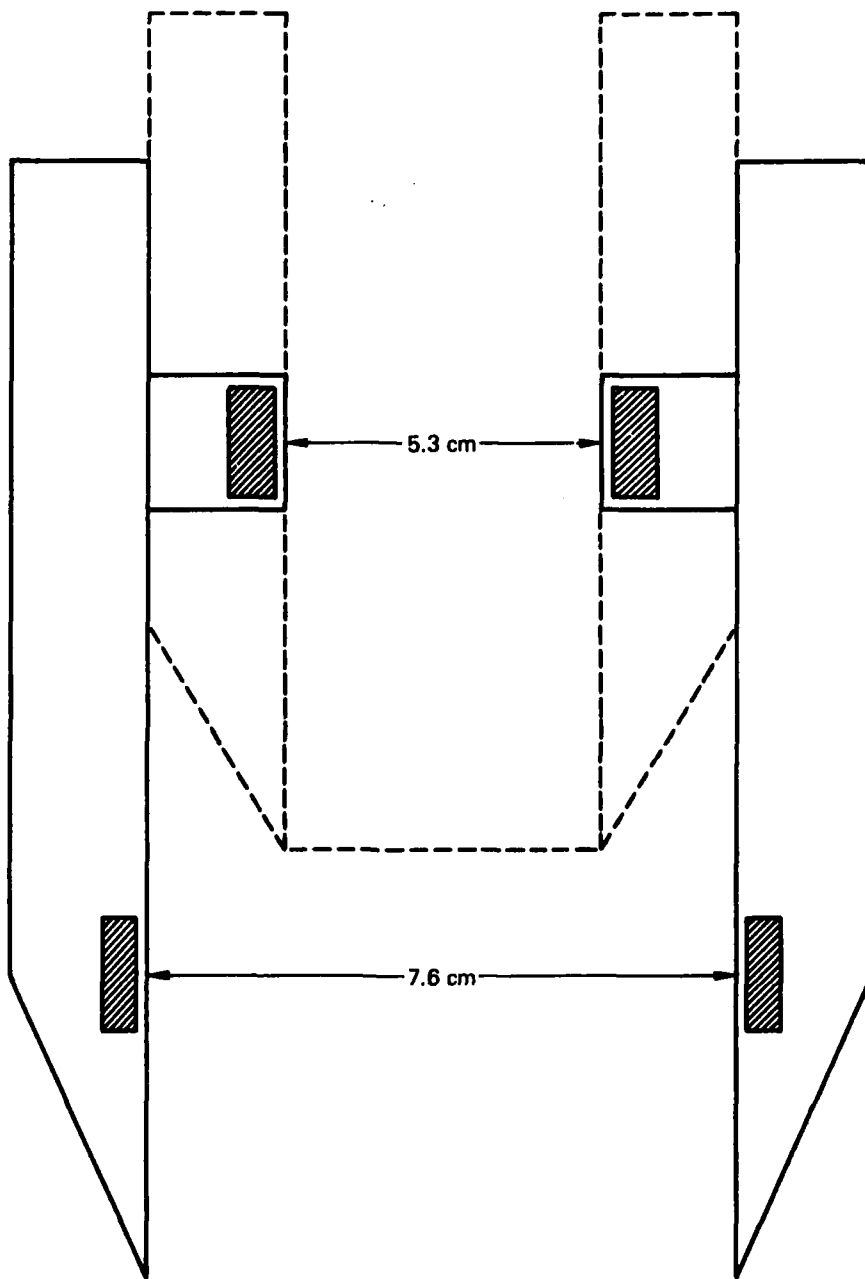


FIGURE 4
SCHEMATIC DRAWING OF THE PROFILOMETER DUAL
COMPRESSIONAL WAVE TRANSDUCER SET SHOWING
RELATIVE POSITIONS OF TRANSDUCER ELEMENTS

ARL:UT
AS-81-418
DJS - GA
4 - 18 - 81

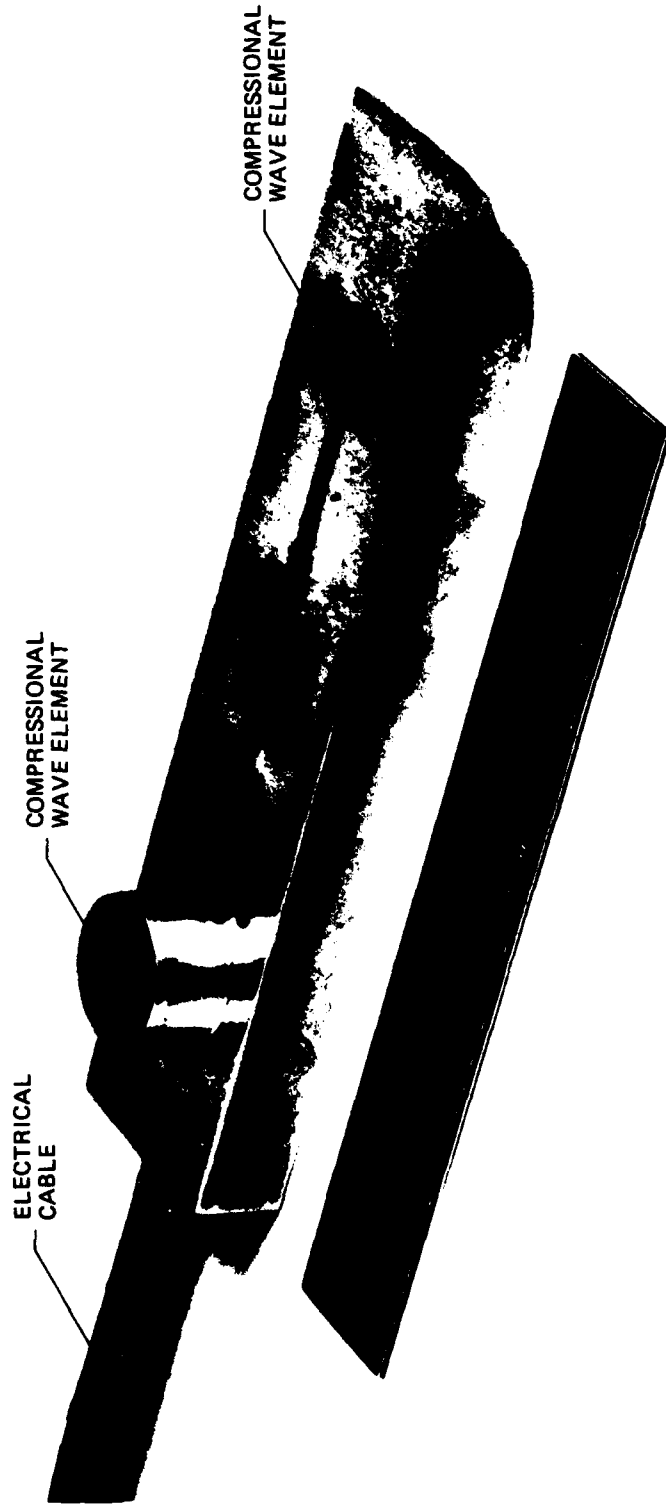


FIGURE 5
TWO-CHANNEL COMPRESSIONAL WAVE PROFILOMETER TRANSDUCER

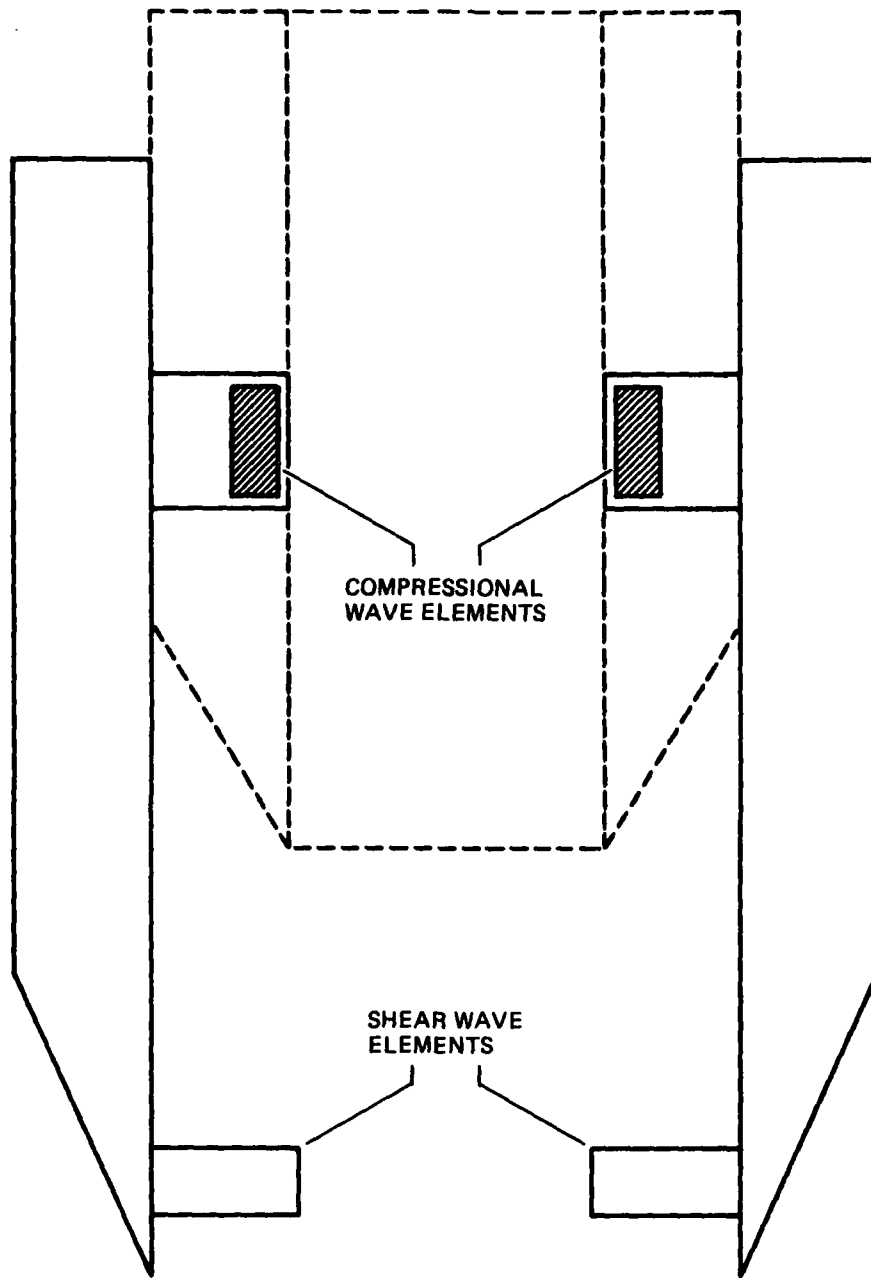


FIGURE 6
SCHEMATIC DRAWING OF THE PROFILOMETER COMPRESSIONAL
WAVE/SHEAR WAVE TRANSDUCER SET SHOWING RELATIVE
POSITIONS OF TRANSDUCER ELEMENTS

ARL:UT
AS-81-419
DJS - GA
4-16-81

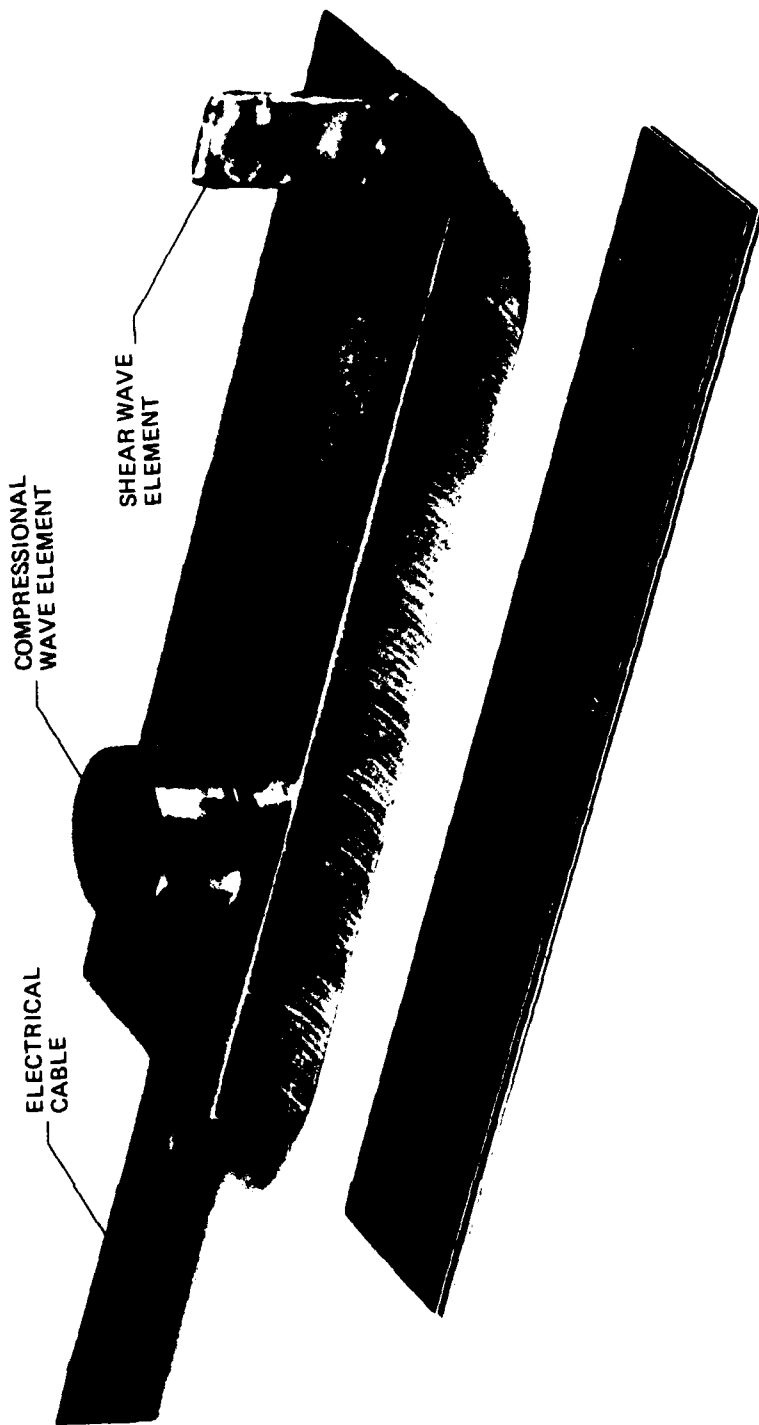


FIGURE 7
SHEAR WAVE/COMPRESSIONAL WAVE PROFILOMETER TRANSDUCER

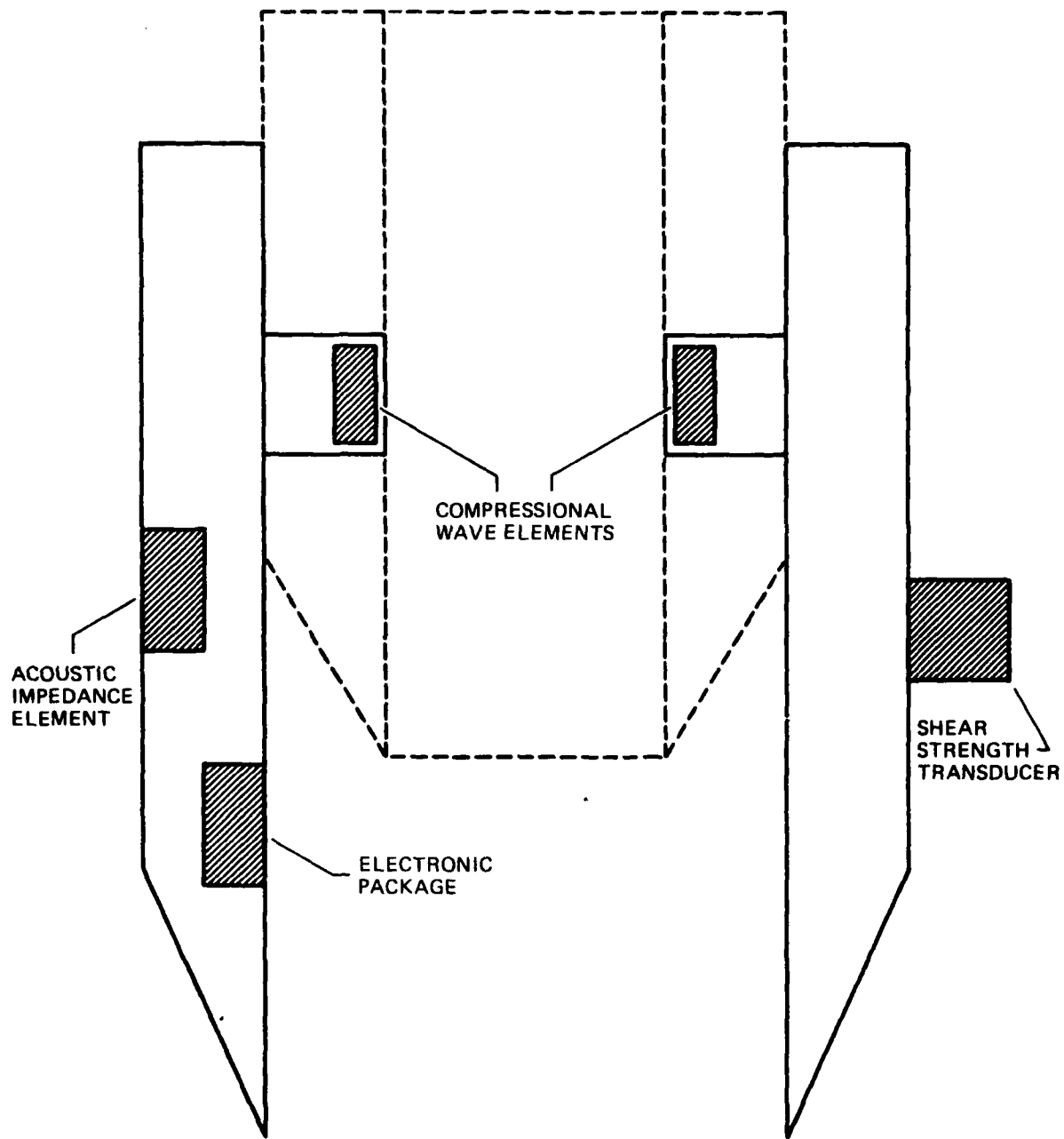


FIGURE 8
SCHEMATIC DRAWING OF THE PROFILOMETER TRANSDUCER SET
TO MEASURE COMPRESSIONAL WAVE SPEED, ACOUSTIC
IMPEDANCE, AND SHEAR STRENGTH

ARL:UT
 AS-81-420
 DJS - GA
 4 - 16 - 81

cutter to allow the whole shear wave element to be in contact with the sediment to increase shear wave coupling to the sediment. The design is identical to that used to successfully obtain a shear wave profile in the Gulf of Mexico in FY 79.⁴ The forward position of the shear wave element increases the hazard from hard layers, so the new design was made more rugged by constructing the bender element from a layer of piezoelectric ceramic and a layer of stainless steel. The resulting shear wave transducer is more rigid and less sensitive than one made from two ceramic layers, but tests indicate that sensitivity is still sufficient to enable operation in most natural sediments. Figure 7 shows a photograph of the transducer set.

The third transducer set is illustrated in Fig. 8. In the previous two transducer sets that have been described, both projector and receiver transducers were identical. For the third set it was necessary to put the active transducers (the compressional wave projector and the acoustic impedance transducer) in one housing and the passive transducers (compressional wave receiver and shear strength transducer) in the other to eliminate interference. A small electronic package is also included in the housing with the acoustic impedance transducer to provide necessary decoupling circuits between the cable capacitance and the transducer element. The two transducers are thus different in construction and are not interchangeable.

Figure 9 shows a photograph of the transducer which incorporates the acoustic impedance element. The design of the element is the same as that first tested in FY 78.¹ A cross sectional drawing of the transducer design is shown in Fig. 10 and illustrates the various components of the device. The radiating head for the present device is made of hardened tool steel and was tested to a pressure of $3.45 \times 10^7 \text{ N/m}^2$ (5000 psi) before the disc ruptured. Such a pressure represents about 3.5 km of water depth. The ceramic element is a 1.59 cm diam disc 1.43 mm thick and is attached to the steel radiating head by rigid epoxy cement. The transducer element is held in place in the housing by a threaded ring and is sealed by an O-ring. A small electronic



FIGURE 9
COMPRESSIONAL WAVE/ACOUSTIC IMPEDANCE PROFILOMETER TRANSDUCER

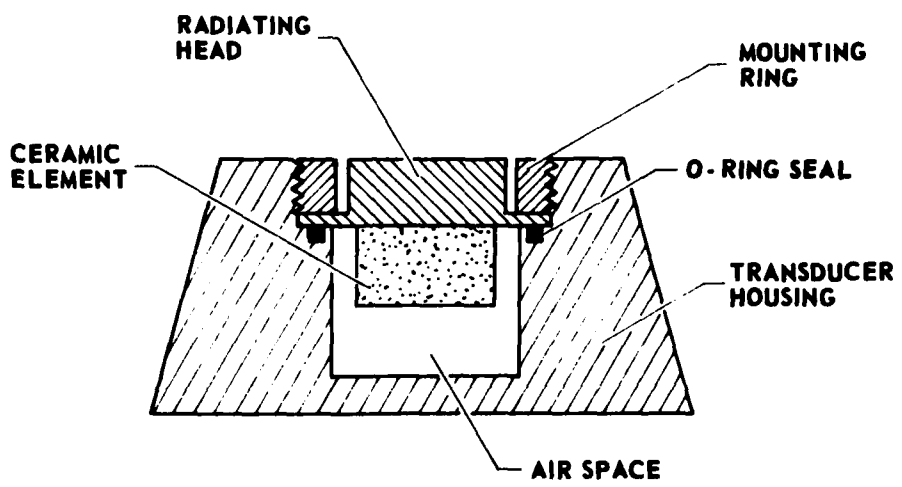


FIGURE 10
CROSS SECTION OF ACOUSTIC IMPEDANCE TRANSDUCER

ARL:UT
AS-79-940
DJS - GA
5-11-79

circuit is also incorporated in the transducer housing and consists of a two-channel operational amplifier integrated circuit. One channel of the amplifier drives the element to isolate it from the capacitance of the interconnecting cable; the other channel rectifies the signal obtained from a current detecting resistor to keep the capacitatively coupled ac driving signal in the cable from interfering with the detected signal. Detailed descriptions of the electronic circuits can be found in Appendix A.

Figure 11 is analogous to Fig. 9 and shows the unit containing the compressional wave receiver and the transducer used to measure shear strength. The shear strength transducer consists of a small penetrometer body 1 cm x 1 cm x 2.5 cm long. The leading edge is sharpened and tapered in an ogive shape and is attached to a 1 cm long cantilever beam welded to the transducer housing. The beam has a pair of metal strain gauges attached to the top and bottom and connected as two arms of a balanced bridge. The beam is encased in epoxy plastic shaped to match the shape of the penetrometer. The force experienced by the penetrometer during penetration of a sediment causes the beam to deflect slightly upward, which reduces the resistance of the upper strain gauge and increases the resistance of the lower. Any change in resistance due to temperature tends to cancel since both strain gauges are identical and in opposite arms of the bridge.

D. Laboratory Tests

The three sets of transducers were tested in a laboratory tank for proper operation. The tank was 0.6 m diam by 2 m deep and had approximately 1 m of sediment and 1 m of overlying water. The sediment consisted of a water saturated ball clay (pottery clay), which has been used for previous transducer tests. The transducers were mounted on a core cutter which was mounted on a 3 m length of aluminum pipe; the transducers were attached to the profilometer recorder by electrical cables. The analog outputs of each of the measurement circuits were

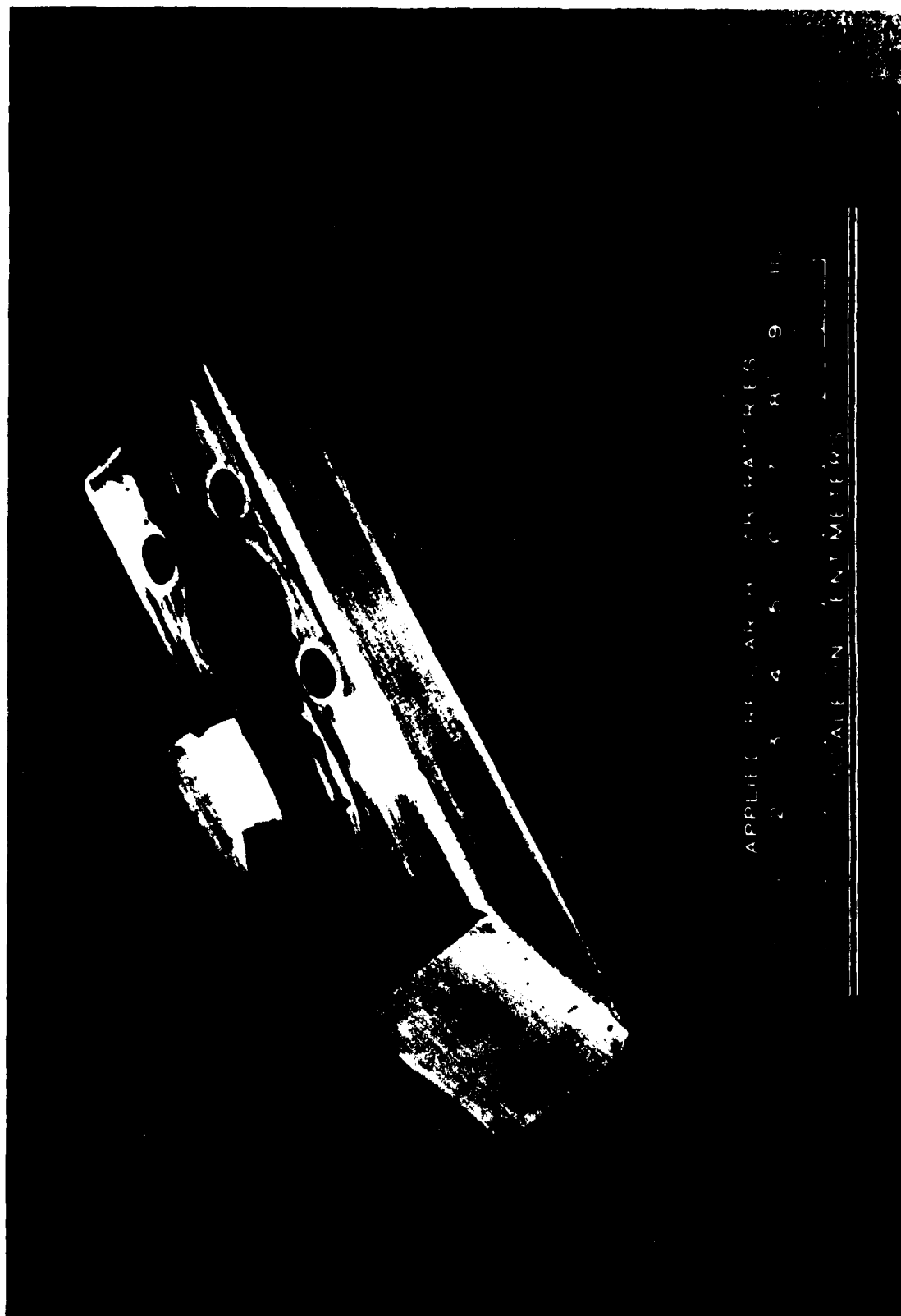


FIGURE 11
COMPRESSIONAL WAVE/SHEAR STRENGTH PROFILOMETER TRANSDUCER

recorded directly on a strip chart recorder since the solid state recording circuits had not been completed at the time of the tests. To test the transducers dynamically, the cutter and pipe were pushed into the sediment by hand while the electrical signals were recorded. An attempt was made to maintain a constant speed of insertion so that the time axis of the strip chart recorder would represent as closely as possible the penetration depth for the test. Figure 12 shows the results of the test using the dual compressional wave transducer set. Because the strip chart recorder had only two channels, only the velocity outputs were recorded. Since the clay had a high porosity, the compressional wave velocity is slightly lower in the sediment than in the overlying water and shows a gradient toward the bottom where the clay tended to increase in stiffness. Apart from a few noise spikes, the profiles are smooth and seem to be identical. There is an offset in the depth axis between the two profiles due to the separation of the transducer element pairs.

Figure 13 shows the results of laboratory tests for the shear wave/compressional wave transducer set. The top trace is the compressional wave velocity and is similar to those shown in Fig. 12, except the profile is less smooth due to disturbance to the sediment during the first test. The lower trace is the shear wave velocity. In general, the shear wave velocity follows fairly closely that of the compressional waves, with a lower velocity at the top of the sediment gradually increasing toward the bottom, with some variations probably due to the sediment having been disturbed by previous tests. While the shear wave elements are in the overlying water at the beginning of the profile, the trace is offscale due to detection of the feedaround signal in the cutter providing a signal to the instrument that appears to be a very fast shear wave (about 400 m/sec). As soon as the shear wave elements contact the sediment, the feedaround signal is damped out and the actual shear wave is measured. The large noise spikes at the end of the shear wave profile are probably due to the cutter striking the bottom of the test tank.

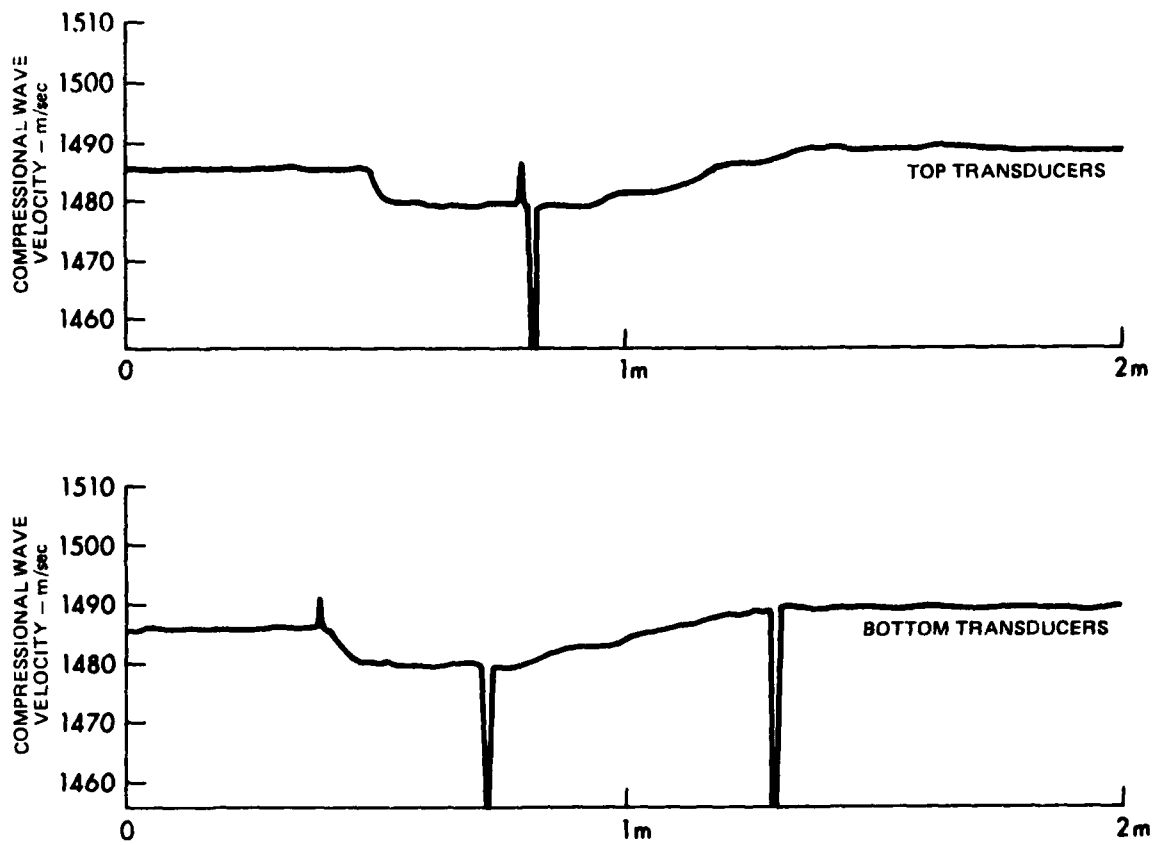


FIGURE 12
COMPRESSIONAL WAVE VELOCITY PROFILES IN A SEDIMENT TEST TANK

ARL:UT
 AS-81-421
 DJS - GA
 4-16-81

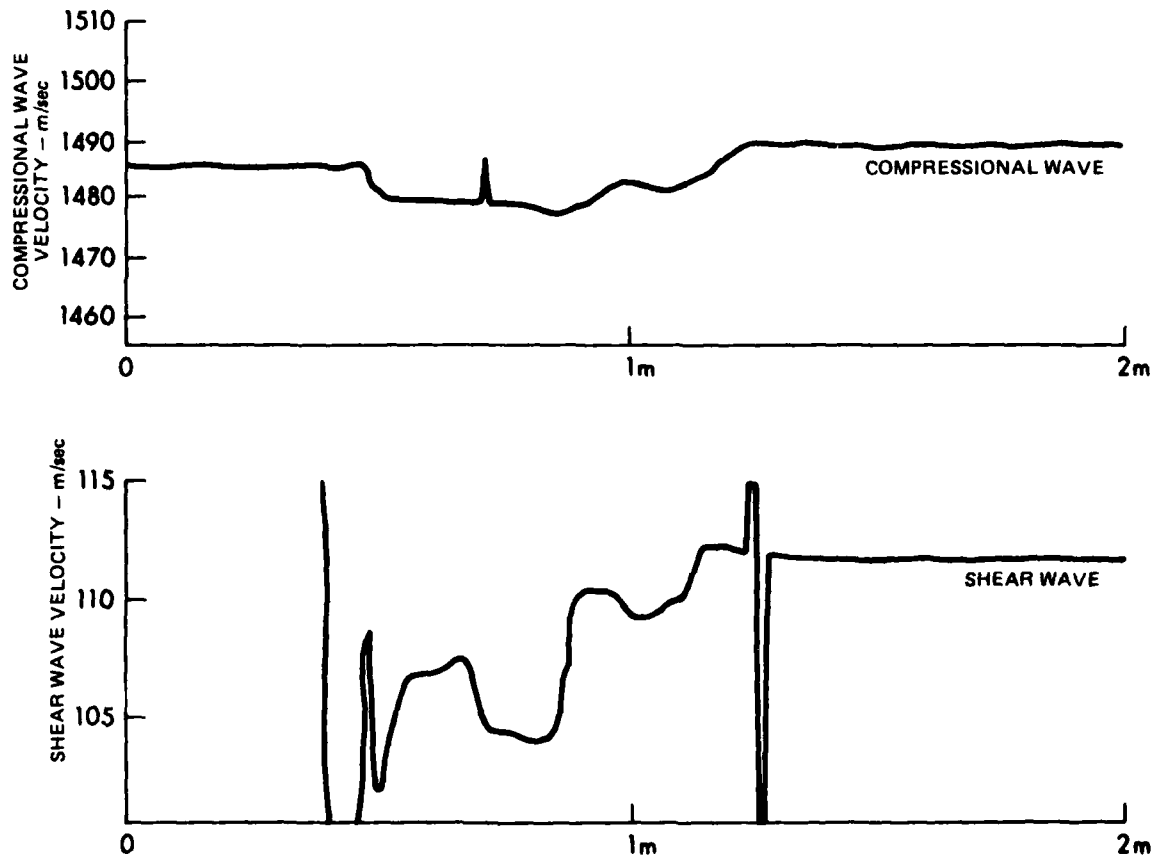


FIGURE 13
COMPRESSIONAL AND SHEAR WAVE VELOCITY PROFILES
IN A SEDIMENT TEST TANK

ARL:UT
 AS-81-422
 DJS - GA
 4-16-81

Figures 14 and 15 show the results of laboratory tests of the third transducer set, which was designed to measure compressional wave velocity, acoustic impedance, and static shear strength. The restriction of two channels on the strip chart recorder required that the acoustic impedance and shear strength measurements be tested separately. Figure 14 shows concurrently made profiles of compressional wave velocity and acoustic impedance. Increased disturbance to the sediment from the series of tests tended to homogenize the sediment so there was little variation of either parameter from top to bottom. Figure 15 also shows little variation, but enough to show that the transducers operated satisfactorily. The variation in acoustic impedance measured during the test was 2.2×10^3 acoustic ohms (1 acoustic ohm = $1 \text{ g/cm}^2 \text{ ga}$) and was smaller than expected, but the sediment was pretty well disturbed by that time even though the tests occurred over a period of three days. The sediment had previously been undisturbed for over a year.

The results of the laboratory tests on the three transducer sets were judged to be satisfactory. The next step, then, is a sea test to evaluate their operation in an environment where stresses on the components are much larger and more uncontrollable.

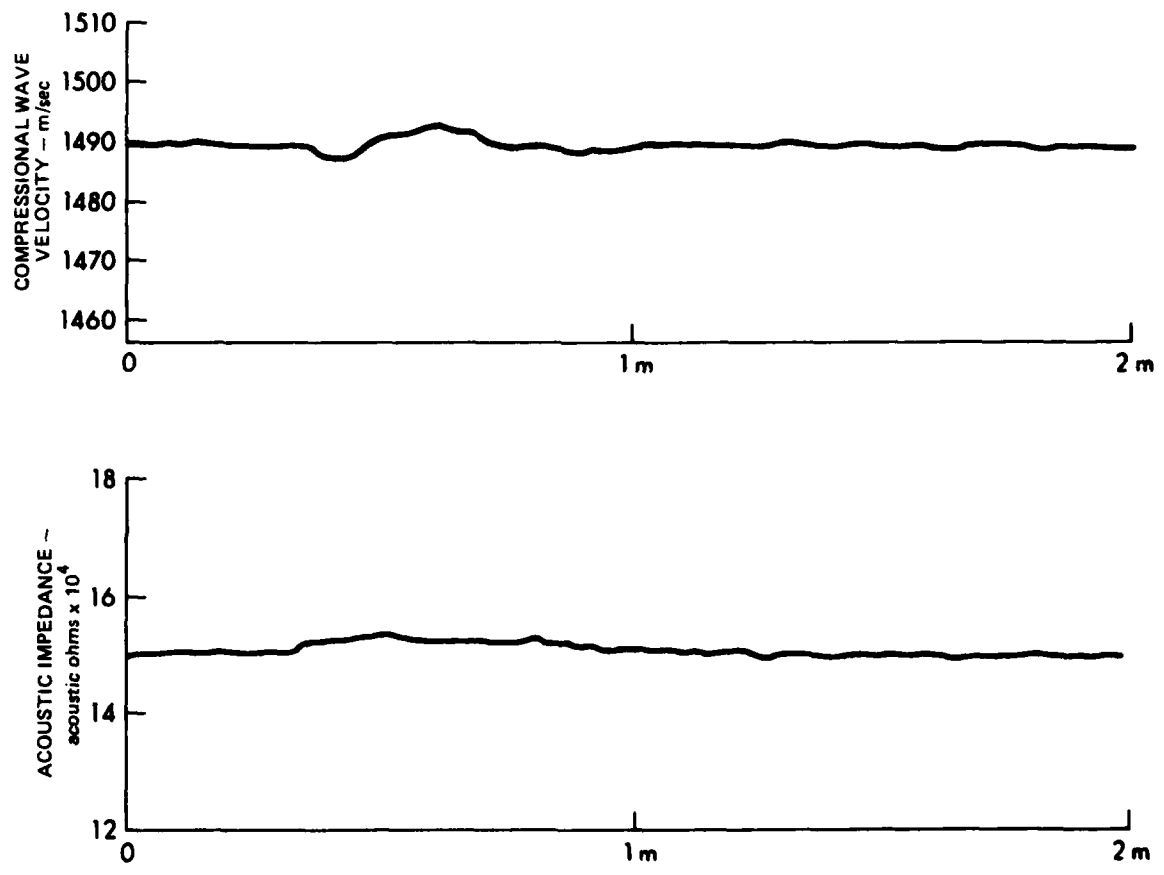


FIGURE 14
COMPRESSIONAL WAVE VELOCITY AND ACOUSTIC IMPEDANCE PROFILES
IN A SEDIMENT TEST TANK

ARL:UT
 AS-81-423
 DJS - GA
 4 - 18 - 81

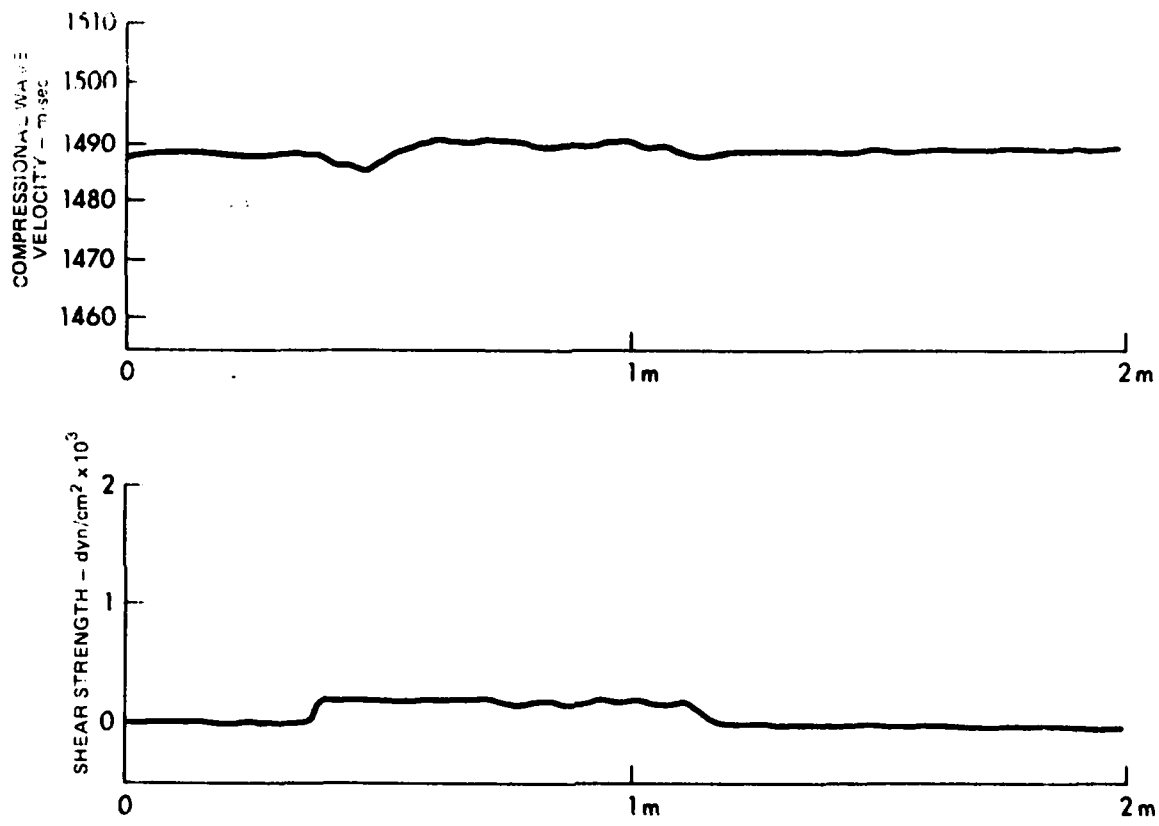


FIGURE 15
COMPRESSIONAL WAVE VELOCITY AND SHEAR STRENGTH PROFILES
IN A SEDIMENT TEST TANK

ARL:UT
 AS-81-424
 DJS:GA
 4 16 81

III. LABORATORY MEASUREMENTS

A. Introduction

An important part of the sediment acoustics program at ARL:UT has been the development of analytical models for the propagation of acoustical energy through sediments and the testing of these models and resulting predictions by acoustical measurements in the laboratory on natural and artificial sediments.

During FY 78 and FY 79, Bell⁸ and Hovem⁹ developed models of acoustical propagation in sediments based on the work of Biot² and Stoll.³ The Biot and Stoll models were intended to be used for propagation in natural sediment types with a wide range of parameter variation. As a consequence, several of the parameters to be inserted in those models have to be assumed from measurements in real sediments. The efforts of Bell and Hovem were directed at developing a specialized model with simple geometry and little variation in parameters. Such a model would have little utility for application to a real sediment, but if the parameters of the model are selected so that they can be easily duplicated in a controlled laboratory environment then predictions and behavior of the specialized model can be more easily understood and evaluated than those of the general model.

During FY 80, the specialized model was used to investigate the acoustical behavior of a sand-type sediment with a single size of spherical grains and a pore fluid of variable viscosity. The work is described in the next section.

B. Background

Hovem and Ingram⁹ previously set up a model based on the Biot theory to examine the frequency response of compressional waves in a spherical grain sand sediment. Hovem showed that the coupled differential equations describing wave propagation could be written in the form

$$\nabla^2 (He - C\xi) = \frac{\partial^2}{\partial t^2} (\rho e - \rho_f \xi) \quad , \quad (1)$$

and

$$\nabla^2 (Ce - M\xi) = \frac{\partial^2}{\partial t^2} (\rho_f e - \rho_c \xi) - \frac{\eta}{B_0} F_r(\kappa) \frac{\partial \xi}{\partial t} \quad , \quad (2)$$

where

- e = dilation of the skeletal frame,
- ξ = relative dilation between frame and fluid,
- ρ_f = bulk density of the pore fluid,
- ρ_s = bulk density of the solid grains,
- ρ_c = effective density parameter, and
- ρ = bulk density of the aggregate.

In turn, ρ is related to the solid and fluid densities by the porosity ϕ in the following equation:

$$\rho = (1-\phi)\rho_s + \phi\rho_f \quad . \quad (3)$$

The coefficients H , C , and M in Eqs. (1) and (2) are elastic coefficients related to the bulk modulus of the grains K_r , the shear modulus of the frame μ_b , the bulk modulus of the frame K_b , and the porosity ϕ as follows:

$$H = K + 4/3 \mu_b \quad , \quad (4)$$

where

$$K = K_r(K_b + Q)/(K_r + Q) \quad , \quad (5)$$

$$Q = (K_f/\phi)(K_r - K_b)/(K_r - K_f) \quad , \quad (6)$$

$$C = QK_r/(K_r + Q) \quad , \quad (7)$$

and

$$M = CK_r/(K_r - K_b) \quad . \quad (8)$$

Hovem also showed that for this particular type of sediment the effective density parameter ρ_c could be described in terms of fluid density, porosity, and a structure constant, γ , by the following equation:

$$\rho_c = \frac{\rho_f}{\phi} (1 + \gamma) \quad , \quad (9)$$

where

$$\gamma = 1 + (\eta\phi/B_o\rho_f) [F_1(\kappa)/\omega] \quad . \quad (10)$$

Here B_o is the permeability of the sediment and η is the absolute viscosity of the pore fluid. The permeability can be related to grain size d_m , porosity ϕ , and a pore size parameter k by the following equation:

$$B_o = (d_m^2/36k) [\phi^3/(1-\phi)^2] \quad . \quad (11)$$

The coefficient k is a function of the pore shape and tortuosity of the pores and, for a spherical grain sediment, has a value between 4 and 5.

Thus, Hovem was able to set up a model for wave propagation in a spherical grain sediment which required only grain size, grain density, porosity, fluid density, fluid viscosity, and the wave propagation frequency as inputs. In preliminary work, model predictions as a function of frequency were investigated and confirmed.⁹

In order to further test the model, investigation of the model predictions as functions of other variable parameters was required. Pore fluid viscosity was decided upon as the parameter to be studied since the viscosity of the fluid could be varied by changing the concentration of an aqueous solution of a material such as alcohol or glycerin. The results of that experiment are discussed in the next section.

C. Experimental Results

In order to vary the viscosity of the pore fluid in a sediment, it was decided to examine the feasibility of changing the concentration of an aqueous solution of a substance to produce a measurable change in viscosity with concentration. Both ethyl alcohol and glycerin have well known characteristics of viscosity and both are soluble in water. Handbook¹⁰ values are available for viscosity as a function of both concentration and temperature for ethyl alcohol and glycerin. Figure 16 shows the variation of viscosity with concentration for both materials at a temperature of 20°C. Glycerin was selected over alcohol due to the fact that glycerin is less volatile than alcohol and would thus provide a more stable pore fluid over a period of time.

Although a variation of viscosity was the object of the experiment, other properties of the fluid such as bulk modulus and density will also be a function of concentration and will affect the acoustical properties of the fluid and of the sediment. Compressional wave velocity and attenuation data were obtained for the pore fluid alone to measure the change in acoustical properties as the concentration and viscosity were varied. Figure 17 shows the velocity data plotted against glycerin concentration while Fig. 18 shows the same data plotted as a function of viscosity. The measurements were made at a frequency of 114 kHz and no extra attenuation due to the presence of glycerin in the solution was observed.

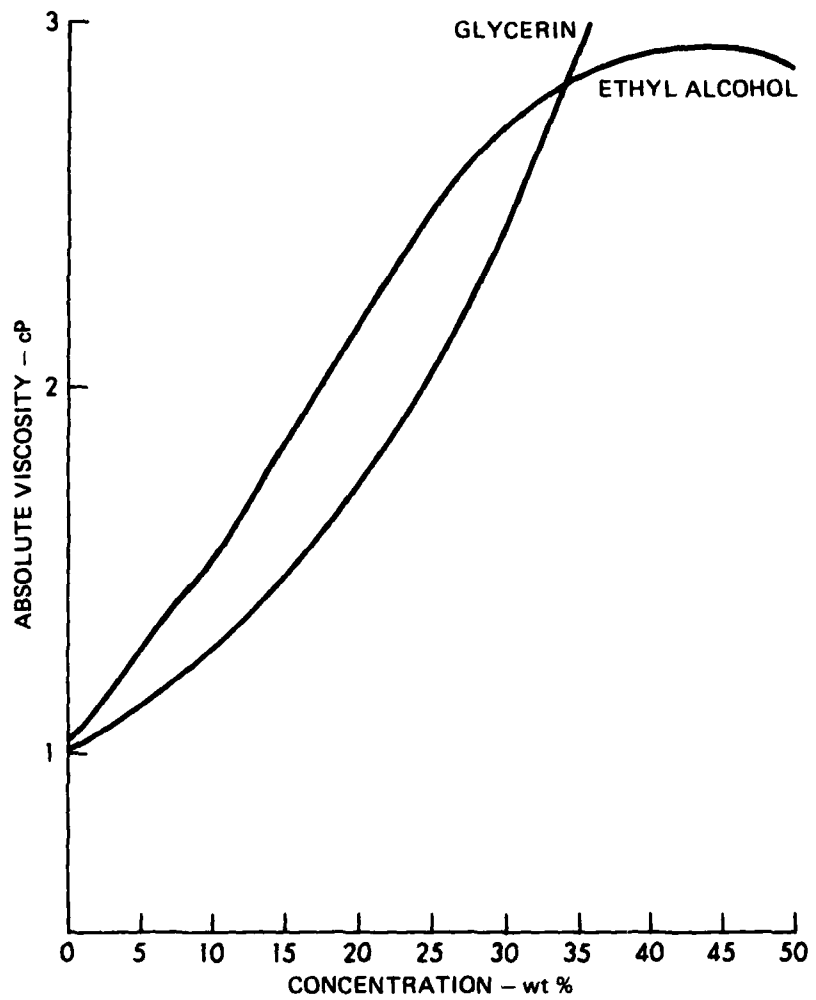


FIGURE 16
BEHAVIOR OF VISCOSITY AS A FUNCTION OF CONCENTRATION
FOR AQUEOUS SOLUTIONS OF ETHYL ALCOHOL AND GLYCERIN

ARL:UT
 AS-81-425
 DJS - GA
 4-16-81

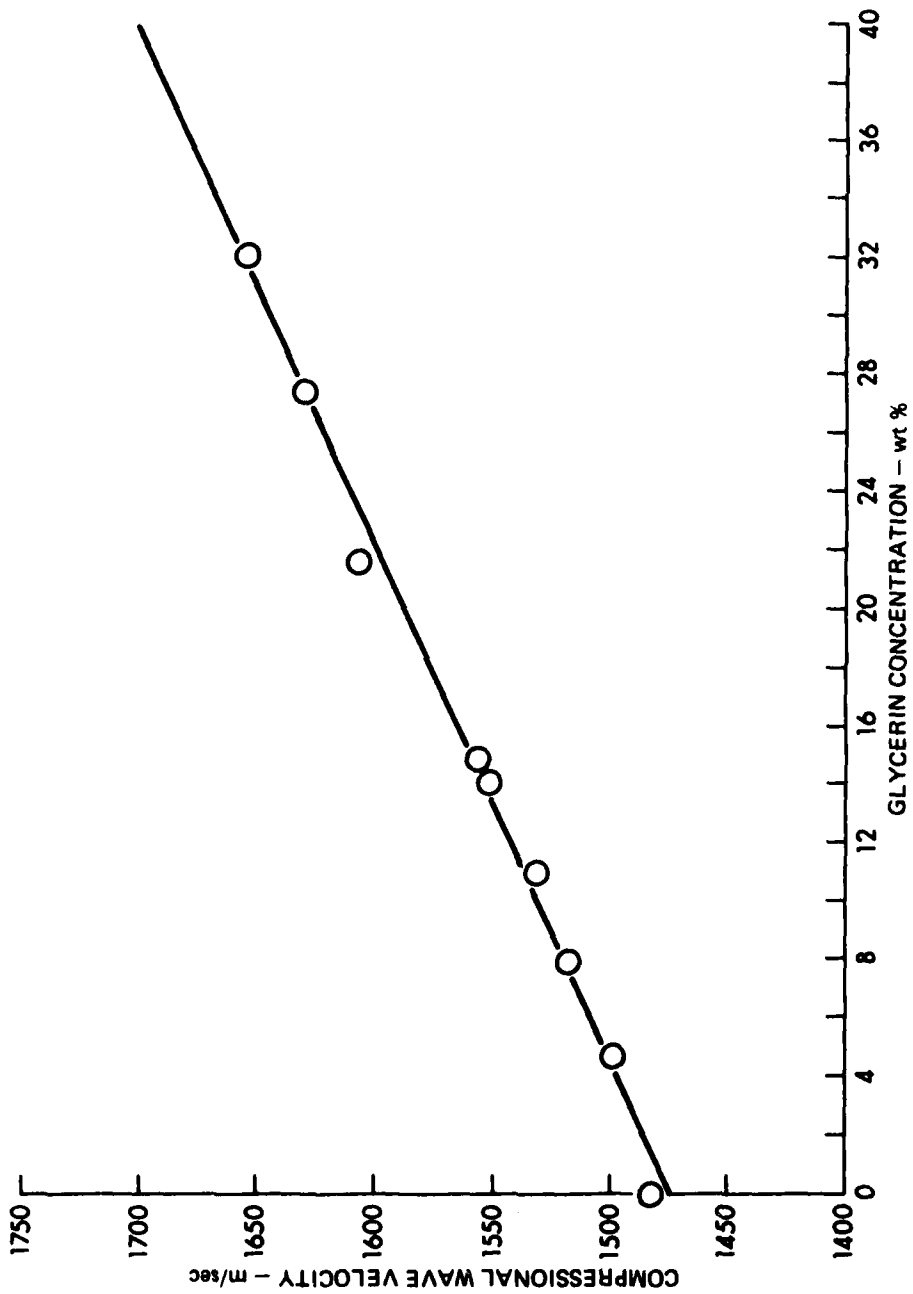


FIGURE 17
COMPRESSIONAL WAVE VELOCITY AS A FUNCTION OF GLYCERIN
CONCENTRATION IN AN AQUEOUS SOLUTION

ARL:UT
 AS-81-426
 DJS - GA
 4-16-81

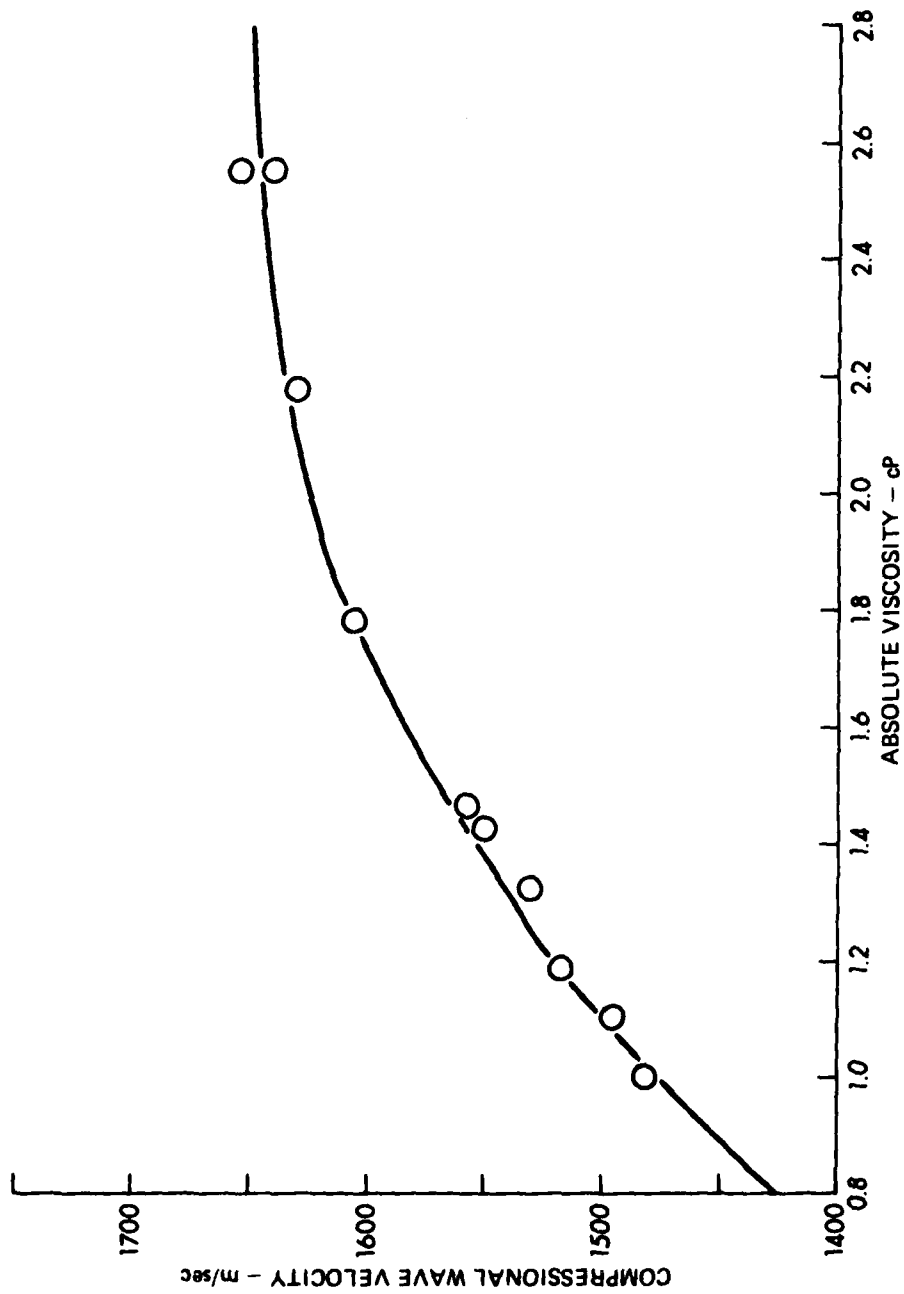


FIGURE 18
 COMPRESSIONAL WAVE VELOCITY OF AN AQUEOUS SOLUTION
 OF GLYCERIN AS A FUNCTION OF VISCOSITY

ARL-UT
 AS-81-427
 DJS - GA
 4-16-81

The velocity data were used in conjunction with handbook values for density of the solutions to calculate the bulk modulus for the material. The bulk modulus data are shown in Figs. 19 and 20 plotted as functions of concentration and viscosity. In each of the figures where data are plotted as a function of concentration, the data points are shown and the solid line is a least squares fit to the data. In the figures showing data plotted versus viscosity, the points are measured data while the solid lines are calculated from the least squares fit from the other figures. The bulk modulus obtained from the above data, as well as density and viscosity, is used in the analytical model to enable predictions of wave velocities and attenuations in a sediment with a pore fluid having the above properties.

A sediment consisting of spherical glass beads mixed with the above pore fluid was selected for study. Various physical properties of the sediment are listed in Table II. Calculations based on the work of Hovem⁹ and Bell⁸ were made of compressional wave velocity and attenuation and shear wave velocity and attenuation for the glass bead sand with variations in viscosity, saturated bulk density, and bulk modulus due to the changing properties of the pore fluid as the concentration of glycerin increased.

Measurements of compressional wave velocity and attenuation and shear wave velocity and attenuation were made in a small sediment tank 16 cm x 30 cm x 20 cm deep. The sediment sample was carefully prepared by adding demineralized water to the initially dry material, boiling the mixture, and then subjecting the cooled sediment to a vacuum for 24 hours. Once the sediment was ready for measurement, the transducers were inserted into the material and the apparatus allowed to remain undisturbed for another 24 hours. Acoustical measurements were then made and again the sediment was allowed to sit undisturbed for another 24 hours, after which the acoustical measurements were repeated. The above procedure was repeated until successive shear wave measurements were essentially identical. It was found that the sediment usually stabilized by the third or fourth 24 hour interval.

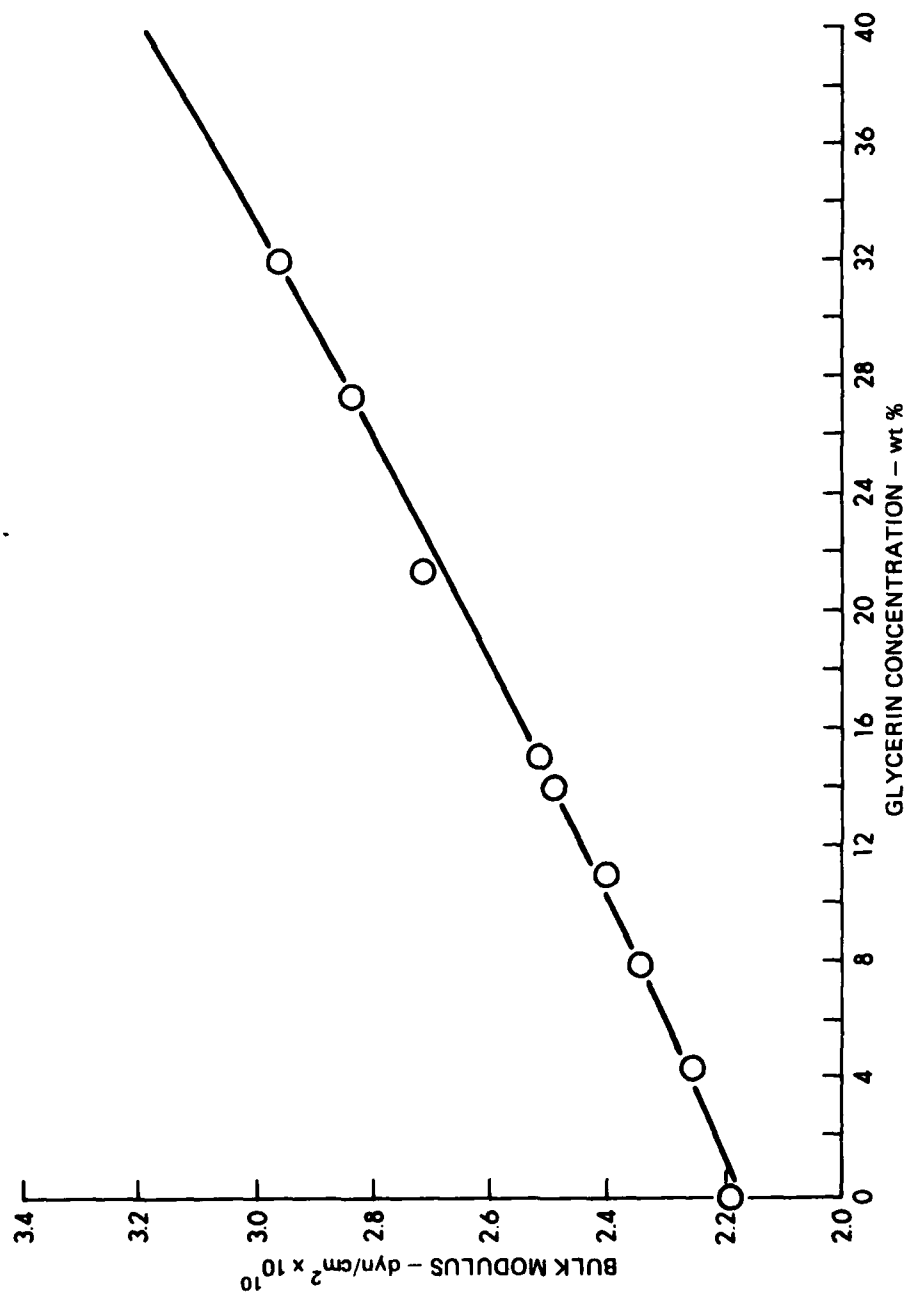


FIGURE 19
BULK MODULUS AS A FUNCTION OF GLYCERIN CONCENTRATION
IN AN AQUEOUS SOLUTION

ARL:UT
 AS-81-428
 DJS-GA
 4-16-81

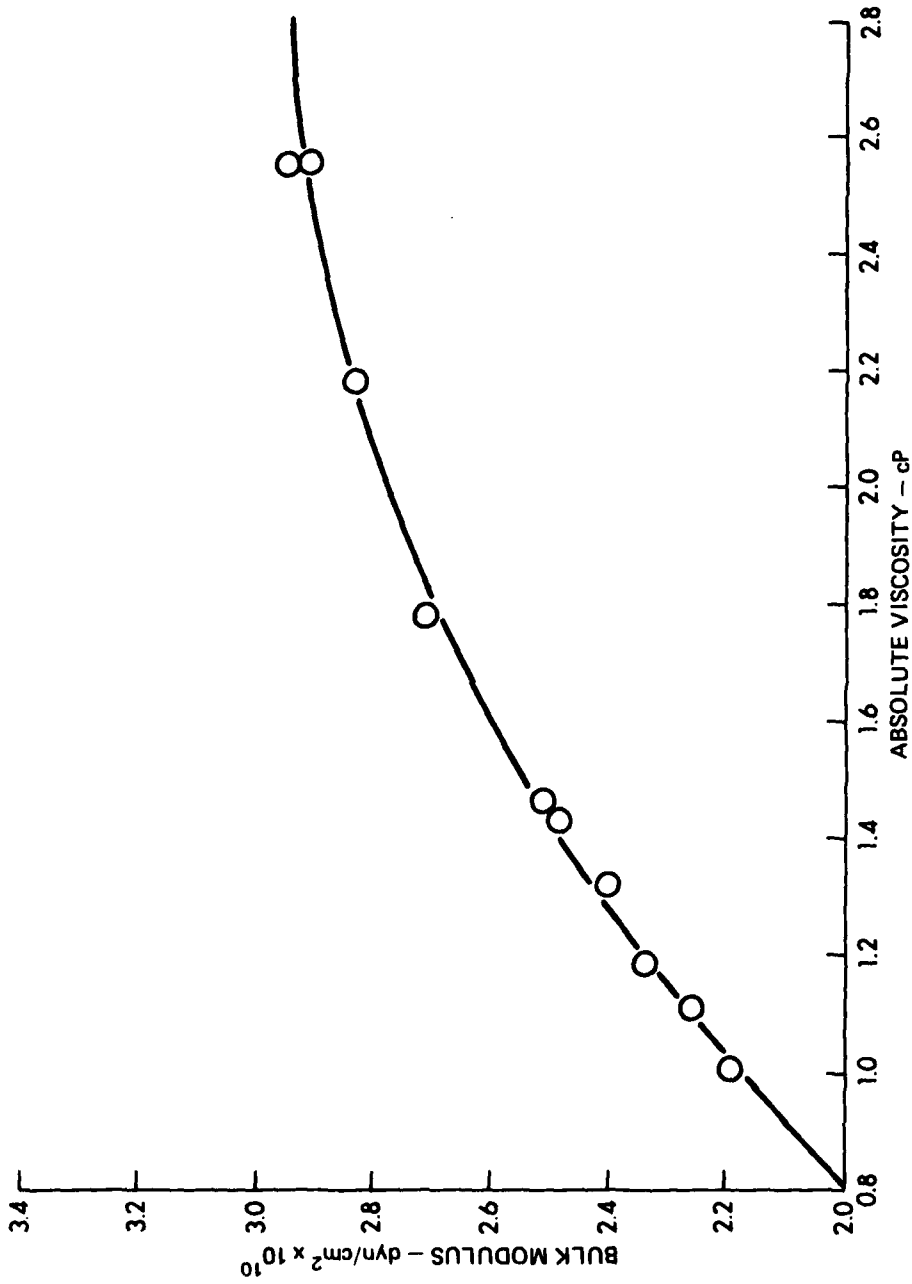


FIGURE 20
BULK MODULUS OF AN AQUEOUS SOLUTION OF GLYCERIN
AS A FUNCTION OF VISCOSITY

ARL:UT
 AS-81-429
 DJS - GA
 4-16-81

TABLE II

PHYSICAL PROPERTIES OF A GLASS BEAD SEDIMENT USED IN ANALYTICAL MODEL
CALCULATIONS

Bead Type	MH
Grain Diameter	1.8×10^{-2} cm
Grain Density	2.50 g/cm^3
Grain Bulk Modulus	1×10^{12} dyn/cm ²
Porosity	0.365
Permeability	2.713×10^{-7} cm ²

Once a set of acoustical measurements had been made, the sediment was removed from the tank, approximately 400 ml of glycerin was added, and the new mixture was thoroughly stirred. The sediment was again evacuated to remove entrained air and the acoustical measurement procedure described above was repeated. After acoustical measurements were completed for a particular concentration of glycerin, a sample of the pore fluid was removed from the tank for viscosity and density measurements. Viscosity was measured at 20°C with a modified Ostwalt viscometer and density was measured at 20°C with a calibrated 50 ml pycnometer. The viscosity and density measurements were used to determine concentration. After successive measurements to a concentration of approximately 25% glycerin, the sediment was discarded and the whole procedure repeated as a check with freshly prepared sediment.

Transducers used to make the compressional and shear wave measurements were similar to those described previously,¹¹ and consisted of a shear wave bender element mounted so that the plane of the bender was vertical, and a small compressional wave element near the bender element. One projector was used with two receivers at different distances so that attenuation could be calculated from the difference in amplitude between the signals at the two receivers. Compressional wave data were obtained at a frequency of 114 kHz and shear wave data at a frequency of 2.8 kHz. Depth of the transducers in the sediment was approximately 10 cm.

Figure 21 shows the response of compressional wave velocity in the sediment to changes in the concentration of glycerin in the pore fluid. These changes in velocity are due mainly to changes in the sediment bulk modulus rather than to any dependence on viscosity. In any event, the predicted curve shows a greater slope than the data. Figure 22 shows that the same relationship holds true for shear wave velocity except that the difference in slope is slightly smaller.

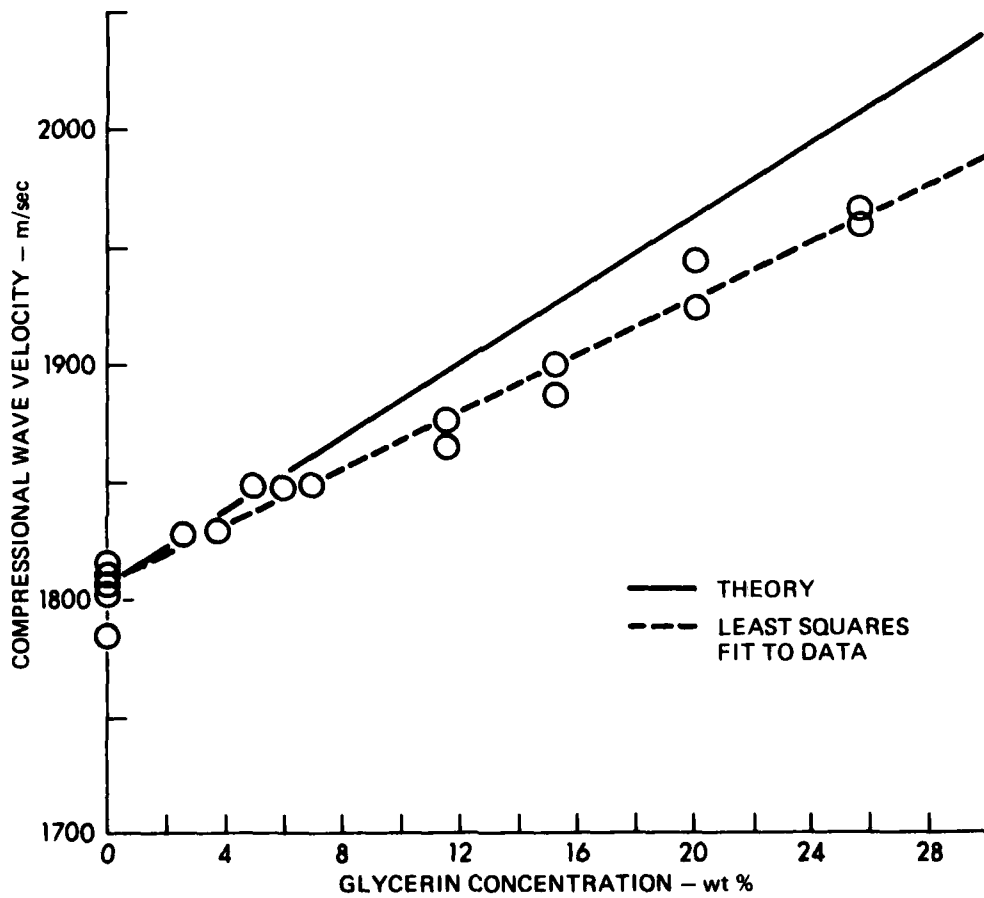


FIGURE 21
COMPRESSIONAL WAVE VELOCITY IN A GLASS BEAD SEDIMENT AS A
FUNCTION OF GLYCERIN CONCENTRATION IN THE PORE FLUID

ARL:UT
 AS-81-430
 DJS - GA
 4-16-81

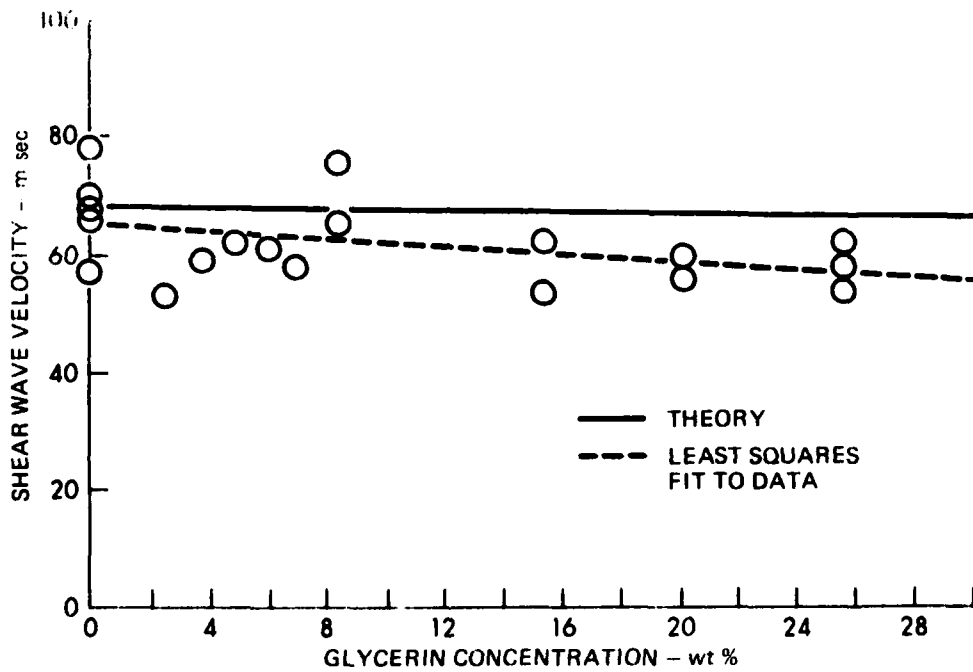


FIGURE 22
SHEAR WAVE VELOCITY IN A GLASS BEAD SEDIMENT AS A FUNCTION
OF GLYCERIN CONCENTRATION IN THE PORE FLUID

ARL:UT
 AS-81-431
 DJS - GA
 4-16-81

Differences between the theoretical predictions and the data also appear in the compressional wave and shear wave attenuations. Figures 23 and 24 show the compressional wave and shear wave data, respectively, compared to the model predictions. In these cases, the attenuations are larger than predicted for both wave types and also have larger slopes than predicted. It could be conjectured here that the viscous loss model does not accurately describe the situation where frame losses due to the lubricating action of the added glycerin can contribute significantly. For whatever reason, the model did not accurately predict acoustical parameters of a sediment for other than plain water as pore fluid.

Since the purpose of the experiment was to examine the effects of viscosity of the pore fluid, the attenuation data have also been plotted as a function of viscosity and are shown in Figs. 25 and 26. The least squares fit to the data from Figs. 23 and 24 have also been included for comparison, replotted for viscosity. It is not proposed here that a linear fit to the data as a function of glycerin concentration or of viscosity is appropriate since the scatter in the data is too large for an accurate determination.

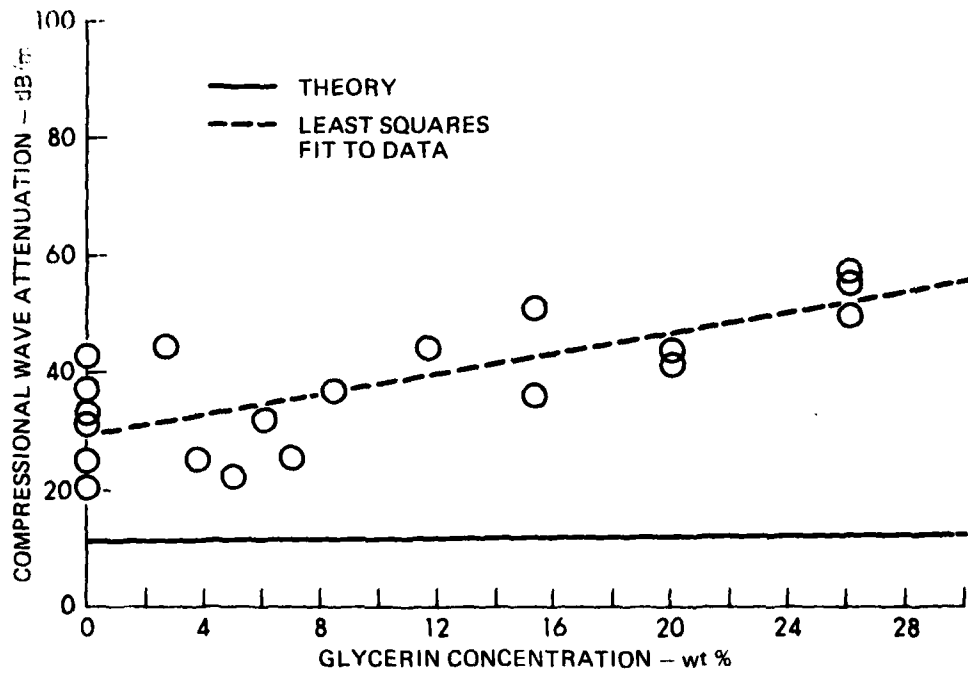


FIGURE 23
COMPRESSIONAL WAVE ATTENUATION AS A FUNCTION OF
GLYCERIN CONCENTRATION IN A GLASS BEAD SEDIMENT
 $f_0 = 114 \text{ kHz}$

ARL:UT
 AS-81-432
 DJS-GA
 4-16-81

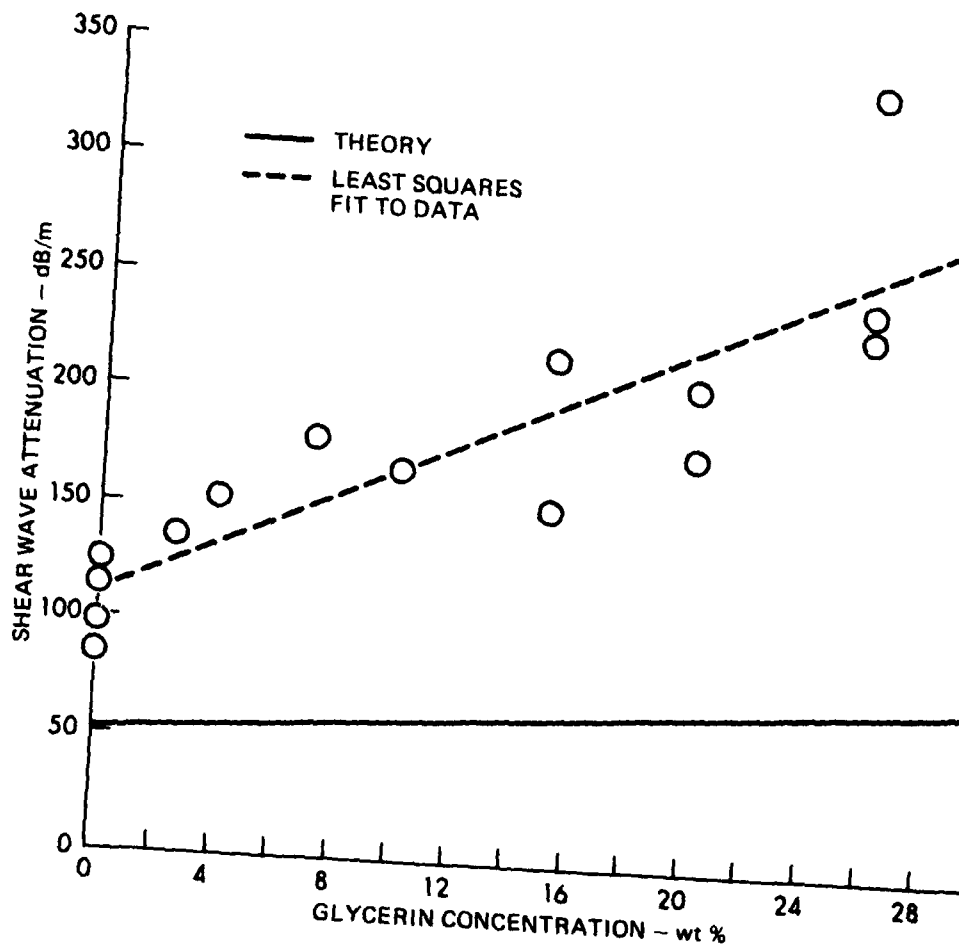


FIGURE 24
SHEAR WAVE ATTENUATION AS A FUNCTION OF GLYCERIN
CONCENTRATION IN A GLASS BEAD SEDIMENT
 $f_0 = 2.8 \text{ kHz}$

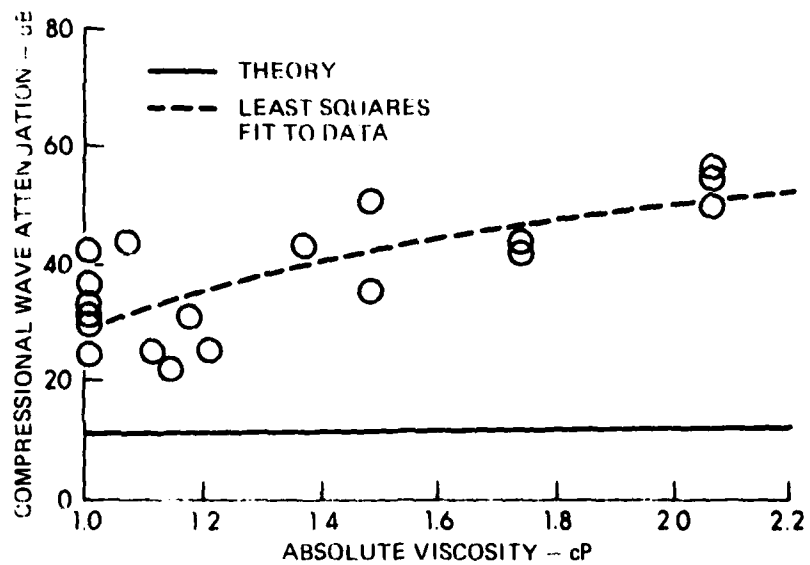


FIGURE 25
COMPRESSIONAL WAVE ATTENUATION versus VISCOSITY
IN A GLASS BEAD SEDIMENT SATURATED WITH
WATER-GLYCERIN MIXTURE

$f_0 = 114 \text{ kHz}$

ARL-UT
 AS-81-434
 DJS-GA
 4-16-81

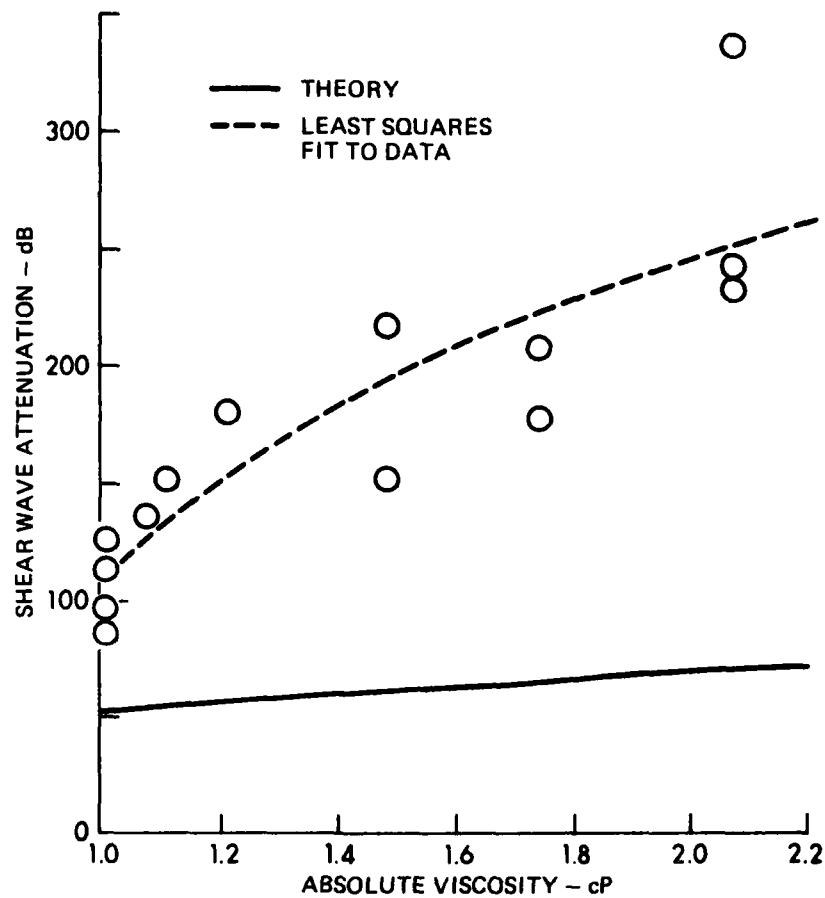


FIGURE 26
SHEAR WAVE ATTENUATION versus VISCOSITY
IN A GLASS BEAD SEDIMENT SATURATED
WITH WATER-GLYCERIN MIXTURE
 $f_0 = 2.8 \text{ kHz}$

ARL:UT
 AS-81-435
 DJS - GA
 4-16-81

IV. SUMMARY

During the past year, the ARL:UT sediment acoustics program has been involved in two areas of work.

1. The in situ acoustic measuring system has been reconfigured to enable concurrent measurement of compressional wave velocity and attenuation, shear wave velocity and attenuation, and acoustic impedance. The recording instrument and transducers have been successfully tested in the laboratory and are being prepared for extensive field testing.

2. A laboratory experiment has been concluded to test predictions of the analytical model developed by Hovem. Viscosity of the pore fluid in an artificial sediment of spherical glass beads was varied by mixing various concentrations of glycerin with water. Results of the experiment indicate that predictions of the model do not match measured data. Further examination and modification of the model, plus repeat of the measurements, are indicated.

Future work under the program will continue to emphasize a balance between analytical modeling, laboratory measurements, and in situ measurements to ensure accurate results. Topics to be investigated include:

1. theoretical model development,
2. physical scale model development,
3. investigation of interface waves,
4. investigation of nonlinear acoustical parameters of sediments,
5. examination of Biot's second type compressional wave,
6. investigation of the effects of salinity on sediment acoustical properties,
7. investigation of the relationship between engineering properties and acoustical properties of sediments,

8. investigation of the density profile and compressional wave/
shear wave velocity ratio in situ,

9. development of a free-fall sediment acoustic measuring system,
and

10. development of a shear wave acoustic reflection profiler
system.

REFERENCES

1. D. J. Shirley, D. W. Bell, and J. M. Hovem, "Laboratory and Field Studies of Sediment Acoustics," Applied Research Laboratories Technical Report No. 79-26 (ARL-TR-79-26), Applied Research Laboratories The University of Texas at Austin, 12 June 1979.
2. M. A. Biot, "Theory of Propagation of Elastic Waves in a Fluid Saturated Porous Solid, I and II," J. Acoust. Soc. Am. 28, 168-191 (1956).
3. R. D. Stoll and G. M. Bryan, "Wave Attenuation in Saturated Sediments," J. Acoust. Soc. Am. 47, 1440-1447 (1970).
4. D. J. Shirley, J. M. Hovem, G. D. Ingram, and D. W. Bell, "Sediment Acoustics," Applied Research Laboratories Technical Report No. 80-17 (ARL-TR-80-17), Applied Research Laboratories, The University of Texas at Austin, 2 April 1980.
5. D. J. Shirley, "A Subseafloor Environmental Simulator," Applied Research Laboratories Invention Disclosure, Navy Case No. 65,339, 10 November 1980.
6. D. J. Shirley and A. L. Anderson, "Compressional Wave Profilometer for Deep Water Measurements," Applied Research Laboratories Technical Report No. 74-51 (ARL-TR-74-51), Applied Research Laboratories, The University of Texas at Austin, 6 December 1974.
7. D. J. Shirley, "Method for Measuring in situ Acoustic Impedance of Marine Sediments," J. Acoust. Soc. Am. 62, 1028-1032 (1977).
8. D. W. Bell, "Shear Wave Propagation in Unconsolidated Fluid Saturated Porous Media," Applied Research Laboratories Technical Report No. 79-31 (ARL-TR-79-31), Applied Research Laboratories, The University of Texas at Austin, 15 May 1979.
9. J. M. Hovem and G. D. Ingram, "Viscous Attenuation of Sound in Saturated Sand," J. Acoust. Soc. Am. 66, 1807-1812 (1979).
10. A. N. Lange, Handbook of Chemistry (Handbook Publishers, Inc., Sandusky, Ohio, 1949).
11. D. J. Shirley, "An Improved Shear Wave Transducer," J. Acoust. Soc. Am. 63, 1643-1645 (1978).

APPENDIX A

Introduction

The purpose of this appendix is to provide detailed circuit descriptions and schematics of the new or revised analog measuring circuits of the profilometer and the new solid state memory which was developed to replace the FM magnetic tape recording system. Included in the analog circuits are (1) a revised pulse generator circuit, (2) a circuit to measure acoustic impedance, and (3) a circuit to measure shear strength. In the digital category are (1) a controller and digitizer for the solid state memory, (2) the memory circuits, and (3) a computer interface to couple stored digital data into the microcomputer.

Pulse Generator

Figure 27 is a schematic diagram of the revised pulse generator circuit used to drive the acoustic transducers to make both compressional and shear wave measurements in the profilometer. The original circuit operated at its own repetition (200 pps) rate to generate a positive going square pulse of the proper length (2.5 μ sec for compressional waves, 250 μ sec for shear waves). The new circuit described here is almost identical except that the repetition rate is controlled by a trigger input from the solid state memory circuits and generates the pulse at a controlled time interval following the trigger. Compressional wave and shear wave circuits are identical except for the RC network used to control pulse width.

Referring to Fig. 27, U1 is a CD4098 dual monostable integrated circuit, part of which is used to generate a constant delay after the trigger, and the other, to generate the driving pulse. The trigger

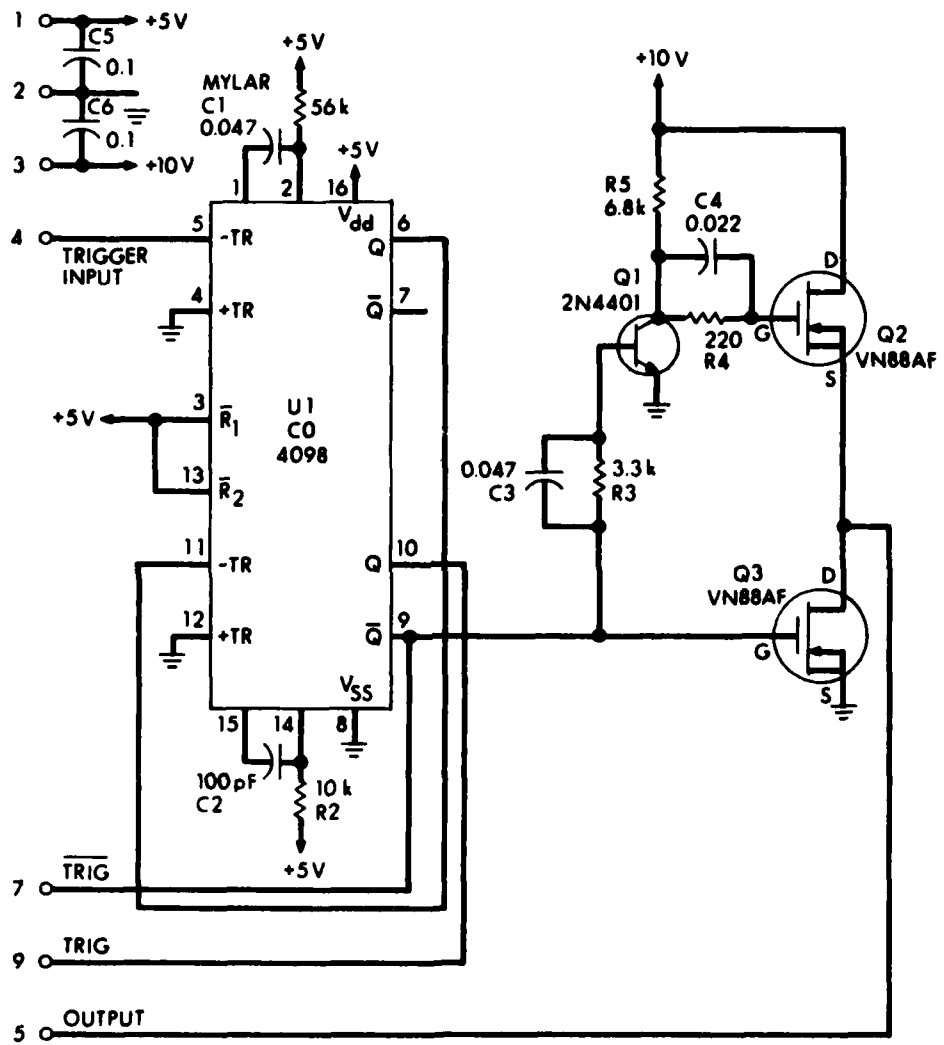


FIGURE 27
SCHEMATIC DIAGRAM OF THE PULSE GENERATOR

ARL:UT
AS-81-503
DJS-GA
5-5-81

input to pin 5 of U1 triggers the monostable on the trailing edge of the trigger pulse. A positive going pulse is generated at the Q output of the monostable, pin 6. The length of the pulse and consequently the delay is controlled by R1 and C1. If no delay is desired, C1 is removed and pin 2 of U1 is connected directly to +5 V. The delay pulse from pin 6 of U1 is coupled into the negative trigger input of the second monostable at pin 11 so that the second monostable is triggered on the trailing edge of the delay pulse. Complementary pulses are generated at the Q and \bar{Q} outputs of U1 and are provided to the card edge connector for triggering other circuits in the profilometer. Pulse width of the second pulse is controlled by the time constant of R2 and C2. Values shown in Fig. 27 are for a 2.5 μsec pulse for compressional wave measurements. Changing C2 to a value of 0.01 μF will provide a 250 μsec pulse appropriate for shear wave measurements.

The \bar{Q} output from the second monostable is applied to the base of transistor Q1, which is configured as a common emitter amplifier. The negative going pulse is inverted and amplified from the nominal 5 V level to a 10 V level and applied to transistor Q2 which is a VMOS power FET arranged in a source-follower circuit to drive the output. Q3 is an identical power FET used as a switch to connect the output line to ground when the driving pulse is not applied. Operation in this manner reduces ringing in the acoustic transducer.

Acoustic Impedance Measurement Circuit

The purpose of the acoustic impedance measuring circuit is to provide a continuous wave (cw) signal to the acoustic impedance transducer at the resonance frequency of that transducer when it is immersed in water, and to detect and amplify the analog voltage from the circuits associated with the transducer which detect the current through the transducer.

Figure 28 is the schematic diagram of the part of the acoustic impedance circuit which is in the pressure case while Fig. 29 shows the schematic diagram for the circuits associated with the transducer.

Referring to Fig. 28, U1 is an NE566 function generator integrated circuit configured to generate a constant frequency, constant amplitude triangular wave signal at pin 4. The frequency of oscillation is controlled by the time constant of R3 and C2 and the frequency can be varied by adjusting R3. The signal is coupled to U2 where it is amplified and then applied to the transducer cable through R7. The series resistance of R7 is used to decouple the cable capacitance from the operational amplifier U2 and thus maintain stability. The analog signal which is proportional to the transducer impedance is filtered by R8, R9, and C4 and applied to the operational amplifier U3 which amplifies the signal by a factor of 10.

In Fig. 29, U4A is used to buffer the signal coming through the cable from the generating circuit and to drive the transducer element at a constant voltage level. R1 senses the current through the element and develops an ac voltage inversely proportional to the impedance of the element. The ac signal from R1 is rectified by U4B which is an operational amplifier configured as a half-wave rectifier circuit. The rectified signal then goes back up the cable to be filtered and amplified and applied to the recording circuits.

Shear Strength Measuring Circuit

The purpose of the shear strength measuring circuits is to provide a dc excitation voltage to the strain gauge bridge elements on the transducer and to measure the resulting bridge output voltage, amplify it, and provide it to the recording circuits. Figure 30 shows the schematic diagram of the circuit. SG1 and SG2 are metal strain gauges mounted on opposite sides of a cantilever bar (see Section II.C) used

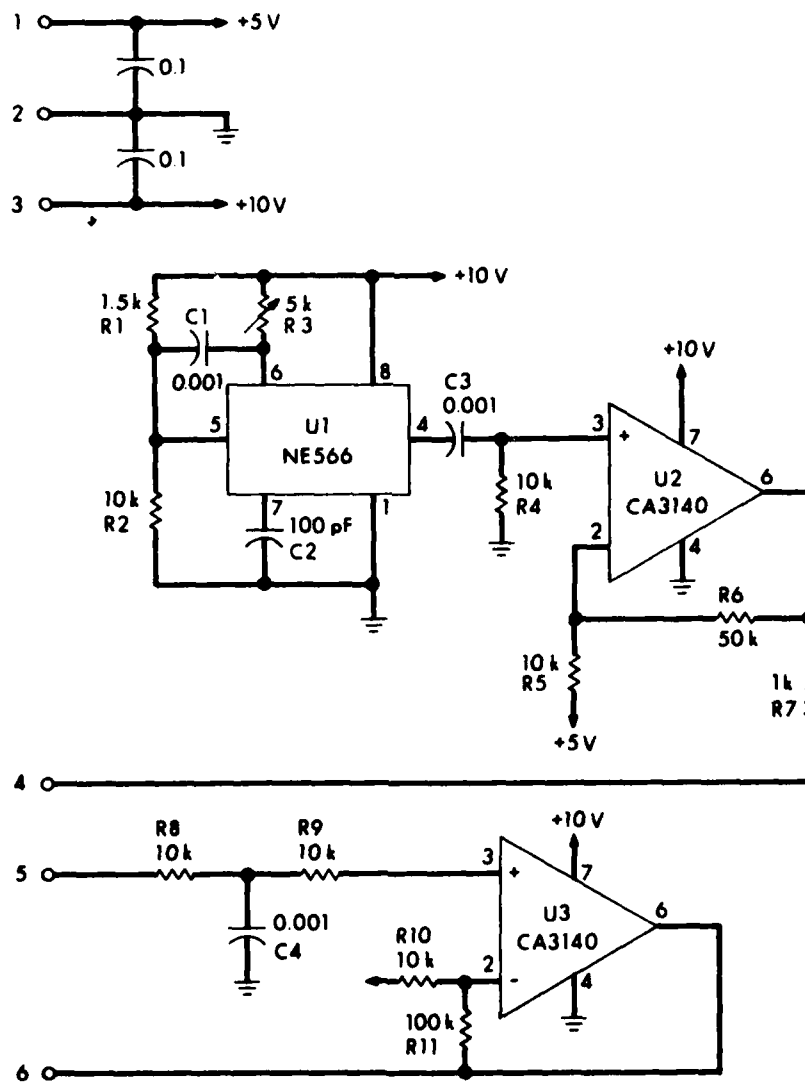


FIGURE 28
SCHEMATIC DIAGRAM OF THE ACOUSTIC IMPEDANCE MEASURING CIRCUIT

ARL:UT
AS-81-504
DJS - GA
5 - 5 - 81

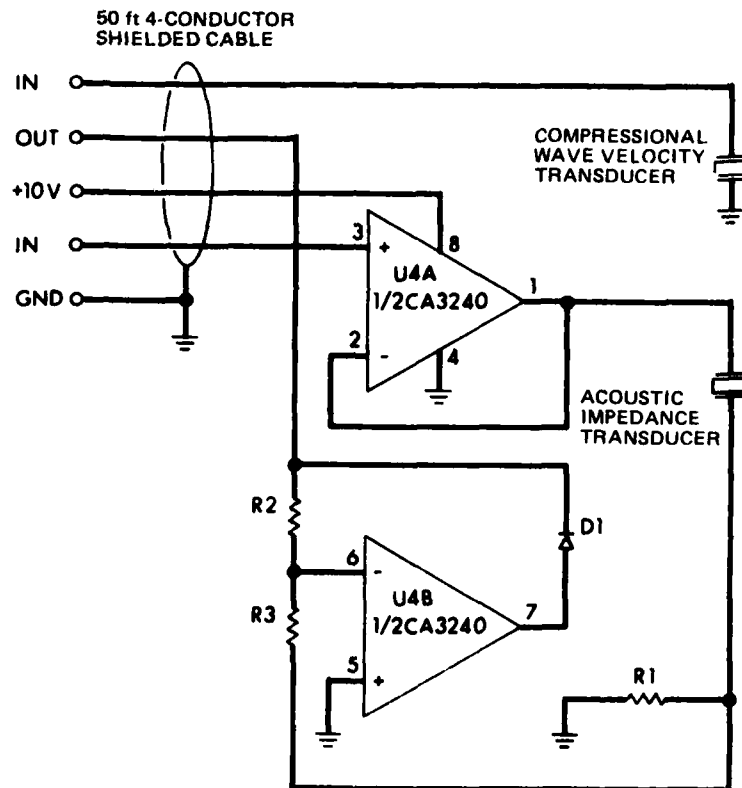


FIGURE 29
SCHEMATIC DIAGRAM OF THE ACOUSTIC IMPEDANCE TRANSDUCER CIRCUIT

ARL:UT
AS-81-505
DJS - GA
5-5-81

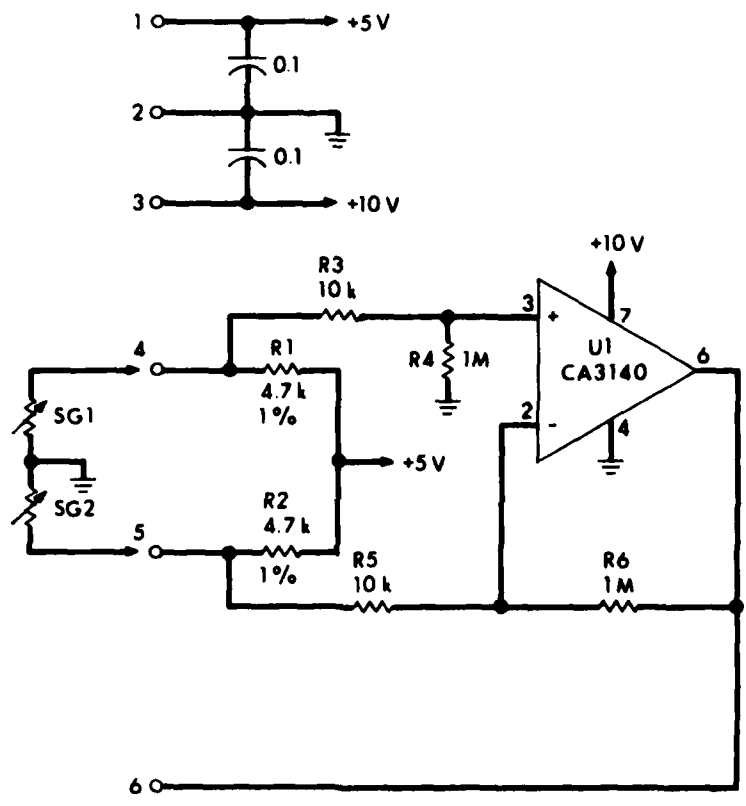


FIGURE 30
 SCHEMATIC DIAGRAM OF THE SHEAR STRENGTH MEASURING CIRCUIT

to sense the force exerted on a penetrometer body attached to the end of the bar. The strain gauges are arranged such that forces on the penetrometer bend the bar and cause one strain gauge to increase in resistance and the other to decrease in resistance by the same amount. The two strain gauges form a bridge network with R1 and R2 to detect the strain gauge resistance changes. The output of the bridge is connected to U1 which is an operational amplifier connected as a differential input amplifier with a voltage gain of 100. The output of the amplifier is provided through the card edge connector to the recorder circuits.

Solid State Memory Controller

The solid state memory controller includes circuits to multiplex six data channels, digitize the analog data, provide chip selects and address signals to the memory, and provide appropriate timing signals to control the operation sequence of all the circuit units in the profilometer.

Figure 31 is the schematic diagram of the control and digitizing circuits. Figure 32 provides a timing diagram of those circuits. The circuits comprise the following individual sections:

- (1) recorder on-off control,
- (2) clock generator and divider,
- (3) input channel multiplexer,
- (4) sample-and-hold amplifier,
- (5) channel select counter,
- (6) A/D converter,
- (7) address counter, and
- (8) chip select control.

The four sections of U15 constitute the recorder on-off control circuit. A free-fall sensing switch located exterior to the pressure case is connected to the input (pins 1 and 2) of NOR gate U15A connected

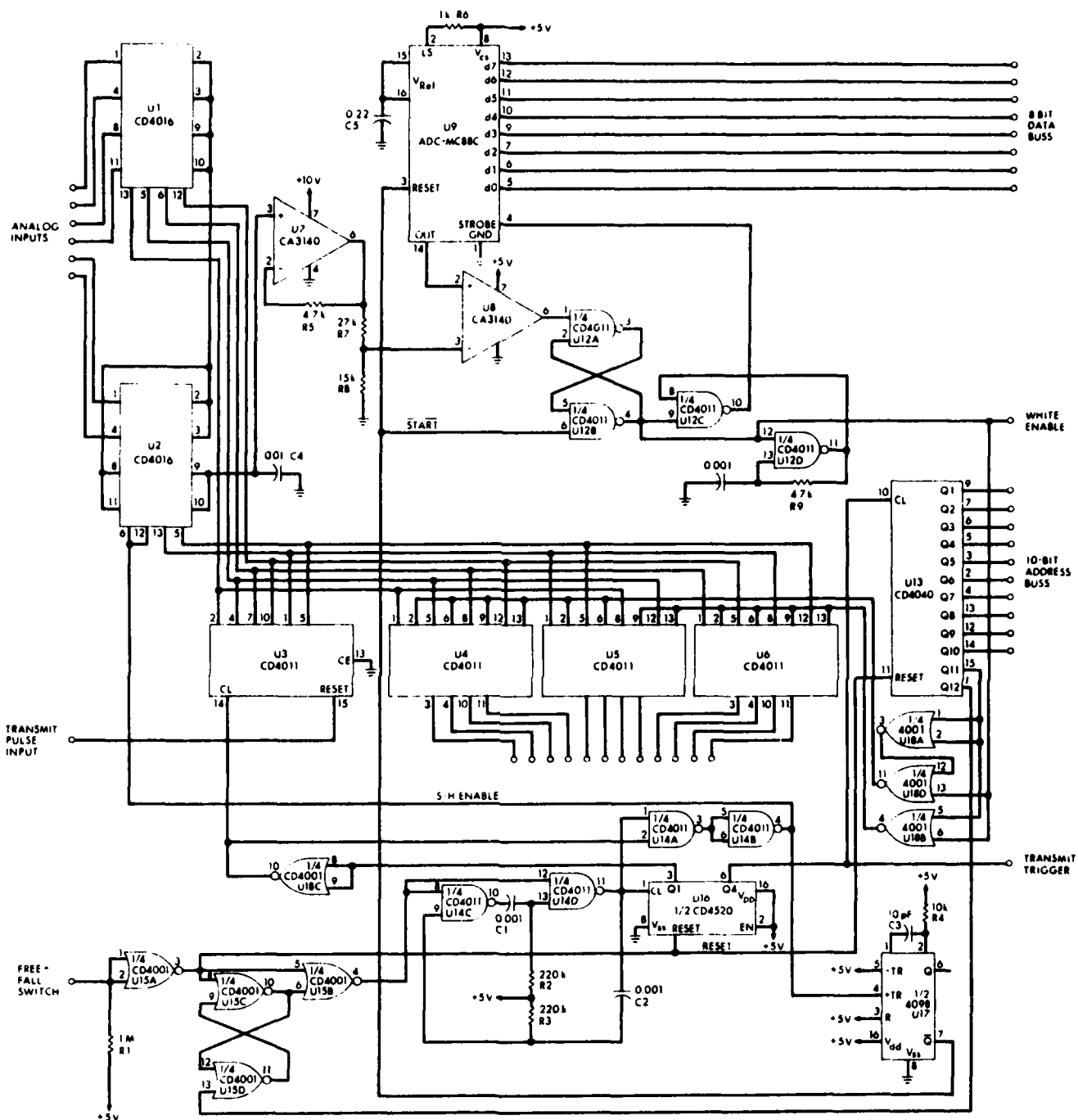


FIGURE 31
SCHEMATIC DIAGRAM OF THE DIGITAL MEMORY CONTROL CIRCUIT

ARL:UT
CS-81-607
DJS - GA
6-6-81

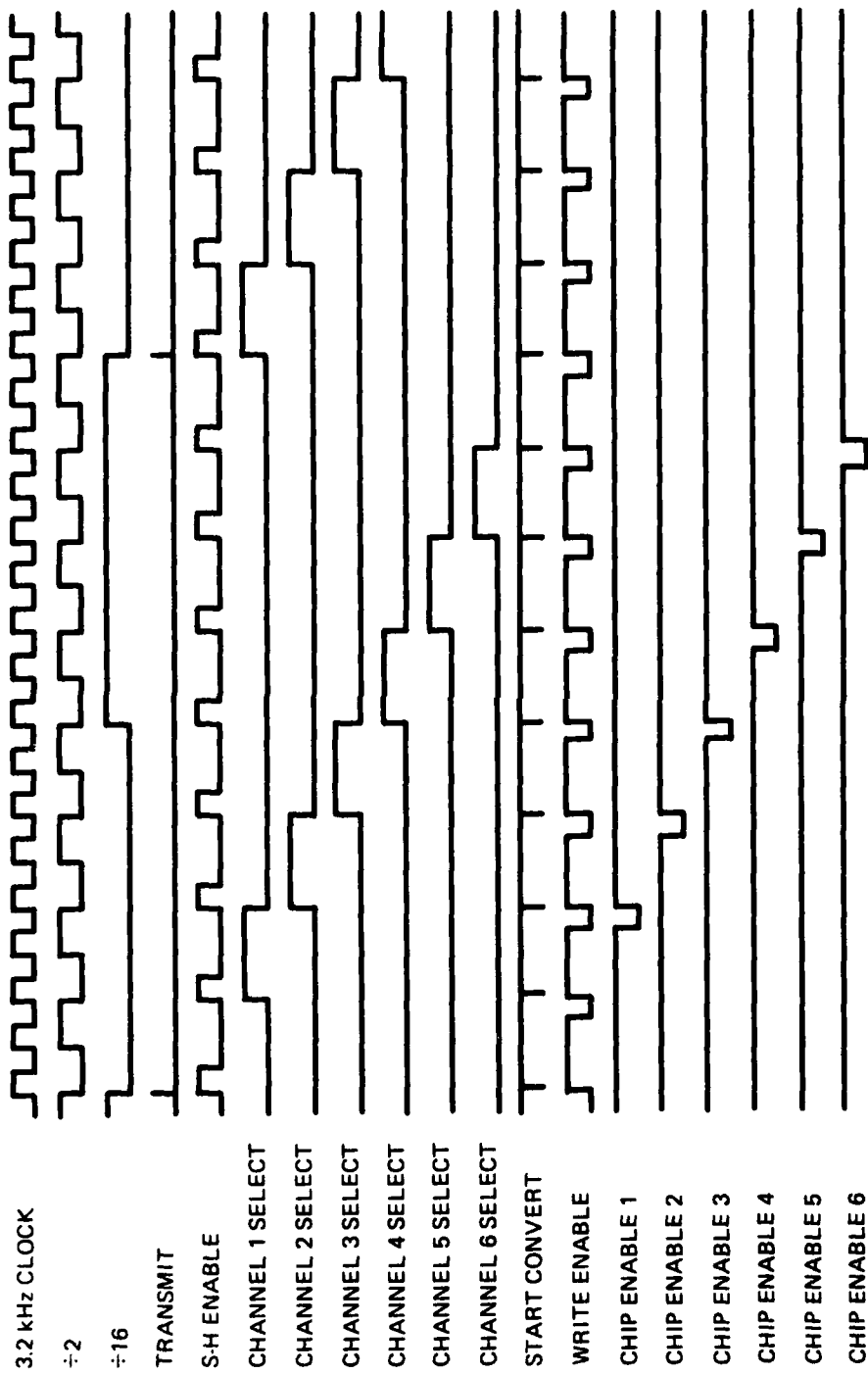


FIGURE 32
TIMING DIAGRAM FOR THE DIGITAL MEMORY CONTROL CIRCUITS

as an inverter. The switch is a normally closed magnetic reed switch which is caused to open when the corer is triggered at the ocean bottom. While the switch is closed, the input to U15A is low so the output will be high. The output line is connected to the reset inputs of counters U16 and U13 which causes their outputs to be low. The output of U15A is also connected to one input (pin 8) of an R-S flip-flop composed of U15C and U15D. Since the other input (pin 13) is connected to an output of counter U13, which is held low by the high reset input, the output of the R-S flip-flop (pin 10) is high. The output of the R-S flip-flop and the reset line are NOR'ed in U15B and with both inputs high the output of U15B is held low. The output from U15B is used to control a gated 3.2 kHz oscillator composed of U14C and U14D and associated RC networks. When the output from U15B is low, the oscillator is off and digitizing and storage of data is inhibited. When the free-fall reed switch is opened at the start of corer free-fall, the reset line is caused to go low, which enables counters U16 and U13 and brings the outputs of U15B high to enable the 3.2 kHz oscillator. The R-S flip-flop remains in its initial state. Counter U16 divides the 3.2 kHz from the oscillator and provides the $\div 2$ and $\div 16$ signals as outputs. These clock signals are shown at the top of the timing diagram, Fig. 32. The $\div 16$ clock pulse is input to the pulse generator in the analog measuring circuits where the falling edge of the $\div 16$ clock pulse initiates the generation of an acoustic pulse and the resultant measurement of the acoustic velocities. The $\div 16$ pulse is also input to the clock of 14-stage counter U13. The first 10 outputs of U13 are used as the address bus for the digital memory circuits. As a result, each time an acoustical measurement is initiated by the $\div 16$ clock pulse, the digital memory is advanced to the next location for storage of the six data bytes associated with each measurement.

The $\div 2$ clock pulse from U16 is inverted by U18C and supplied as the clock pulse to decimal counter U3. The outputs of counter U3 are decoded to provide a single positive going pulse at one of its 10 outputs, starting at Q0 and going to Q9 each time the counter is clocked. During reset, Q0 goes high. Six of the outputs of U3 (Q1 through Q6)

are used as the channel select signals and are shown in Fig. 32. The inverted $\div 2$ clock pulse going to U3 is also AND'ed with the 3.2 kHz main clock signal by NAND gates U14A and U14B to produce the sample-and-hold enable pulse. When this pulse is high, the sample-and-hold amplifier samples the level of the selected analog signal and when the pulse goes low the analog level is held constant by the amplifier.

The analog multiplexer and the sample-and-hold gate are implemented in the two CD4016 analog gate IC's, U1 and U2. The gates operate as single-pole/single-throw switches controlled by the outputs of U3 and the sample-and-hold signal. The multiplexer sequentially connects each of the six inputs to the sample-and-hold switch. Immediately after each input is connected, the sample-and-hold switch is closed and allows sampling capacitor C4 to charge to the analog voltage level. U7 is an operational amplifier connected as a X1 gain buffer to keep the load of following circuits from discharging C4.

As each of the six analog inputs is selected by the outputs of counter U3, one of six digital memory chips must be selected for storage of that datum. There are a total of 12 memory chips, two for each of the analog channels. The data from each channel is stored in each chip by selecting that chip through a low level CHIP ENABLE (\overline{CE}) input. After cycling through the six inputs and six chips, the addresses for all memory chips are advanced by clocking address counter U13. After a set of six chips are filled with data (1024 bytes) all 10 address lines (Q1 through Q10 of U13) will be high. The next clock pulse into U13 will set all address lines low again and set Q11 of U13 high. This action will select the next bank of six memory chips for storage.

The low going \overline{CE} pulses are generated from the high going channel select signals by first NOR'ing the Q11 output from U13 in NOR gates U18B and U18D with the WRITE ENABLE (\overline{WE}) pulse from the A/D converter and NAND'ing the result with the channel select signals in NAND gates U4, U5, and U6. Both the noninverted and inverted versions of the Q11

output of U13 are used in this way so that when Q11 is low, the first six \overline{CE} signals are enabled and when Q11 is high, the other six \overline{CE} signals are enabled and the first six are disabled.

After each of the six input channels is selected, a short, low going pulse is generated which is used to initiate the analog-to-digital conversion. The leading edge of the sample-and-hold enable pulse is applied to the trigger input of monostable multivibrator U17. The \overline{Q} output of U17 is a low going pulse whose duration is controlled by the RC time constant of R4 and C3. The output pulse is applied to the reset input of the analog-to-digital converter (ADC) chip U9 which sets all eight bits of its output low. The start pulse is also applied to one input of R-S flip-flop formed by U12A and U12B and sets the output of the flip-flop high. This output is used as the END OF CONVERSION (\overline{EOC}) signal and also as the WRITE ENABLE (\overline{WE}) signal. When \overline{EOC} is high, the ADC is busy converting and output data are not valid.

The input of the ADC is connected through resistance R7 and R8 to the output of the sample-and-hold amplifier. R7 and R8 are used to set the calibration of the unit so that 5 V input will produce a digital output from the ADC with all bits high. With zero input, all bits from the ADC will be low. The input voltage is connected to the noninverting input of operational amplifier U9 which is configured as a voltage comparator. The inverting input of the comparator is connected to the analog output of the ADC chip.

At the start of conversion when \overline{EOC} goes high, a 500 kHz clock generator formed by U12C and U12D is enabled and provides a 500 kHz pulse string to the strobe input (pin 4 of U9) of the ADC. As the counters internal to the ADC are incremented by the strobe input, an internal digital-to-analog converter (DAC) circuit provides a linearly increasing voltage at the analog output, pin 14. When the ADC output voltage reaches the same level as the input voltage, voltage comparator U8 switches its output low which resets the RS flip-flop (U12A and B) which in turn disables the ADC clock circuit, stops the ADC counters, and

sets \overline{EOC} and \overline{WE} low. The result is that the digital output of the ADC counters available on the eight data lines is directly proportional to the analog input voltage. The \overline{WE} pulse is then used to store the data word in an appropriate space in the digital memory.

After 2048 samples of data have been obtained for each of the six inputs, Q12 of address counter U13 will go high. Q12 is connected to the reset input of RS flip-flop U15C and U15D. Pin 10 of U15 will return to a high level bringing pin 4 low and thus turning off the 3.2 kHz oscillator. With the oscillator disabled, the profilometer circuits cannot function and operation is effectively halted.

Solid State Memory Circuit

Figure 33 shows the schematic diagram of one of three identical memory boards used in the profilometer recorder. Each board carries four memory chips, which is sufficient for two channels of data. The data lines (D0 through D7) and the address lines (A0 through A9) are connected in parallel to all 12 chips in the memory circuit. The 12 \overline{CE} lines are connected to the 12 outputs of the control circuit and to the \overline{CE} inputs of the memory chips. The \overline{WE} line is connected to all 12 chips and in conjunction with the \overline{CE} signals determines where each digital datum will be stored.

Memory Power Supply

Power for most of the control and digitizing operations is supplied by the profilometer power unit. However, the operating time for the profilometer main battery is limited to about 18 h; it will also be disconnected when the unit is lifted out of the water upon retrieval. If power is lost, all data stored in the memory will also be lost. For this reason, the memory chips and selected portions of the control circuitry are operated from a separate battery system.

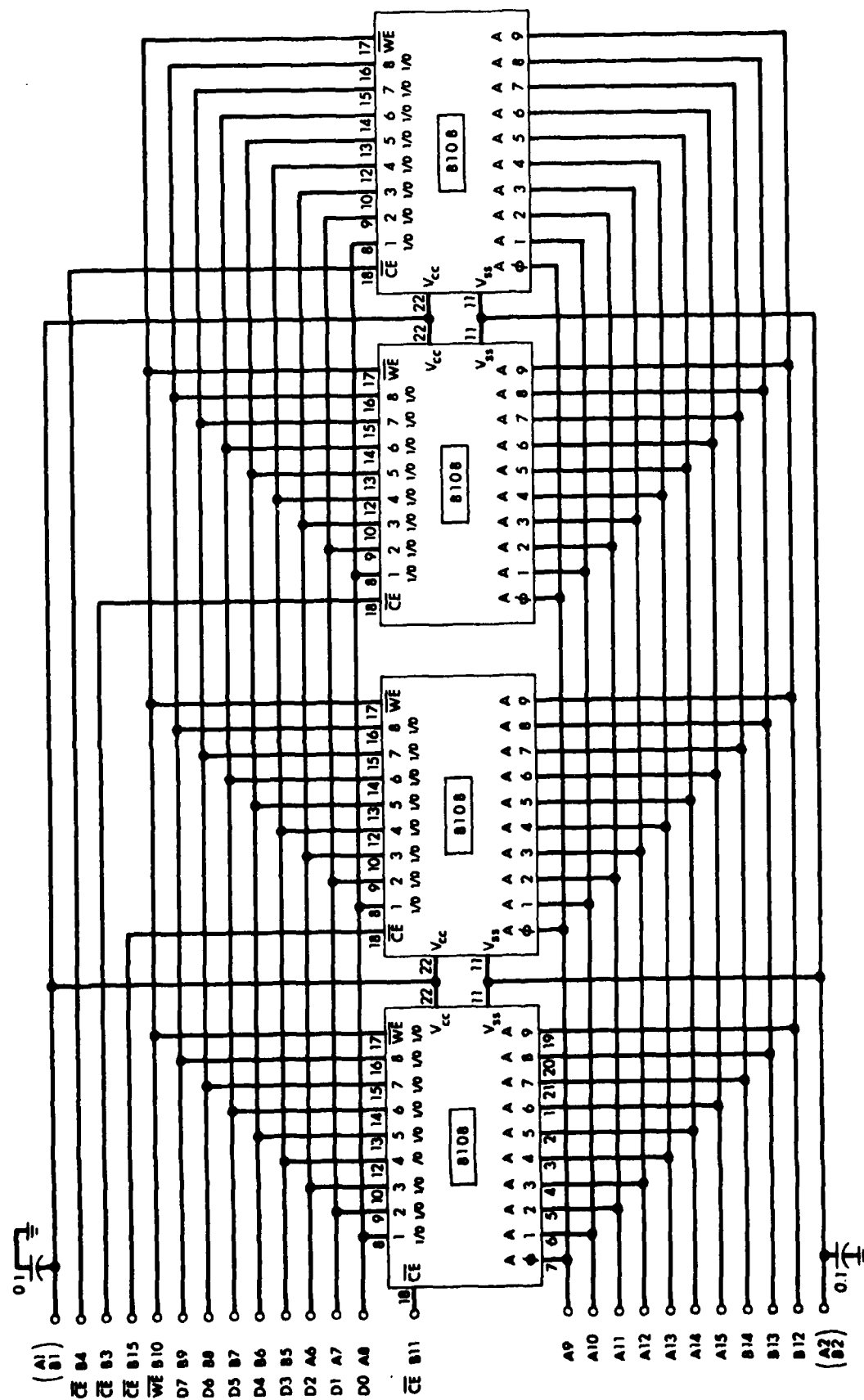


FIGURE 33
SCHEMATIC DIAGRAM OF THE DIGITAL MEMORY BOARD

Figure 34 is the schematic of the memory power supply. Power is supplied by a 7.2 V, 1.8 A·h NiCad battery pack. Q1 is a silicon controlled rectifier (SCR) which acts as a power switch and keeps power to the memory circuits turned off until the unit is deployed. As the profilometer unit is immersed in the ocean, a saltwater sensor turns on the main power supply in the profilometer. The +5 V level on the main power bus turns on the SCR and thus applies power to the memory circuits. Once turned on, the SCR will remain on regardless of whether the main supply remains on or not. The battery pack is able to supply power to the memory for a period of 70 h.

The circuit composed of Q2, R3, D1, D2, C1, and C2 is a low power voltage regulator to regulate the battery voltage to the +5 V level required by the memory chips.

To ensure that data are retained in memory and that minimum power is used, the \overline{CE} inputs to all the memory chips must be kept at a high level at all times except during the actual storage time interval. R4 through R15 are used to ensure that all \overline{CE} inputs are pulled up to the +5 V supply rail even if other parts of the control circuit are disabled. For the same reason, the memory power supply is used to supply power to the board that contains the chip enable gates U4, U5, and U6.

Computer Interface

Once the profilometer has been deployed, and has recorded data and been retrieved, the data must be removed from the digital memory circuits inside the profilometer and stored in memory inside the minicomputer unit. To accomplish the transfer of digital data, the two printed circuit cards containing the multiplexer-A/D converter circuit and the address counter/channel select counter circuits are removed from the card cage of the profilometer recording unit, and two other printed circuit cards, which are attached by electrical cable to the microcomputer playback unit, are inserted in their place. The new cards generate address and

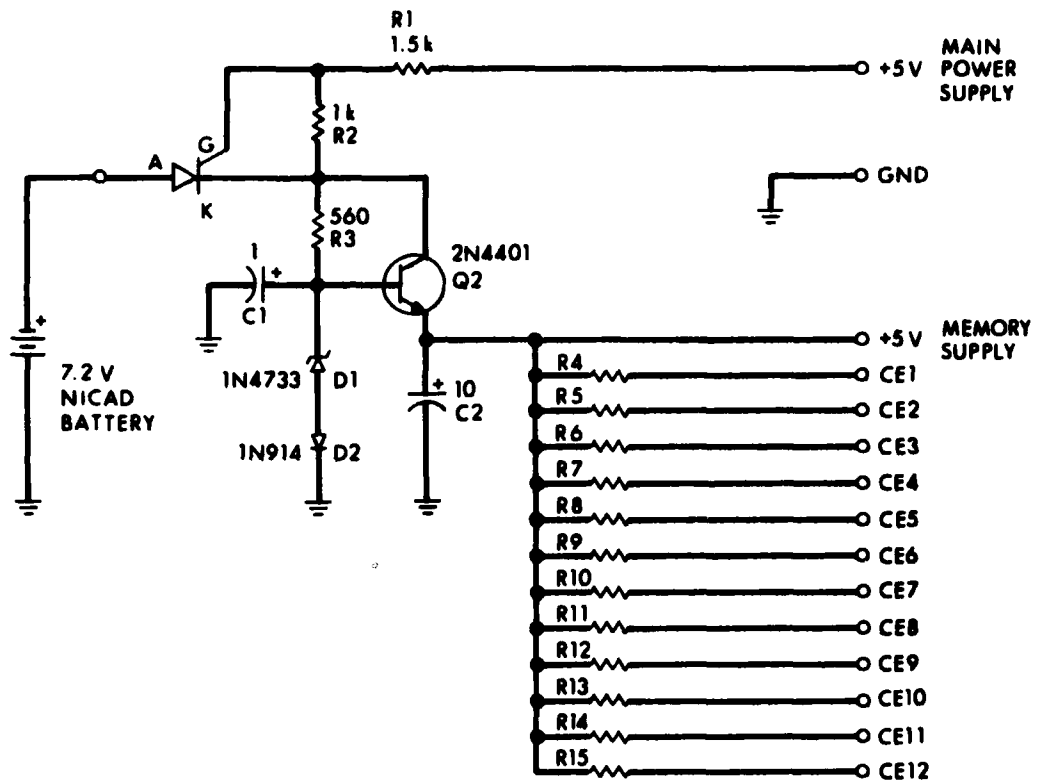


FIGURE 34
SCHEMATIC DIAGRAM OF THE MEMORY POWER SUPPLY

ARL:UT
AS-81-510
DJS-GA
5-5-81

chip enable signals under control of the computer to enable the computer to read the data from the memory chips.

Figure 35 is a diagram of the interface unit. An 18-conductor flat ribbon cable is connected to the input-output connector of the MPU board of the microcomputer. The interface part of the microcomputer consists of a peripheral interface adapter (PIA) chip which has two programmable 8-bit data buses and four control lines. The data buses are labeled PA0 through PA7 and PB0 through PB7 and the control lines are CA1, CB1, CA2, and CB2. The buses and control lines can be programmed by the computer as either inputs or outputs. In this case, the PA bus is programmed as inputs to read the memory data bus in the profilometer and the PB bus is programmed as outputs to generate the chip enable signals for the profilometer memory chips. Since there are not enough data lines available to also generate the address signals, a CD4040 counter controlled by the CA2 and CB2 lines is used.

Operation of the microcomputer is explained in more detail in Appendix B.

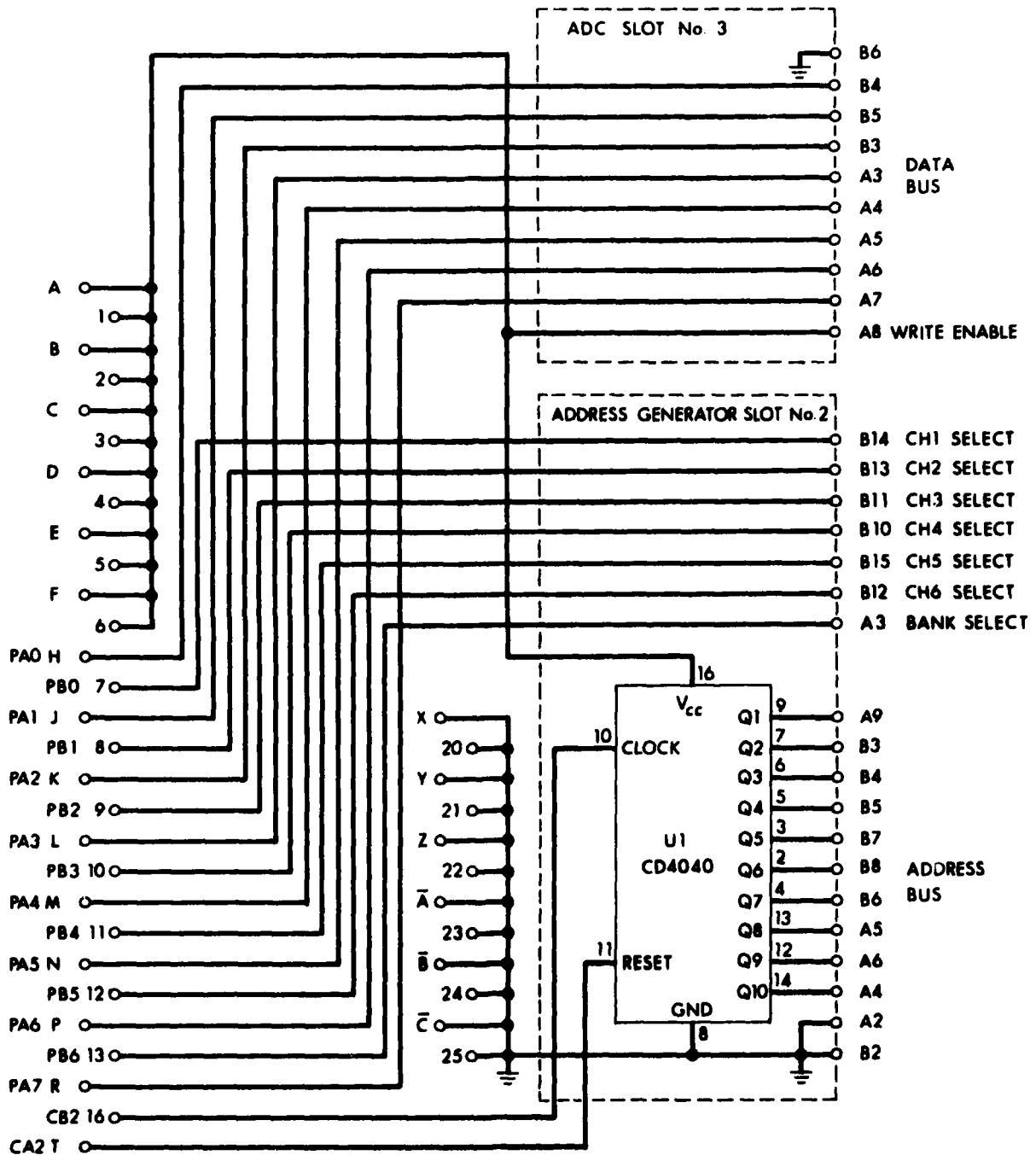


FIGURE 35
SCHEMATIC DIAGRAM OF THE MICROCOMPUTER TO MEMORY INTERFACE BOARD

APPENDIX B

Introduction

The microcomputer unit used with the profilometer acoustical measurement system is built around a Motorola MEK6800D2 evaluation kit. The kit consists of a complete microprocessor unit (MPU) on a finished printed circuit board with a hexadecimal keyboard and associated readout. The microcomputer unit was completed by adding a power supply, a 16-kilobyte static memory board, and an input-output board. The input-output board enables the computer to digitize 8 channels of data and to provide signals to an X-Y plotter so that data stored in memory can be plotted. Only the memory board and the input-output board will be explained in detail. A detailed explanation and schematic for the MPU board can be obtained from the Motorola MEK6800D2 manual.

Figure 36 shows a photograph of the complete microcomputer unit with the top cover removed and the card cage raised to the test position.

Memory Board

Figure 37 is the schematic diagram of the microcomputer memory board which implements a 16-kilobyte static memory. U1 through U32 are type 2142 static memory chips comprising 4098 bits organized as 1024 4-bit words each. A total of 32 chips are used to implement the 16 kilobytes of memory.

The 8 data lines (D0 through D7) and the first 10 address lines (A0 through A9) from the MPU board are connected in parallel to all 32 of the memory chips to form an 8-bit data bus and a 10-bit address bus. The next 3 address lines (A10, A11, and A12) are decoded by a 3 line-to-8 line decoder, U33, to enable the selection of appropriate chips. The top 3 address lines (A13, A14, and A15) are decoded on the MPU board and provide the 2/3 and 4/5 selection signals to select

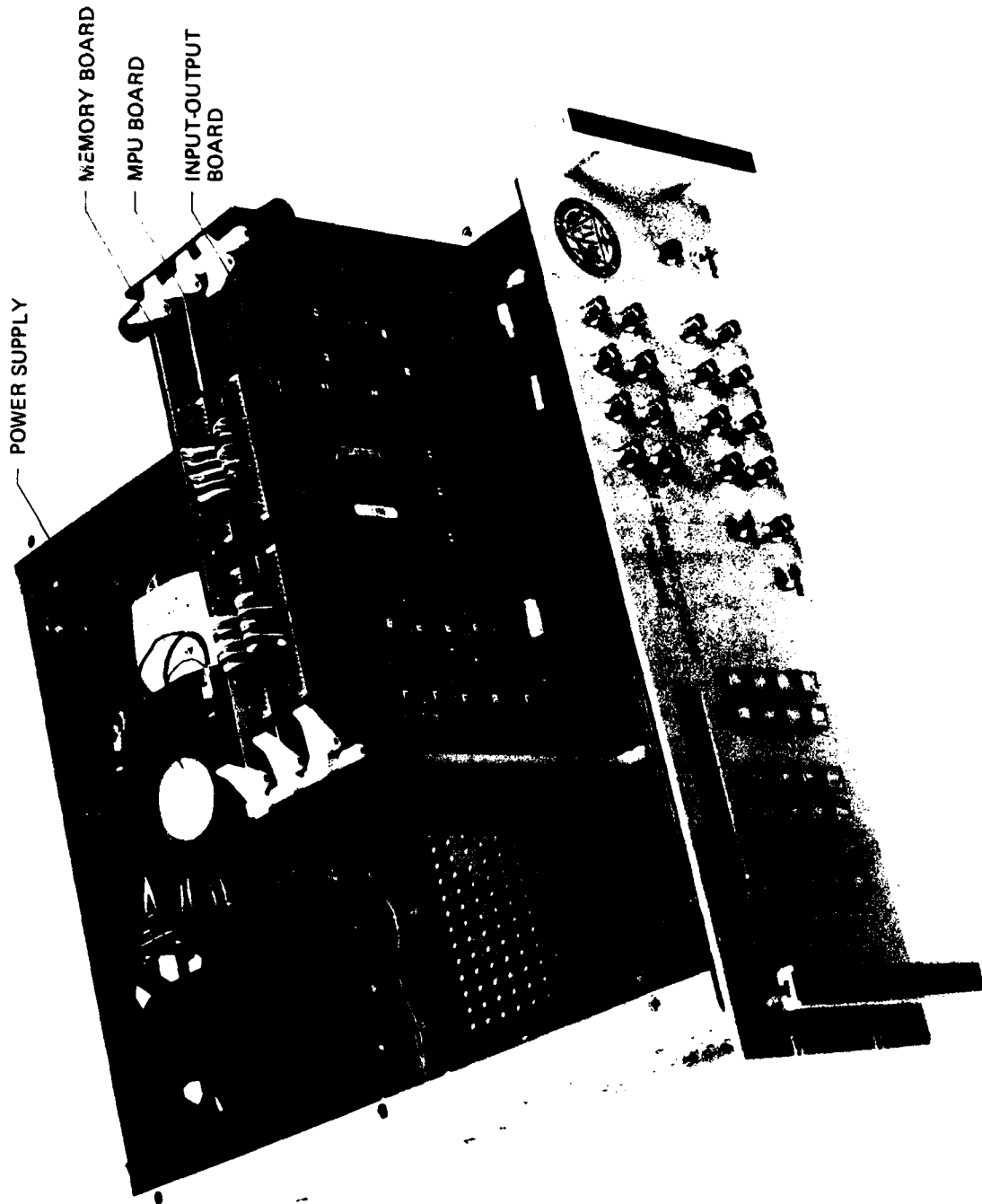


FIGURE 36
PROFILOMETER PLAYBACK MICROCOMPUTER UNIT

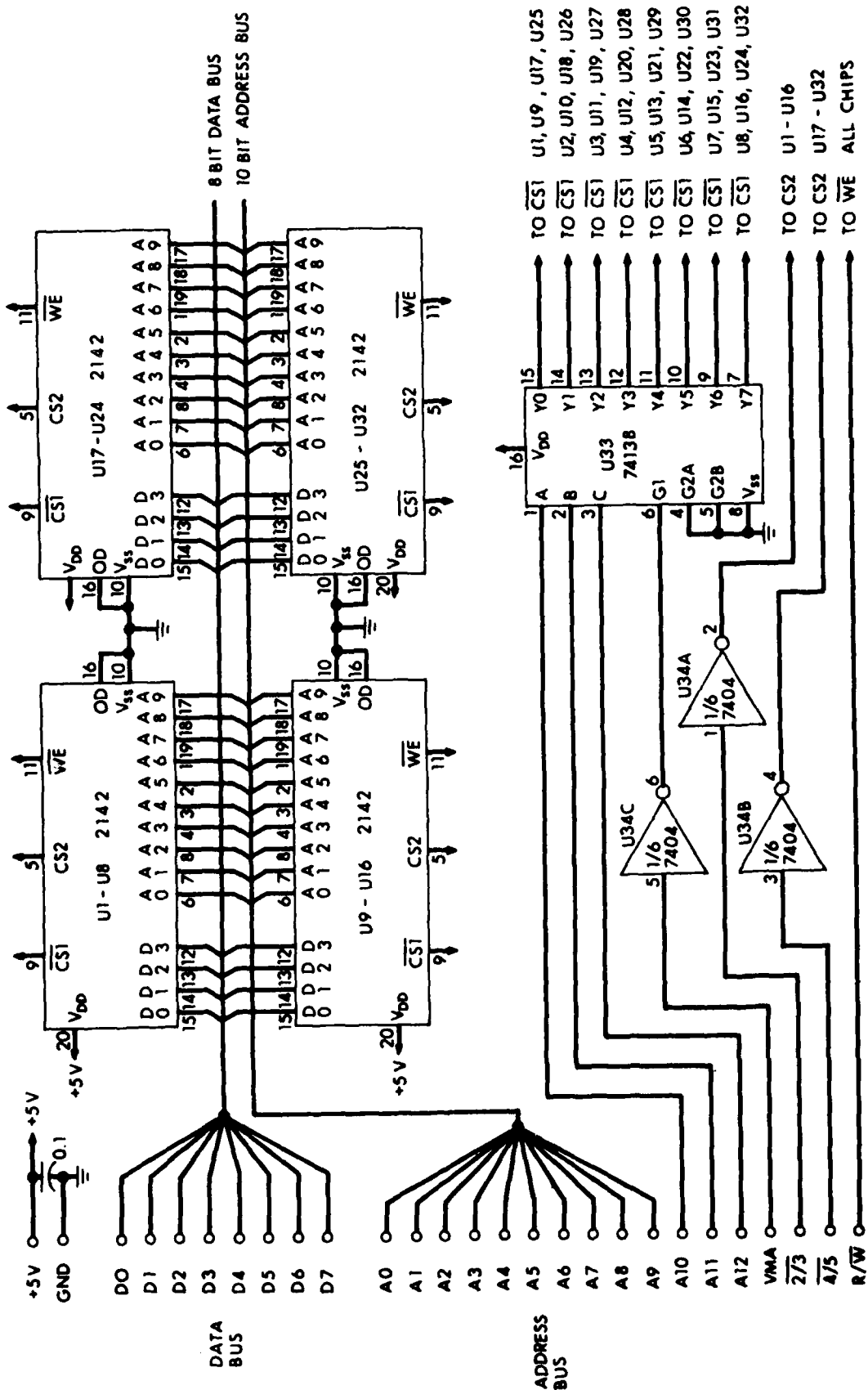


FIGURE 37
SCHEMATIC DIAGRAM OF THE MICROCOMPUTER MEMORY BOARD

ARL:UT
AS-81-512
DJS - GA
5-5-81

either of the two 8K pages of memory. The READ/WRITE (R/W) signal controls the writing of data into the memory chips and is connected to the WRITE ENABLE (\overline{WE}) inputs.

Input-Output Board

Figure 38 is the schematic diagram of the microcomputer input-output board which is used to input analog data to the microcomputer and to output analog data to an X-Y plotter from the computer.

The MPU board of the microcomputer has two 16-bit parallel interface connections implemented with MC6821 peripheral interface adapters (PIA). One of the ports is dedicated to the keyboard/display circuits and the other is available for user access. This second port is used for connection to either the interface circuit (see description in Appendix A) or to the input-output board. The port connections of the PIA can be controlled by the MPU to be either an input or an output. For use with the input-output board, 8 of the parallel lines (PA0 through PA7) are programmed to be the data port and are set up to be inputs or outputs, depending on direction of data flow. The other 8 lines (PB0 through PB7) are set up as outputs to control the various circuits on the input-output board.

U1 is an 8-input multiplexer under program control through PB5, PB6, and PB7, which select the analog input channel to be digitized. U2 is an operational amplifier which, in conjunction with C3 and the multiplexer, operates as a sample-and-hold amplifier to hold the analog signal constant during the digitization process. U3 is an 8-bit analog-to-digital converter module with an internal clock. The A/D process is started under program control through PB4. After the input signal has been digitized and the digital output of U3 is stable, the MPU is signaled through the end of conversion line (EOC) CB1 which serves as an interrupt line to the MPU. U4 and U5 serve as interface buffers with 3-state outputs to enable bus operation on the board. The data output to the data bus from the ADC is enabled under program control

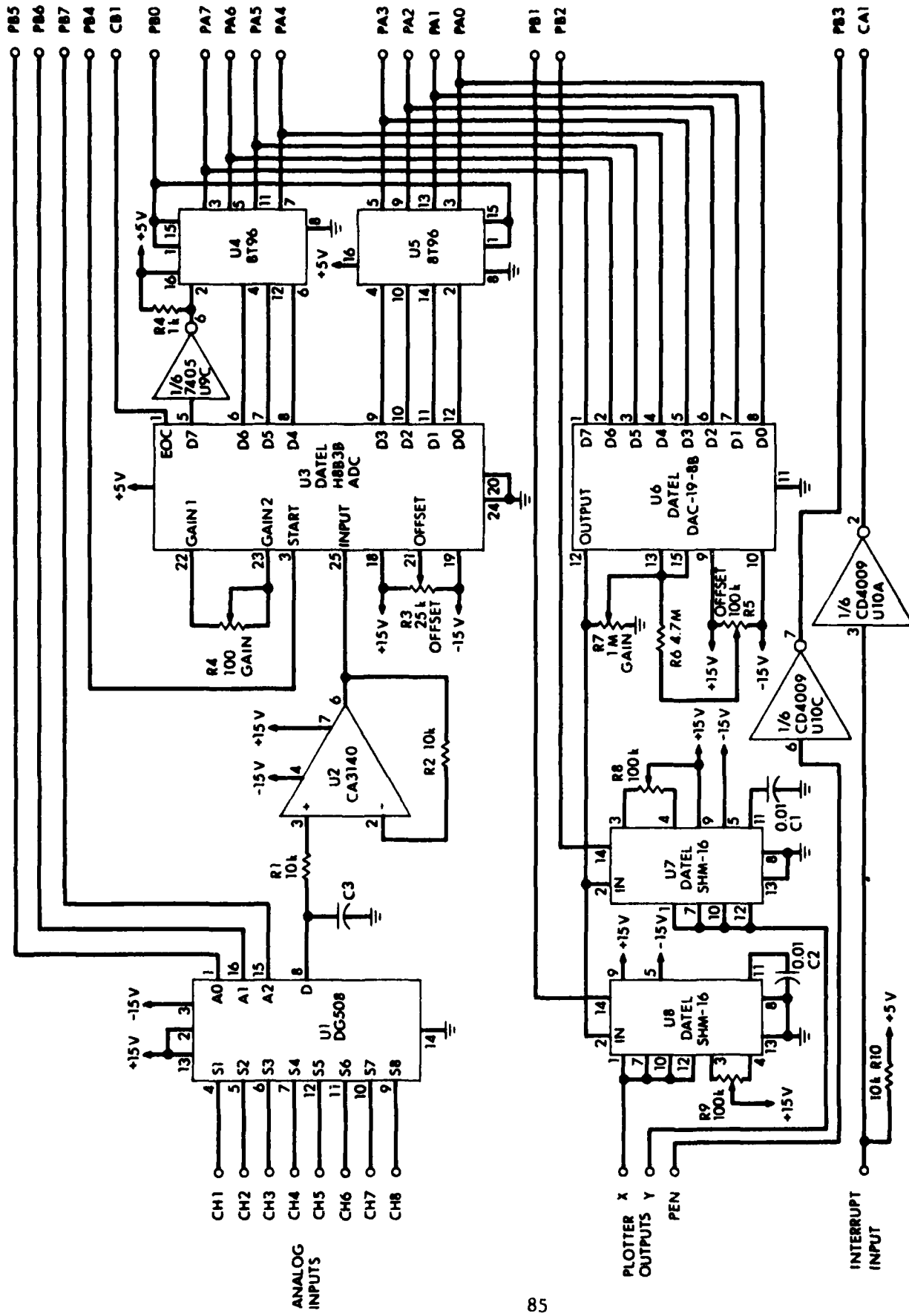


FIGURE 38
SCHEMATIC DIAGRAM OF THE MICROCOMPUTER INPUT-OUTPUT BOARD

ARL:UT
A661-513
DJ8-GA
6-6-81

through PBO. U9C is an inverter for the most significant data bit (MSB) to change the straight binary output of the ADC to a 2's complement output which is compatible with arithmetic operations of the MPU.

When the board is used for an output, the data are routed to the digital-to-analog converter module U6. The sample-and-hold amplifiers are used to store the X and Y coordinates for the X-Y plotter during the pen relocation time of the plotter. The sample-and-hold amplifiers are under program control through PB1 and PB2.

There are two direct digital lines from the MPU through PB3 and CA1. The CA1 line is used as an interrupt line from a front panel switch to control the time the MPU starts digitizing data from the inputs. The PB3 signal allows the MPU to control pen up or pen down positions on the X-Y plotter.

APPENDIX C

I. Introduction

The software to enable the microcomputer to operate in the appropriate modes to digitize data, to plot data, or to extract digital data directly from the profilometer is contained on 2 ultraviolet erasable programmable read only memories (EPROM) on the MPU board. Computer printouts and flow diagrams of the programs are included in this Appendix. Section II contains instructions for setting up and running the programs.

II. Profilometer Microcomputer Unit Programs

A. Use with magnetic tape system

1. Attach BNC cable from Profilometer Playback Unit acceleration channel to input channel 1 on microprocessor front panel; from time delay channel to input 2; and from amplitude channel to input 3.
2. Connect cable from X-Y plotter output on back panel of microprocessor to plotter input.
3. OPTIONAL: To monitor X and Y outputs from microprocessor, connect BNC cables from microprocessor output channel 1 (Y) and channel 2 (X) to storage oscilloscope.
4. Turn on microprocessor. DASH prompt will appear on left side of display.
5. Enter program constants:
 - (1) Enter 0000. Punch "M".
Now enter desired x axis parameter according to the following table.

01 - Acceleration

02 - Time Delay

03 - Amplitude

04 - Velocity

- 05 - Depth
- 06 - Time
- 07 - Sound Speed

- (2) Punch "G". Address "0001" appears. Enter y-axis parameter as in Step 5(1).
- (3) Punch "G". Enter A/D sample period (16-bit hexadecimal number greater than zero). At address "0002" enter most significant 2 digits of sample period.
- (4) Punch "G". Enter least significant 2 digits of sample period. A/D sample period is found by the following formula:

Sample period = $(13 \mu\text{sec} \times N1) + 295 \mu\text{sec}$,
 where N1 is the hexadecimal number entered into 0002 and 0003. Total A/D time is given by:
 A/D time = $(13 \mu\text{sec} \times N1) + 295 \mu\text{sec} \times 2048 \text{ bytes}$.

Solving for N1 yields:

$$N1 = \frac{[\text{A/D time (sec)/2048}] - 295 \mu\text{sec}}{13 \mu\text{sec}}$$

This gives N1 in decimal, which must be converted to hexadecimal before entering into memory.

- (5) Enter D/A sample period into locations 0004 (most significant byte) and 0005 (least significant byte). D/A sample period is given by:

Sample period = $13 \mu\text{sec} \times N2 + 255 \mu\text{sec}$.

D/A time varies depending on whether or not the x axis represents time.

A good value for N2 is 1500.

6. Program is now ready to run.

- (1) Punch escape "E".
- (2) Enter "6000".
- (3) Punch "G".

Program is now initialized and waiting for an interrupt to start digitizing. Just before the area of tape to be analyzed passes by the read head of the playback unit, punch MANUAL INTERRUPT on front panel. Program will stop at 603D when it is through digitizing. Memory changes made:

1. Locations 2000 - 27FF: Acceleration
2. Locations 2800 - 2FFF: Time Delay
3. Locations 3000 - 37FF: Amplitude .

Acceleration is normalized by taking the average of the last 64 bytes = 0.

To check the contents of these locations.

- (1) Punch ESCAPE.
- (2) Enter address to be examined (2000 above, e.g.).
- (3) Punch "M". Contents of that particular memory location will be displayed.

7. (1) Punch ESCAPE.

(2) Enter 603E. Punch "G". Program will now integrate acceleration to get velocity, integrate velocity to get depth, and invert time delay to get sound speed. Memory changes:

1. 3800 - 3FFF: Velocity
2. 4000 - 47FF: Depth
3. 4800 - 4FFF: Sound Speed
4. 0006 - DVCNT1: Number of times acceleration was divided by 2 to get velocity.
5. 0007 - DVCNT2: Number of times velocity was divided by 2 to get depth.
6. 0008 - SCNT: Number of times sound speed was multiplied by 2 before plotting. Scale on the sound speed plot is found from

$$SS = (\$FFFF/td) \times 2^N ,$$

where

SS - Sound Speed,

td = Time Delay, and

N = Shift Count (SCNT).

The last 3 values above (DVCNT1, DVCNT2, SCNT) should be noted on the plots. These are necessary to determine scale and will usually be different for each profile.

8. Data can be plotted now.
 - (1) Punch ESCAPE.
 - (2) Enter 607B. Punch "G". Program will stop at 60AA.
9. Any other parameters can be plotted now by punching ESCAPE, entering new values into location \$0000 and \$0001 (Steps 5(1) and 5(2) and repeating Step 8.

B. Use with solid state memory system

1. After data have been recorded in the recording unit, be sure that during retrieval of the unit from the corer that the switch cable is unplugged and that a blank cover is installed on the waterproof connector.
2. Remove recorder unit from the pressure case and place on a workbench near the microprocessor unit. Attach bench test switch cable with switch in the OFF or center position. Check that main battery voltage is at least 12 V.
3. Attach the interface cable to the IO port on the MPU board in the microprocessor unit.
4. Remove board 2 (address generator board) and board 3 (ADC board) and plug the interface into the two open slots of the profilometer unit.
5. Turn on power to the microprocessor unit and wait for "DASH" prompt signal to appear on the microprocessor readout.
6. Turn switch on profilometer recorder to P/S.
7. Enter C000 into address space of microprocessor and push the "G" button.

8. Data will then be extracted from the profilometer recorder unit and C048 will appear on readout. The following address spaces will contain the listed blocks of data:

2000-27FF	Channel 1 data
2800-2FFF	Channel 2 data
3000-37FF	Channel 3 data
3800-3FFF	Channel 4 data
4000-47FF	Channel 5 data
4800-4FFF	Empty

9. The data blocks should be stored on a magnetic tape via the MPU cassette interface to ensure that the data are not lost.
10. Next enter C07B and push "G" button. The acceleration data will be normalized (last 64 bytes averaged and the average value subtracted from all the data to ensure that the acceleration at rest is zero), then integrated twice to get depth. This process is similar to that in Section II.A. The address of DVCNT1 is 0007 and of DVCNT2 is 0008. Data are stored in memory as follows:

2000-27FF	CH 1 Acceleration
2800-2FFF	Ch 2
3000-37FF	Ch 3
3800-3FFF	Ch 4
4000-47FF	Ch 5
4800-4FFF	Velocity
5000-57FF	Depth

11. Data can now be plotted as in Section II.A except that the address of the beginning byte of data to be plotted on each coordinate must be entered directly in memory as follows:
- (1) Enter 001C and push "M".
 - (2) Enter MSB of x axis starting data address (for example, to plot with depth as x axis the starting address would be 5000, so 50 would be entered in 001C).
 - (3) Push "G"; address 001D will appear in readout.

- (4) Enter LSB of x axis starting data address (for above example, 00).
- (5) Push "G"; address 001E will appear in readout.
- (6) Enter MSB of y axis address.
- (7) Push "G"; address 001F will appear in readout.
- (8) Enter LSB of y axis address.
- (9) If data are to be plotted with time as the x axis, enter 0000 in steps 2 and 4.
- (10) Push "E" and enter CIOE in address after prompt dash appears.
- (11) Push "G"; data will be plotted on X-Y plotter.

MOTOROLA M6854M CROSS-ASSEMBLER

M6854M IS THE PROPERTY OF MOTOROLA SPD, INC.
COPYRIGHT 1974 TO 1976 BY MOTOROLA INC.

MOTOROLA M6800 CROSS ASSEMBLER. RELEASE 1.3

```
00001          NAM      RTI
00002          *-----*
00003          *
00004          *
00005          *
00006          *          APPLIED RESEARCH LABS
00007          *          UNIVERSITY OF TEXAS, AUSTIN
00008          *          JUNE 19, 1979
00009          *          W. TOMPKINS
00010          *
00011          *
00012          *-----*
00013          *
00014          *
```


RT1

MOTOROLA M68SAM CROSS-ASSEMBLER

```
00016 *
00017 *
00018 * THIS PROGRAM DIGITIZES 3 CHANNELS OF ANALOG
00019 * DATA. INPUT CONNECTIONS ARE:
00020 * CH. 1 = ACCELERATION
00021 * CH. 2 = TIME DELAY
00022 * CH. 3 = AMPLITUDE
00023 *
00024 * AFTER DIGITIZING, TIME DELAY DATA ARE
00025 * INVERTED, YIELDING SOUND SPEED, AND
00026 * ACCELERATION IS INTEGRATED TO YIELD
00027 * VELOCITY AND DEPTH. ANY ONE PARAMETER
*
* MAY THEN BE PLOTTED AS A FUNCTION OF
* ANY OTHER OR OF TIME.
*
00028 *
00029 * PARAMETERS TO BE PLOTTED ON THE X AND
00030 * Y AXES ARE SELECTED BY ENTERING ONE OF
00031 * THE FOLLOWING ASSIGNMENTS INTO
00032 * LOCATIONS *XSEL* AND *YSEL*.
00033 * 01. ACCELERATION
00034 * 02. TIME DELAY
00035 * 03. AMPLITUDE
00036 * 04. VELOCITY
00037 * 05. DEPTH
00038 * 06. TIME
00039 * 07. SOUND SPEED
*
00040 *
00041 * THE FOLLOWING CONSTANTS MUST BE ENTERED
00042 * INTO MEMORY BEFORE PROGRAM EXECUTION:
00043 * 1. ENTER DESIRED X OUTPUT PARAMETER INTO
00044 * XSEL, LOCATION $0000.
00045 * 2. ENTER DESIRED Y OUTPUT PARAMETER INTO
00046 * YSEL, $0001.
00047 * 3. ENTER 2 BYTE INPUT LOOP DELAY LENGTH.
00048 * MOST SIGNIF. BYTE INTO INDEL, $0002.
00049 * LEAST SIGNIF. INTO $0003.
00050 * 4. ENTER 2 BYTE OUTPUT LOOP DELAY LENGTH.
00051 * MS BYTE INTO OUTDEL, $0004. LS BYTE
00052 * INTO $0005
*****
```

AD-A103 726

TEXAS UNIV AT AUSTIN APPLIED RESEARCH LABS
ACOUSTICAL PROPERTIES OF SEDIMENTS.(U)
MAY 81 D J SHIRLEY
ARL-TR-81-20

F/G 8/10

N00014-76-C-0117

UNCLASSIFIED

NL

11
26
81-882-4



END
DATE
FILMED
11 81
DTIC

RT1

MOTOROLA M68SAM CROSS-ASSEMBLER

```
00054 *
00055 *
00056 *
00057 F0E0 DELAY EQU $F0E0
00058 2000 ACCBLK EQU $2000 DATA BUFFERS
00059 2800 TDBLK EQU $2800
00060 3000 AMPBLK EQU $3000
00061 3400 VELBLK EQU $3400
00062 4000 DEPRBK EQU $4000
00063 4800 SSBK EQU $4800
00064 5000 SCR16 EQU $5000
00065 0000 TIME EQU $0000
00066 6000 FTN EQU $6000 END
00067 *

00068 0000 ORG $0000
00069 0000 0001 XSEL RMB 1 X-AXIS PARAMETER
00070 0001 0001 YSEL RMB 1 Y-AXIS PARAMETER
00071 0002 0002 INDEL RMB 2 A/D DELAY
00072 0004 0002 OUTDEL RMB 2 U/A DELAY
00073 0006 0001 DVCNT1 RMB 1 FIRST INTEGRATION DIV.
00074 0007 0001 DVCNT2 RMB 1 2ND INTEGRATION DIV. COUNT
00075 0008 0001 DIVCNT RMB 1 SCRATCH DIVISION COUNT
00076 0008 0008 SCNT EQU $0008 BUFFER POINTERS
00077 0009 0002 ACCIX RMB 2
00078 0008 0002 TDIX RMB 2
00079 000D 0002 AMPIX RMB 2
00080 000F 0002 VELIX RMB 2
00081 0011 0002 DEPTX RMB 2
00082 0013 0002 SSIX RMB 2
00083 0015 0002 IX16 RMB 2
00084 0017 0002 IX2 RMB 2
00085 0019 0001 AVGMSB RMB 1
00086 001A 0001 AVGLSB RMB 1
```

```

00087 001A 0001 XTOUT RMB 1
00088 001C 0002 XSCRCH RMB 2
00089 001E 0002 YSCRCH RMB 2
00090 0020 0002 IX3 RMB 2
RT1 MOTOROLA M68SAM CROSS-ASSEMBLER

```

```

00091 0022 0001 NEGFLG RMB 1
00092 0023 0001 XKDVSH RMB 1
00093 0024 0002 XKDVND RMB 2
00094 0026 0002 XKDQDT RMB 2
00095 0028 0001 XKDSPL RMB 1
00096 0029 0001 INITX RMB 1
00097 002A 0001 INITY RMB 1
00098 002H 0002 HIGGST RMB 2
00099      8004 PRA EQU $8004 PERIPH. REG. A (PIA)
00100      8004 DDRA EQU $8004 DATA DIRECTION REG A
00101      8005 CRA EQU $8005 CONTROL REG A
00102      8006 PRH EQU $8006 PERIPH. REG. H
00103      8006 DDRH EQU $8006 DATA DIRECTION REG H
00104      8007 CRH EQU $8007 CONTROL REG. H
00105 *****
RT1 MOTOROLA M68SAM CROSS-ASSEMBLER

```

```

00107 6000          ORG    $6000
00108                *
00109                *
00110 6000 RD 60A8    JSR    INSET    SET PIA INPUTS.
00111 6003 RD 60E4    JSR    CLRMEM   CLEAR DATA MEMORY.
00112 6006 CE 601A    LDX    =INTVEC
00113 6009 FF A000    STX    $A000
00114 600C 7F 0006    CLR    DVCNT1
00115 600F 7F 0007    CLR    DVCNT2
00116 6012 7F 0017    CLR    IX2      CLEAR PSEUDO-IX.
00117 6015 7F 001A    CLR    IX2+1
00118 6018 0E
00119 6019 3E        WAT
00120                *
00121 601A RD 60F1 INTVEC JSR    A2D1    LOOP TO DIGITIZE.
00122 601D RD 6106    JSR    A2D2
00123 6020 RD 611B    JSR    A2D3
00124 6023 DE 17     LDX    IX2
00125 6025 09        INX
00126 6026 DF 17     STX    IX2
00127 6028 AC 0800   CPX    =80800   THRU DIGITIZING+
00128 6028 2C 07     HGE    A2DEND
00129 602D DE 02     LDX    INDEL
00130 602F RD F0E0   JSR    DELAY
00131 6032 20 E6     HRA    INTVEC
00132                *
00133 6034 RD 6130 A2DEND JSR    AVG
00134 6037 RD 615A    JSR    NORM
00135 603A 7F 0008    CLR    DIVCNT1
00136 603D 3F
00137                *

```

RT1

MOTOROLA M68SAM CROSS-ASSEMBLER

```

00139          ***** ** ** ** **
00140          *
00141 603E CE 2000 MAIN1 LDX  EACCHLK
00142 6041 RD 6167      JSR  MOV16    COPY ACC. DATA INTO
00143          *                               WORK AREA.

00144 6044 RD 6199      JSR  INTGPI    INTEGRATE ONCE.
00145 6047 5D          TST  R        CHECK FOR OVERFLOW
00146 6048 27 09      BEQ  MAIN2
00147 604A 7C 0006    INC  DIVCNT1  DIVCNT1 = NUMBER OF TIMES
00148          *                               ACCELERATION HAS BEEN
00149 604D 96 06      LDA  A  DIVCNT1  DIVIDED BY 2 WHILE
00150          *                               GETTING VELOCITY.
00151 604F 97 08      STA  A  DIVCNT  DIVCNT = SCRATCH.
00152 6051 20 FB      BRA  MAIN1
00153          *
00154 6053 CE 3800 MAIN2 LDX  EVELHLK
00155 6056 RD 618F      JSR  MOV16B   MOVE INTEGRATED ACC. DATA
00156          *                               TO VELOCITY BLOCK.
00157          *
00158 6059 CE 3800 MAIN3 LDX  EVELHLK  MOVE VELOCITY TO
00159 605C RD 6167      JSR  MOV16    WORK AREA.
00160          *
00161 605F RD 6199      JSR  INTGRI
00162 6062 5D          TST  R        OVERFLOW CHECK
00163 6063 27 09      BEQ  MAIN4
00164 6065 7C 0007    INC  DIVCNT2  NO. OF TIMES VEL. WAS
00165 6068 96 07      LDA  A  DIVCNT2  DIVIDED BY 2 WHILE
00166 606A 97 08      STA  A  DIVCNT  GETTING DEPTH.
00167 606C 20 FB      BRA  MAIN3
00168 606E RD 638F MAIN4 JSR  FUDGE    MODIFY RESULTS OF
00169          *                               2ND INTEGRATION.
00170 6071 CE 4000 MAIN5 LDX  EDEPHLK  MOVE INTEGRATED VEL.

```

```

00171 6074 RD 618F      JSR    NOV160    INTO DEPTH.
00172                    *
00173                    *
00174                    *
00175 6077 RD 630C MAIN6 JSR    INVERT    INVERT TIME DELAY TO
RTI                    MOTOROLA M68SAM CROSS-ASSEMBLER

```

```

00176                    *                                GET SOUND SPEED.
00177 607A 3F          S4I
00178                    *
00179                    *
00180                    *      *      *      *      *      *      *      *
00181                    *
00182                    *                                NOW OUTPUT DATA.

```

```

00183                    *
00184 607H RD 61DH      JSR    OUTSET    SET PIA OUTPUTS.
00185 607E 96 00      LDA    A        XSEL    INZ OUTPUT POINTERS.
00186 6080 RD 62A0      JSR    SETHLK
00187 6083 DF 1C      STX    XSCRCH
00188 6085 96 01      LDA    A        YSEL
00189 6087 RD 62A0      JSR    SETHLK
00190 608A DF 1E      STX    YSCRCH
00191 608C RD 6285      JSR    PNSTRI    INZ PEN POSITION.
00192 608F CE 0000     LDX    #0000
00193 6092 DF 17      OUTDTA STX    TX?
00194 6094 RD 61FH      JSR    OUTX      OUTPUT X VALUE.
00195 6097 RD 6220      JSR    OUTY      OUTPUT Y VALUE.
00196 609A DE 04      LDX    OUTDEL
00197 609C RD F0E0      JSR    DELAY
00198 609F DE 17      LDX    TX?
00199 60A1 08          INX
00200 60A2 8C 0800     CPX    #0800    THRU PLOTTING
00201 60A5 20 FH      BLT    OUTDTA
00202 60A7 RD 6269      JSR    PENUP

```

```

00203 60AA 3F          SWI
00204                *
00205                *
00206                *****
00207                *          ***SUBROUTINE TO SET PIA INPUTS,
00208                *          AND INITIALIZE BUFFER POINTERS
00209                *
00210 60AB 7F 8006 INSET CLR   DDRB
00211 60AF 7F 8007          CLR   CRA
00212 60B1 86 FF          LDA   A  E9FF
RTI                MOTOROLA M6800 CROSS-ASSEMBLER

```

```

00213 60B3 87 8006          STA   A  DDRB
00214 60B6 86 14          LDA   A  E914
00215 60B8 87 8007          STA   A  CRA
00216 60BB 7F 8005          CLR   CRA
00217 60BE 7F 8004          CLR   DDRA
00218 60C1 4C          INC   A
00219 60C2 87 8005          STA   A  CRA
00220 60C5 CF 2000          LDX   EACCHLK
00221 60C8 DF 09          STX   ACCIA
00222 60CA CE 2800          LDX   ETDRLK
00223 60CD DF 08          STX   TDIX
00224 60CF CE 3000          LDX   EAMPBLK
00225 60D2 DF 00          STX   AMPIX
00226 60D4 CE 3800          LDX   EVELBLK
00227 60D7 DF 0F          STX   VELIX
00228 60D9 CE 4000          LDX   EDPBRLK
00229 60DC DF 11          STX   DEPIX
00230 60DE CF 4800          LDX   ESSHLK
00231 60F1 DF 13          STX   SSIX
00232 60F3 34          RTS
00233                *

```


00234
00235
RTI

*
*
MOTOROLA M68SAM CROSS-ASSEMBLER

```
00237      ****
00238      *          SUBROUTINE TO CLEAR ALL OF DATA MEMORY
00239 60F4 CE 2000 CLRMEM LDX      EACCHLK
00240 60F7 4F          CLR A
00241 60F8 A7 00     ZLOOP STA A  0*X
00242 60FA 08          INX
00243 60FB 8C 6000          CPX      EFIN
00244 60FE 20 F8          HLT      ZLOOP
00245 60F0 39          RTS
00246      *
00247      *
00248      *
00249      ****
00250      *          **SUBROUTINE TO GET ONE ACC. DATUM.**
00251 60F1 DE 09     A201 LDX      ACCIX
00252 60F3 86 1E          LDA A  E01E
00253 60F5 87 8006          STA A  PR8
00254 60F8 86 06          LDA A  =806
00255 60FA 87 8006          STA A  PR8
00256 60FD 86 8004          LDA A  PR4
00257 6100 A7 00          STA A  0*X
00258 6102 08          INX
00259 6103 DF 09          STX      ACCIX
00260 6105 39          RTS
00261      *
```

00262
RT1

*
MOTOROLA M68SAM CROSS-ASSEMBLER

```
00264 *****
00265 * **SUBROUTINE TO GET ONE TIME DELAY DATUM.**
00266 * **IX RETURNS INCREMENTED.**
00267 6106 DE 08 A2D2 LDX T0IX
00268 6108 R6 3E LDA A E3F
00269 610A R7 8006 STA A PR8
00270 610D R6 26 LDA A E26
00271 610F R7 8006 STA A PR8
00272 6112 R6 8004 LDA A PR4
00273 6115 A7 00 STA A 00X
00274 6117 08 INX
00275 6118 DF 08 STX T0IX
00276 611A 39 RTS
00277 *
00278 *
00279 *****
00280 * **SUBROUTINE TO GET ONE AMPLITUDE DATUM.**
00281 * **IX RETURNS INCREMENTED.**
00282 6118 DE 0D A2D3 LDX AMPIX
00283 611D R6 5E LDA A E5E
00284 611F R7 8006 STA A PR8
00285 6122 R6 46 LDA A E46
00286 6124 R7 8006 STA A PR8
00287 6127 R6 8004 LDA A PR4
00288 612A A7 00 STA A 00X
00289 612C 08 INX
00290 612D DF 0D STX AMPIX
00291 612F 39 RTS
00292 *
```

00293
00294
RTI

*
*
MOTOROLA M6800 CROSS-ASSEMBLER

```
00296 *****
00297 * **SUBROUTINE TO FIND AVG. OF LAST 64
00298 * **ACCELERATION VALUES. RESULTS

00299 * **RETURNED IN B REG.
00300 6130 7F 001A AV6 CLR AVGLSB
00301 6133 7F 0019 CLR AVGMSB
00302 6136 CE 2800 LDX =DIRLK
00303 6139 C6 40 LDA H =64
00304 613B 09 AVGLP1 DEX
00305 613C A6 00 LDA A 0*X
00306 613E 9B 1A ADD A AVGLSB
00307 6140 97 1A STA A AVGLSB
00308 6142 24 03 BCC DECNTX
00309 6144 7C 0019 INC AVGMSB
00310 6147 5A DECNTX DEC R
00311 6148 26 F1 BNE AVGLP1
00312 * *****NOW SHIFT RIGHT 5 PLACES.***
00313 614A C6 06 LDA H =06
00314 614C 74 0019 AVGLP2 LSR AVGMSB
00315 614F 76 001A ROR AVGLSB
00316 6152 5A DEC R
00317 6153 26 F7 HNE AVGLP2
00318 6155 D6 1A LDA H AVGLSB
00319 6157 39 RTS
```

00320
00321

*
*

RT1

MOTOROLA M68SAM CROSS-ASSEMBLER

00323
00324
00325
00326
00327

*

*
*
*

***SUBROUTINE TO NORMALIZE ACC. DATA.**
***ENTRY: R REG. CONTAINS RESULT OF
***AVG. SUBROUTINE.

00328 6158 CE 2000
00329 6158 A6 00
00330 615D 10
00331 615E A7 00
00332 6160 08
00333 6161 8C 2800
00334 6164 2D F5
00335 6166 39

NORM LDX =ACCHLK
NORM1 LDA A 0*X
SHA
STA A 0*X
INX
CPX =TDRLK
BLT NORM1
RTS

00336
00337
00338

*
*
*

00339

**SUBROUTINE TO MOVE ANY 2K BYTES
**OF 8 BIT WORDS INTO AN AREA OF
**4K 16 BIT WORDS CALLED SCR16.
**STARTING ADDRESS OF 8 BIT BLOCK
**IS PASSED IN IX. MSB IS
**STORED FIRST.

00340
00341
00342
00343
00344
00345
00346 6167 DF 17
00347 6169 CE 5000
00348 616C DF 15
00349 616E DE 17
00350 6170 A6 00

MOV16 STX IX2
LDX =SCR16
STX IX16
M1 LDX IX2
LDA A 0*X

00351
00352
00353
00354
00355
00356

*
*
*
*
*
*

**NOW TEST DIVCNT. IF DIVCNT NOT
**EQUAL TO 0, A PREVIOUS OPERATION
**ON THE 16 BIT DATA HAS OVERFLOWED.
**NOW THE 16 BIT BLOCK IS RELOADED
**AND EACH VALUE IS SHIFTED RIGHT THE
**NO. OF PLACES IN DIVCNT.

```

00357 6172 7D 0008      TST      DIVCNI
00358 6175 27 06      HFQ      M3
00359 6177 06 08      LDA R    DIVCNI
RTI
MOTOROLA M68SAM CROSS-ASSEMBLER

```

```

00360 6179 47          M2      ASR A
00361 617A 5A          DEC H
00362 617B 26 FC          BNE     M2
00363 617D 48          M3      ASL A      CHECK SIGN.
00364 617E 24 04          HCC     M4
00365 6180 C6 FF          LDA H   2>FF    B=SIGN EXTENSION.
00366 6182 20 01          HRA     M5
00367 6184 5F          M4      CLR B
00368 6185 46          M5      ROR A
00369 6186 08          INX
00370 6187 0F 17          STX     IX2
00371 6189 0F 15          LDA     IX16
00372 618B E7 00          STA H   00X
00373 618D 08          INX
00374 618E A7 00          STA A   00X
00375 6190 08          INX
00376 6191 0F 15          STX     IX16
00377 6193 8C 6000        CPX     6000
00378 6196 2D 06          HLT     M1
00379 6198 39          RTS
00380          *
00381          *
10382          *
RTI
MOTOROLA M68SAM CROSS-ASSEMBLER

```

```

00384
00385
00386
00387
00388
00389 6109 0F 6000 INTGRT LDX      EFIN
00390 610C 0F 15      STX      IX16
00391 610E 09      DEX
00392 610F 09      DEX
00393 6110 09      DEX
00394 6111 09      DEX
00395 6112 5F      CLR  R
00396 6113 A6 03  I1  LDA  A  3*X
00397 6115 A8 01      ADD  A  1*X      ADD L.S. BYTES
00398 6117 A7 01      STA  A  1*X
00399 6119 A6 02      LDA  A  2*X
00400 611B A9 00      ADC  A  0*X      ADD MS BYTES.
00401 611D 28 04      HVC  12      OVERFLOW*
00402 611F C6 FF      LDA  B  2*FF
00403 6121 70 08      BRA  13
00404 6123 A7 00  I2  STA  A  0*X
00405 6125 09      DEX
00406 6126 09      DEX
00407 6127 0F 15      STX      IX16
00408 6129 8C 5000  CPX      ESCR16
00409 612C 2C F5      BGE  11
00410 612E 39      13  RTS
00411
00412
00413
RTI

```

MOTOROLA M68SAM CROSS-ASSEMBLER

```

00415 *****
00416 *                               **SUBROUTINE TO MOVE MOST SIGNIF.
00417 *                               **BYTES FROM 16 BIT DATA BLOCK
00418 *                               **TO 8 BIT WORD DATA BLOCK
00419 *                               **WITH STARTING ADDRESS PASSED
00420 *                               **IN IA.
00421 61rF DF 17  MOV16r STX   IA2
00422 61r1 CE 5000 LDX   =SCR16
00423 61r4 DF 15   STX   IX16
00424 *
00425 61r6 A6 00  MH1   LDA  A  0*x
00426 61r8 0R     INX
00427 61r9 0R     INX
00428 61rA DF 15   STX   IX16
00429 61rC DE 17   LDX   IX2
00430 61rE A7 00   STA  A  0*x
00431 61n0 0R     INX
00432 61n1 DF 17   STX   IA2
00433 61n3 DE 15   LDX   IX16
00434 61n5 8C 6000 CPX   =FIN
00435 61n8 2D FC   BLT   MH1
00436 61nA 39     RTS
00437 *
00438 *
00439 *
RTI                               MOTOROLA M68SAM CROSS-ASSEMBLER

```

```

00441          *****
00442          *                               **SUBROUTINE TO SET PIA OUTPUTS.
00443 610B 7F R005 OUTSET CLR     CRA
00444 610E 7F R007          CLR     CRH
00445 61F1 86 FF          LDA A   E$FF
00446 61F3 87 R004          STA A   DDRB
00447 61F6 87 R006          STA A   DDRH
00448 61F9 86 17          LDA A   E$17
00449 61FB 87 R005          STA A   CRA
00450 61FF 86 14          LDA A   E$14
00451 61F0 87 R007          STA A   CRH
00452 61F3 86 R0          LDA A   E$R0
00453 61F5 97 1B          STA A   XTOUT   INITIAL TIME VALUE.
00454 61F7 39          RTS

00455          *
00456          *
00457          *
00458          *****
00459          *                               **SUBROUTINE TO OUTPUT 1 BYTE
00460          *                               **FROM REG. A TO X-AXIS WITH
00461          *                               **PEN DOWN.
00462 61FB 96 1C          OUTX   LDA A   XSCRCH
00463 61FA 27 09                   BEQ    OUT1
00464 61FC DE 1C                   LDX    XSCRCH
00465 61FE A6 00                   LDA A   0.0
00466 6200 08                   INX
00467 6201 DF 1C                   STX    XSCRCH
00468 6203 20 05                   BRA    OUTX
00469 6205 96 1B          OUT1   LDA A   XTOUT
00470 6207 7C 001B                   INC    XTOUT
00471          *                               NOW OUTPUT ONE BYTE FROM REG. A
00472          *                               TO X-AXIS WITH PEN DOWN.

```



```

00473 620A B7 8004 OUT1X STA A 000A
00474 620D 86 08 LDA A 0000
00475 620F B7 8006 STA A 0004
00476 6212 63 00 COM 00X THESE 4 COMPLETES
00477 6214 63 00 COM 00X KILL 7 CYCLES EACH
RTI MOTOROLA M6800 CROSS-ASSEMBLER

```

```

00478 6216 63 00 COM 00X WHILE D TO A CONV.
00479 6218 63 00 COM 00X AND S-H SETTLE.
00480 621A 86 0F LDA A 000F
00481 621C B7 8006 STA A 0004
00482 621F 39 RTS
00483 *
00484 *
00485 *
00486 *
00487 *****
00488 *
00489 * RESUBROUTINE TO OUTPUT 1 GATE
00490 * FROM REG. A TO Z-AXIS.
00491 *
00492 6220 DF 1E OUT1Y LDA YSCRCH
00493 6222 A6 00 LDA A 00X
00494 6224 D6 1C LDA B XSCRCH X AXIS = 1111*
00495 6226 76 16 HNE OUT1Y3
00496 6228 C6 08 LDA B 008 THIS IS TO ADD 8
00497 622A D8 18 ADD B IX2+1 TO THE IX2 INDEX
00498 622C D7 18 STA B IX2+1 IF X=1111.
00499 622E 24 03 HCC OUT1Y2
00500 6230 7C 0017 INC IX2
00501 6232 C6 08 OUT1Y2 LDA B 008
00502 6234 D8 1F ADD B YSCRCH+1 LIKEWISE WITH
00503 6236 D7 1F STA B YSCRCH+1 Y INDEX.
00504 6238 24 03 HCC OUT1Y3

```

```

00505 6238 7C 001E      INC      YSCRCH
00506                      *
00507 623E DF 1E      OUTY3  LDX      YSCRCH
00508 6240 08          INX
00509 6241 DF 1E      STX      YSCRCH
00510                      *
00511                      *      OUTPUT 1 BYTE FROM REG. A
                                TO Y AXIS. PEN DOWN.
00512 6243 B7 R004  OUTLY  STA  A  PRA
00513 6246 B6 0D      LDA  A  E$0D
00514 6248 B7 R006      STA  A  PRR
RTI                      MOTOROLA M68SAM CROSS-ASSEMBLER

```

```

00515 6248 63 00      COM      0*X      WAITING HERE FOR
00516 624D 63 00      COM      0*X      D TO A AND S-H
00517 624F 63 00      COM      0*X      TO SETTLE.
00518 6251 63 00      COM      0*X
00519 6253 B6 0F      LDA  A  E$0F
00520 6255 B7 R006      STA  A  PRR
00521 6258 39          RTS
00522                      *
00523                      *
00524                      *

```

RT1

MOTOROLA M68SAM CROSS-ASSEMBLER

```
00526                                     *****
00527                                     *                               **SUBROUTINE TO OUTPUT REG. A
00528                                     *                               **TO X-AXIS. PEN UP.
00529 6259 R7 R004 OUTIXU STA A PRA
00530 625C R6 03                               LDA A E03
00531 625E R7 R006                               STA A PRR
00532 6261 63 00                               COM 00X           TIME KILLING HERE.
00533 6263 63 00                               COM 00X
00534 6265 63 00                               COM 00X
00535 6267 63 00                               COM 00X
00536 6269 86 07 PENIJP LDA A E07           HERE TO LEFT PEN.
00537 626R R7 R006                               STA A PRR
00538 626E 39                               RTS
00539                                     *
00540                                     *
00541                                     *****
00542                                     *                               **SUBROUTINE TO OUTPUT REG. A
00543                                     *                               **TO Y-AXIS. PEN UP.
00544 626F R7 R004 OUTIYL STA A PRA
00545 6272 R6 05                               LDA A E05
00546 6274 R7 R006                               STA A PRR
00547 6277 63 00                               COM 00X           KILLING TIME...
00548 6279 63 00                               COM 00X
00549 627B 63 00                               COM 00X
00550 627D 63 00                               COM 00X
00551 627F 86 07                               LDA A E07
00552 6281 R7 R006                               STA A PRR
00553 6284 39                               RTS
00554                                     *
00555                                     *
00556                                     *****
00557                                     *                               **SUBROUTINE TO INITIALIZE PEN
```

00558				*		**POSITION.
00559	62A5	96	1C	PNSTR1	LDA A	XSCRCH
00560	62A7	26	04		HNE	P1
00561	62A9	A6	80		LDA A	E\$R0
00562	62AH	20	04		HRA	P2
RT1				MOTOROLA M68SAM CROSS-ASSEMBLER		

00563	62AD	DE	1C	P1	LIX	XSCRCH
00564	62AF	A6	00		LDA A	0*X
00565	6291	80	C6	P2	BSR	OUT1XU
00566	6293	DE	1E		LIX	YSCRCH
00567	6295	A6	00		LDA A	0*X
00568	6297	80	D6		BSR	OUT1YU
00569	6299	CE	FFFF		LIX	E\$FFFF
00570	629C	80	FUEU		JSR	DELAY
00571	629F	39			RTS	

00572
00573
RTI

*
*
MOTOROLA M68000 CROSS-ASSEMBLER

```
00575 *****
00576 *                               **SUBROUTINE TO INITIALIZE INDEX
00577 *                               **DEPENDING ON DESIRED OUTPUT
00578 *                               **BLOCK. REG. A CONTAINS EITHER
00579 *                               **ASEL OR YSEL.
00580 62A0 CE 62A9 SELHLK LDX      LDTRL-2
00581 62A3 08      SI        INX
00582 62A4 08      INX
00583 62A5 4A      DEC A
00584 62A6 26 FB      HNE      SI
00585 62A8 EE 00      LDX      0*x
00586 62AA 39      RTS
00587 62AB 2000      LDTRL    FDB      $2000
00588 62AD 2800      FDB      $2800
00589 62AF 3000      FDB      $3000
00590 62B1 3800      FDB      $3800
00591 62B3 4000      FDB      $4000
00592 62B5 0000      FDB      0000
00593 62B7 4800      FDB      $4800
00594 *
00595 *
00596 *****
00597 *
00598 *                               SUBROUTINE TO DIVIDE AN UNSIGNED 4 DIGIT
00599 *                               HEX NUMBER (16 BIT BINARY) BY AN UNSIGNED
00600 *                               2 DIGIT HEX NUMBER (8 BIT BINARY).
00601 *                               THE DIVISOR AND THE DIVIDEND MUST BE
00602 *                               LOADED INTO XKDVR AND XKDND(XKDND+1)
00603 *                               RESPECTIVELY. THEN JSR TO XKDVID.
00604 *                               THE REMAINDER WILL BE IN XKDND,
00605 *                               SHIFTED LEFT THE E OF BITS INDICATED IN
00606 *                               XKDSPL. THE DIVISOR WILL BE
00607 *                               BINARYLY LEFT JUSTIFIED.
00608 *
```

```

00609 62R9 C6 08   XKDIVD LDA R   E08   INITIAL S=8.
00610 62RH 7F 0026   CLR   XKQUOT ZERO QUOTIENT BUFFER
00611 62RE 7F 0027   CLR   XKQUOT+1
RT1      MOTOROLA M68SAM CROSS-ASSEMBLER

```

```

00612 62C1 5C           DVOLP0 INC H
00613 62C2 C1 10           CMP H   E16
00614 62C4 2F 34           HGT   DVDERH IF S>16, DIVIDE ERROR.
00615 62C6 78 0023         ASL   XKDVSR IF S<16 LEFT SHIFT DIVISOR.
00616 62C9 24 F6           HCC   DVOLP0 IF C=0, CONT. LOOP
00617 62CB 07 28           STA R   XKDSPL IF C=1 XKDSPL = SHIFT CNT.
00618 62CD 76 0023         ROR   XKDVSR SHIFT DIVISOR BACK 1 SHIFT
00619           *           COUNT NOW IN ACCR.
00620           *           DIVISOR LEFT JUST. IN X
00621 62D0 96 24           LDA A   XKDVND
00622 62D2 91 23   DVOLP1 CMP A   XKDVSR IF DIVIDEND < DIVISOR
00623 62D4 25 0D           HCS   DVNSUB DON'T SUBTRACT.
00624 62D6 0D           DVOLP2 SEC   IF THE DIVIDEND >OR= DIVISOR
00625 62D7 79 0027         ROL   XKQUOT+1 SHIFT LEFT 1 BIT.
00626 62DA 79 0026         ROL   XKQUOT WITH LSH = 1.
00627 62DD 90 23           SUB A   XKDVSR Y(M)=Y(M)-X
00628 62DF 97 24           STA A   XKDVND
00629 62F1 20 07           BRA   DVSHFT
00630 62F3 0C           DVNSUB CLC   SHIFT Q LEFT WITH
00631 62F4 79 0027         ROL   XKQUOT+1 LSH=0
00632 62F7 79 0026         ROL   XKQUOT
00633 62FA 5A           DVSHFT DEC R   S= S-1
00634 62FB 27 12           BEQ   DVDFND IF S=0 STOP
00635 62FD 0C           CLC   IF S>0 SHIFT DIVIDEND
00636 62FE 79 0025         ROL   XKDVND+1 LEFT 1 BIT, LSH=0.
00637 62F1 79 0024         ROL   XKDVND MSB INTO CARRY.
00638 62F4 96 24           LDA A   XKDVND

```

```

00639 62F6 25 DE          RCS      DVDLP2      IF C=1 GO TO LOOP2.
00640 62F8 20 DB          HRA      DVDLP1
00641 62FA CE FFFF DVDERR LDX      =FFFF
00642 62FD DF 26          STX      XKQ101
00643 62FF D6 28          DVDEND LDA      XKD5PL      GET SHIFT CNT INTO
00644 6301 C0 09          SU4      =9      ACCR. XKD5PL=XKD5PL-9.
00645 6303 C1 04          CMP      =4      XKD5PL < 4?
00646 6305 25 02          RCS      DVDLP3      YES...RETURN
00647 6307 C0 04          SU4      =4      NO...XKD5PL=XKD5PL-4

```

```

00648 6309 D7 28          DVDLP3 STA      XKD5PL      DISPLACEMENT OF
RTI                          MOTROLA M68SAM CROSS-ASSEMBLER

```

```

00649                      *          REMAINDER STORED IN XKD5PL.
00650 630B 39          *          RTS
00651                      *
00652                      *
00653                      *
00654                      *
00655                      *
00656                      *
00657                      * *****
00658                      *          SUBROUTINE TO INVERT ENTIRE TIME.
00659                      *          DELAY DATA BLOCK AND PUT IT IN
00660                      *          SOUND SPEED BLOCK (SSBLK). LEAVING
00661                      *          TIME DELAY DATA INTACT.
00662                      *
00663 630C CE 2800 INVERT LDX      =IDBLK
00664 630F DF 08          STX      =IX
00665 6311 CF 5000          LDX      =SCR16
00666                      *          ADDING =XRO MAKES ALL VALUES
00667                      *          UNSIGNED IN PREPARATION FOR
00668                      *          DIVISION.
00669 6314 DF 15          INV1  STX      =X16
00670 6316 DF 0B          LDX      =IX

```

00671	631A	A6	00	LDA	A	0*X
00672	631A	AA	80	ADD	A	=580
00673	631C	0A		INX		
00674	631D	0F	0B	STX		101X
00675	631F	97	23	STA	A	XKDVSH
00676	6321	CE	FFFF	LDX		=FFFFF
00677	6324	DF	24	STX		XKDVND
00678	6326	8D	6289	JSR		XKDIVD
00679	6329	DE	15	LDX		1X16
00680	632H	96	26	LDA	A	XKQUOI
00681	632D	A7	00	STA	A	0*X
00682	632F	0A		INX		
00683	6330	96	27	LDA	A	XKQUOI+1
00684	6332	A7	00	STA	A	0*X
00685	6334	0A		INX		
RTI						

MOTOROLA M68SAM CROSS-ASSEMBLER

00686	6335	8C	6000	CPX		FIN
00687	6338	2D	DA	HLT		INV1
00688			*			
00689			*			LOOK FOR BIGGEST RESULT.
00690	633A	CE	5000	LDX		=SCRIB
00691	633D	0F	15	STX		1X16
00692	633F	EE	00	LDX		0*X 1ST VALUE INTO BIGGEST.
00693	6341	0F	2H	STX		BIGGEST
00694			*			
00695			*			TEST OTHER VALUES.
00696	6343	DE	15	INV2	LDX	1X16
00697	6345	8C	6000	CPX		FIN
00698	6348	2E	0E	HGT		INV3
00699	634A	0A		INX		
00700	634B	0A		INX		
00701	634C	DF	15	STX		1X16
00702	634E	FF	00	LDX		0*X


```

00703 6350 9C 28      CPX      RIGGS1
00704 6352 2D FF      HLT      INV2
00705 6354 0F 28      STX      RIGGS1
00706 6356 20 FB      BPA      INV2
00707
00708
00709
00710 6358 C6 FF      INV3    LDA B  E3FF
00711 635A 0C          CLC
00712 635B 96 28      LDA A  RIGGS1
00713 635D 5C          INV4    INC H
00714 635E 48          ASL A
00715 635F 24 FC      BCC     INV4
00716 6361 D7 08      STA H  SCNT
00717
00718 6363 CE 5000     LDX     -SCRIP
00719
00720
00721 6366 D6 08      INV5    LDA B  SCNT
00722 6368 27 07      INV6    BEQ   INV7
RTI
MOTOROLA M68SAM CROSS-ASSEMBLER

```

```

00723 636A 68 01      ASL     1*x
00724 636C 69 00      ROL     0*x
00725 636E 5A          DEC H
00726 636F 20 F7      BRA     INV6
00727
00728 6371 08          INV7    INX
00729 6372 08          JNX
00730 6373 8C 6000     CPX     =FIN
00731 6376 2D FE      HLT     INV5
00732
00733
00734
          ADDING =EB0 PREPARES DATA
          FOR OUTPUT.

```

```

00735 637A CF 4800      LDX      =SSBLK
00736 637B RD 612F      JSR      =CV160
00737 637E C6 80        LDA      =980
00738 63A0 CF 4800      LDX      =SSBLK
00739 63A3 A6 00      INVR     LDA      1*X
00740 63A5 1A          ABA
00741 63A6 A7 00      STA      0*X
00742 63A8 0A          INX
00743 63A9 8C 5000     CPX      =5000
00744 63AC 2D F5       HLT      INVR
00745 63AE 39          RTS

```

```

00746
00747
00748
00749
00750
00751
00752
00753
00754
00755
00756
00757
00758
00759
RTI

```

```

*
*      SUBROUTINE TO CHANGE RESULTS OF VELOCITY
*      INTEGRATION SO THAT BOTH POS. AND NEG NUMBERS
*      ARE OUTPUT. THIS ALLOWS BETTER HORIZONTAL RES-
*      OLUTION WHEN DEPTH IS USED AS X-AXIS. EACH BYTE
*      IS SHIFTED LEFT. AND ALL MS BYTES ARE SEARCHED
*      FOR THE LARGEST POS. VALUE. THIS VALUE IN THE
*      R REG. IS SUBTRACTED FROM ALL OTHERS AND 87E IS
*      ADDED TO ALL.

```

MOTOROLA M6800 CROSS-ASSEMBLER

```

00760 63AF 5F          FUDGE  CLR      R
00761 63B0 CF 5000     LDX      =5000
00762 63B3 6A 01      FUDGE  ASL      1*X
00763 63B5 69 00      ROL
00764 63B7 E1 00      CMPS   0*X

```

```

00765 6399 2A 02      RPL      FUD2
00766 639H F6 00      LDA R    0*X
00767 639D 08          INX
00768 639E 08          INX
00769 639F 8C 6000     CPX      =FIN      FOUND BIGGEST YET
00770 63A2 2D FF      HLT      FUD1
00771 63A4 CE 5000     LDX      =SCR16
00772 63A7 A6 00      FUD3     LDA A    0*X
00773 63A9 10          SHL
00774 63AA 8B 7F      ADD A    =87F      ADD OFFSET.
00775 63AC A7 00      STA A    0*X
00776 63AE 08          INX
00777 63AF 08          INX
00778 63B0 8C 6000     CPX      =FIN
00779 63B3 2D F2      HLT      FUD3
00780 63B5 39          RTS
00781
00782
00783
00784
00785
*****
      FND)

```

RT1

MOTOROLA M68SAM CROSS-ASSEMBLER

SYMBOL TABLE

DELAY	EAEO	ACCBLK	2000	TDBLK	2800	AMPBLK	3000	VFLBLK	3800
DEPRLK	4000	SSBLK	4800	SCR16	5000	TIME	0000	FIN	6000
XSEL	0000	YSEL	0001	INDEF	0002	OUTDEL	0004	DVCNT1	0006
DVCNT2	0007	DIVCNT	0008	SCNT	0008	ACCIX	0009	TDIX	0008
AMPIX	0000	VFLIX	000F	DEPIX	0011	SSIX	0013	IX16	0015
IX2	0017	AVGMSB	0019	AVG1SB	001A	XTOU1	001H	XSCRCH	001C
YSCRCH	001E	IX3	0020	NEGFLG	0022	XKOVSR	0023	XKOVND	0024
XKQUOT	0026	XKDSPL	0028	INITX	0029	INITY	002A	RIGGST	002F
CRA	8004	DDRA	8004	CRA	8005	PRH	8006	DDRB	8006
CRB	8007	INTVEC	601A	A2DFND	6034	MAIN1	603E	MAIN2	6053
MAIN3	6059	MAIN4	606E	MAIN5	6071	MAIN6	6077	OUTDIA	6092
NSFT	60AH	CLRMEM	60E4	ZLOOP	60E8	A2D1	60F1	A2D2	6106
203	611H	AVG	6130	AVGLP1	6138	DEFCTR	6147	AVGLP2	614C
ORM	6158	NORM1	6158	MOV16	6167	M1	616E	M2	6179
3	6170	M4	6184	M5	6185	INTGRT	6199	I1	61A3
2	61B3	I3	619E	MOV16B	61BF	MRI	61C6	OUTSET	61D8
ITX	61F8	OUT1	6205	OUT1X	620A	OUTY	6220	OUTY2	6233
ITY3	623E	OUT1Y	6243	OUT1XU	6259	PFNDP	6269	OUT1YU	626F
NSTRT	6285	P1	6280	P2	6291	SFLBLK	62A0	S1	62A3
OTHL	62AH	XKDIVD	62R9	DVDLPI	62C1	DVDLPI	62D2	DVDLP2	62D5
INSUB	62E3	DVSHFT	62FA	DVDPRH	62FA	DVDEND	62FF	DVDLP3	6300
INVERT	630C	INV1	6314	INV2	6343	INV3	6358	INV4	635D
NV5	6366	INV6	6368	INV7	6371	INV6	6383	FUDGE	638F
IDI	6393	FUD2	639D	FUD3	63A7				

.00.18.UCLP. AA31.

1.00RKLNS.

JUMP TO SUBROUTINE

6000

JSR INSET TO SET
PIA INPUTS

JSR CLRMEM

STORE INTERRUPT VECTOR
AT \$A000

CLEAR INTEGRATION
OVERFLOW COUNTS
DVCNT1, DVCNT2

CLEAR IX2

CLEAR INTERRUPT FLAG
WAIT FOR INTERRUPT

601A

JSR TO DIGITIZE
SUBROUTINES

LDX IX2

INX

STX IX2

THROUGH
DIGITIZING?
IX = \$400?

YES

NO

LDX INDEL, JSR DELAY

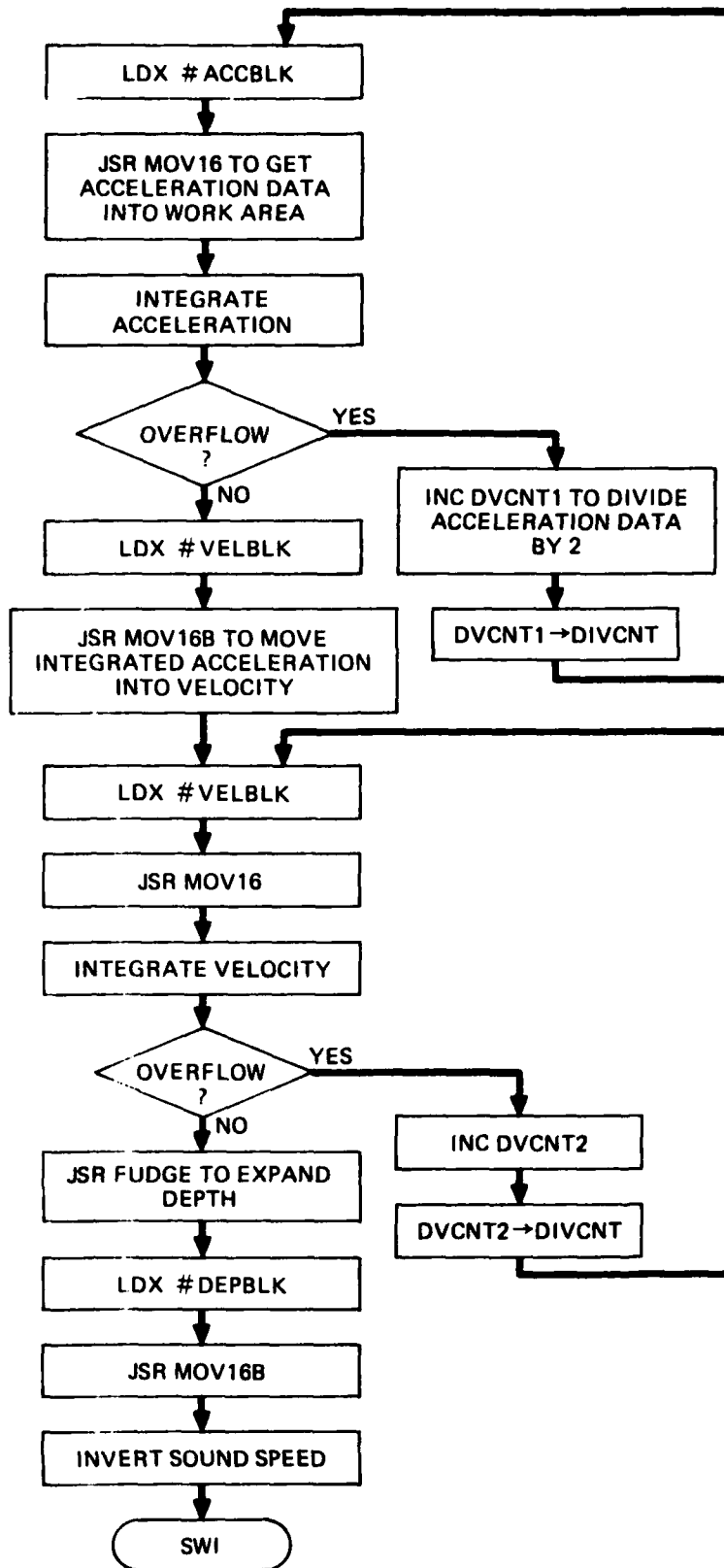
6034

JSR AVG

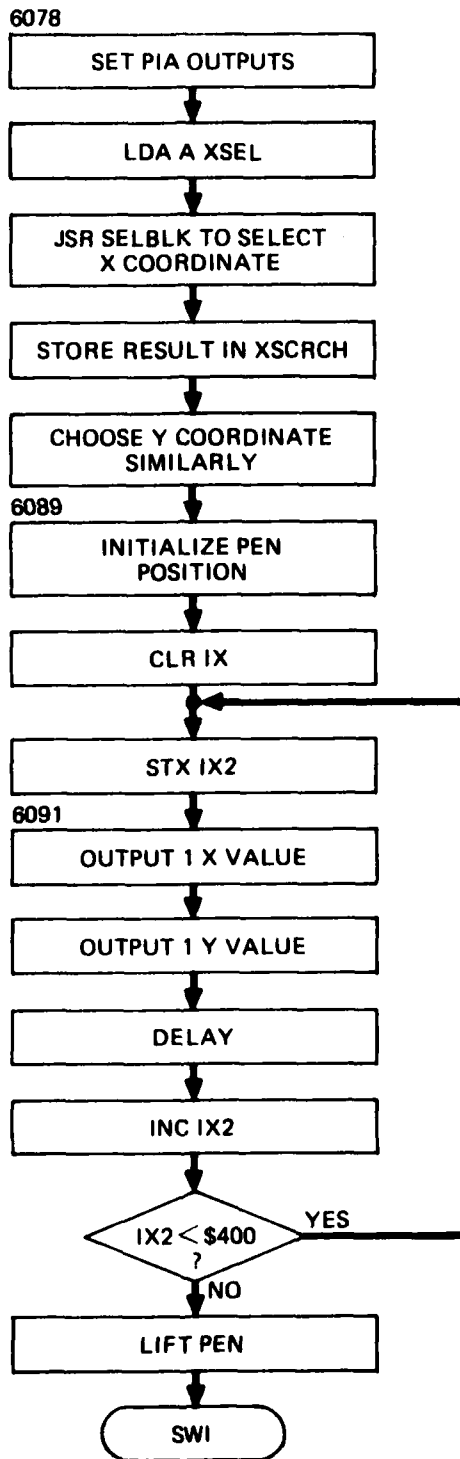
JSR NORM (NORMALIZE
ACCELERATION)

SWI

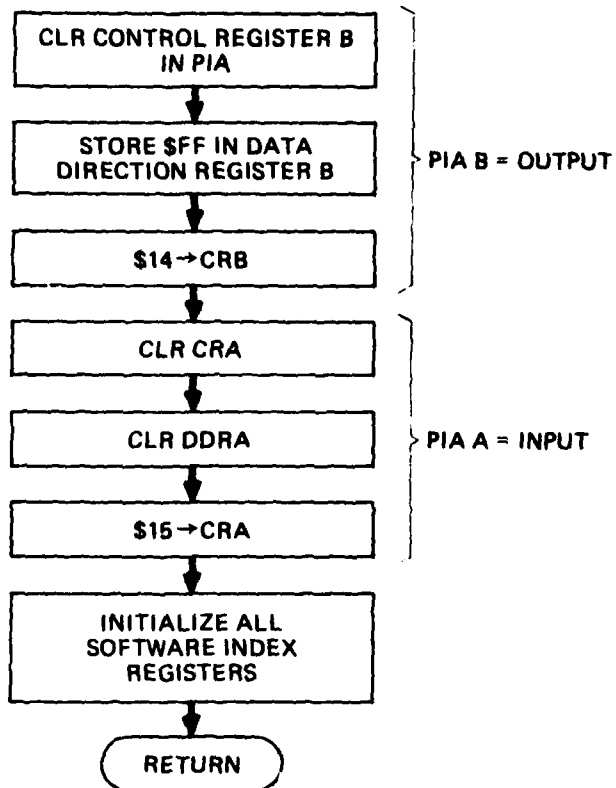
MAIN PROGRAM



MAIN PROGRAM (Cont'd)

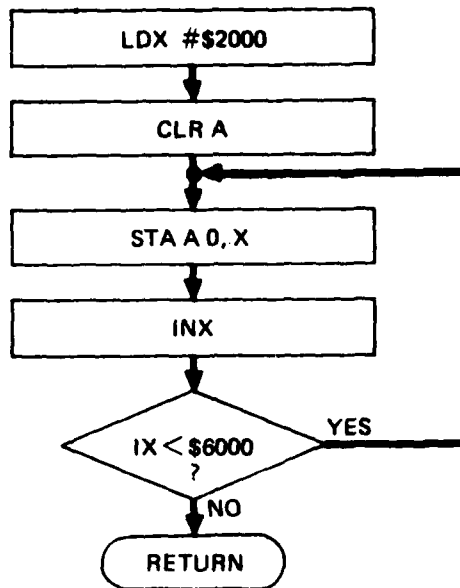


MAIN PROGRAM (Cont'd)

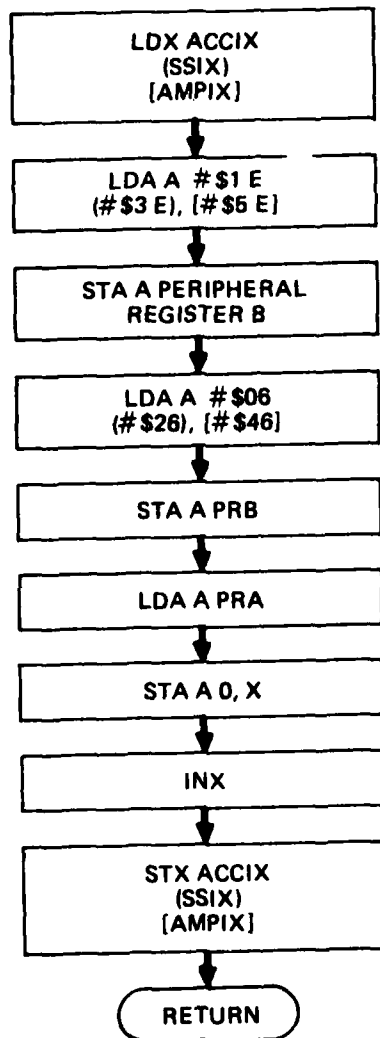


SUBROUTINE INSET

ARL:UT
AS-81-858
RTT - GA
8-3-81

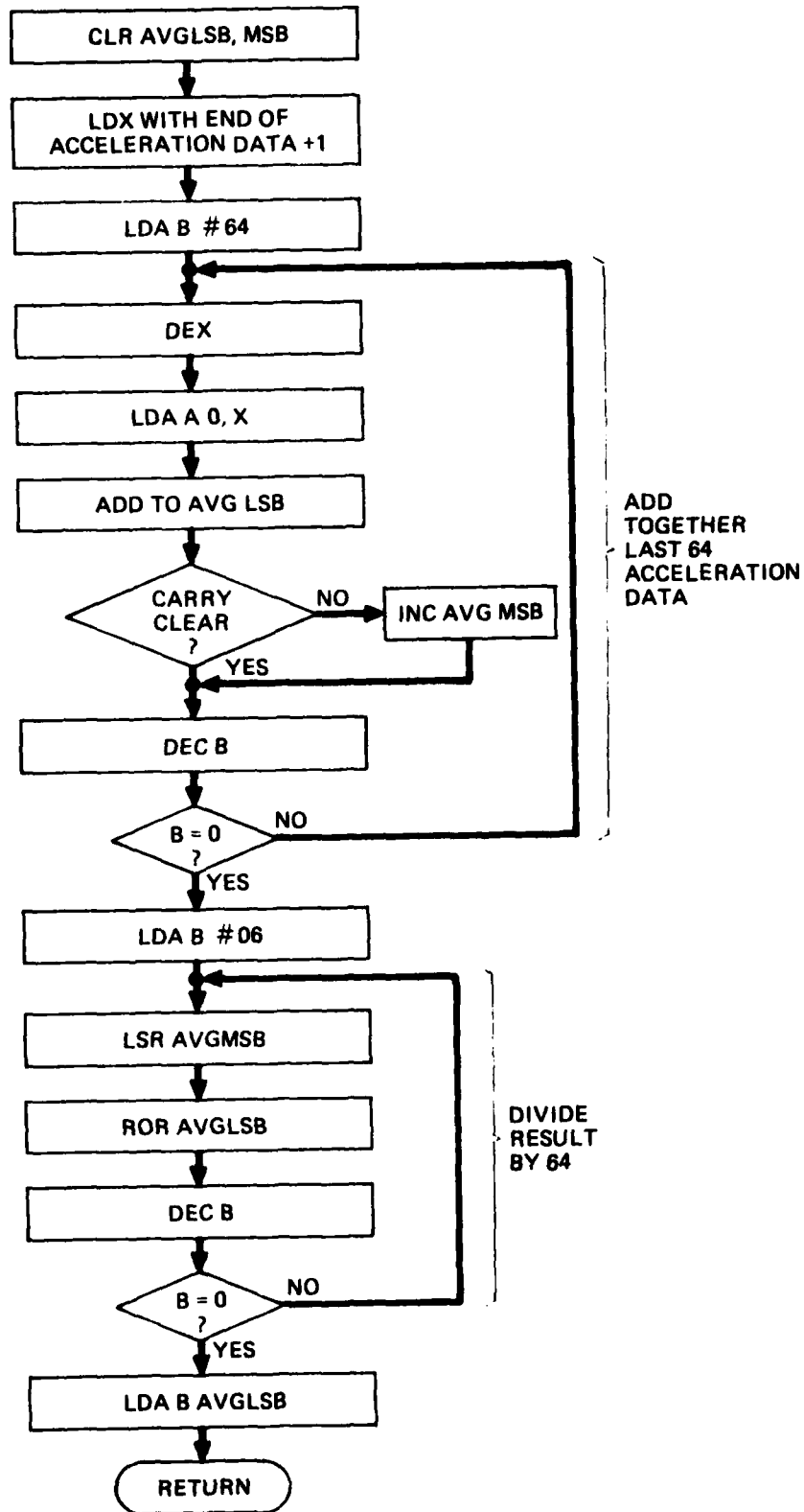


SUBROUTINE CLRMEM

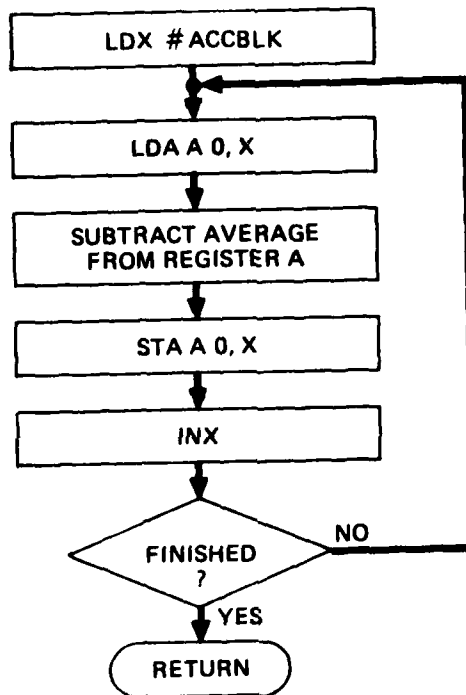


SUBROUTINES A2D1,
(A2D2), [A2D3]

ARL:UT
AS-81-880
RTT - GA
8-3-81

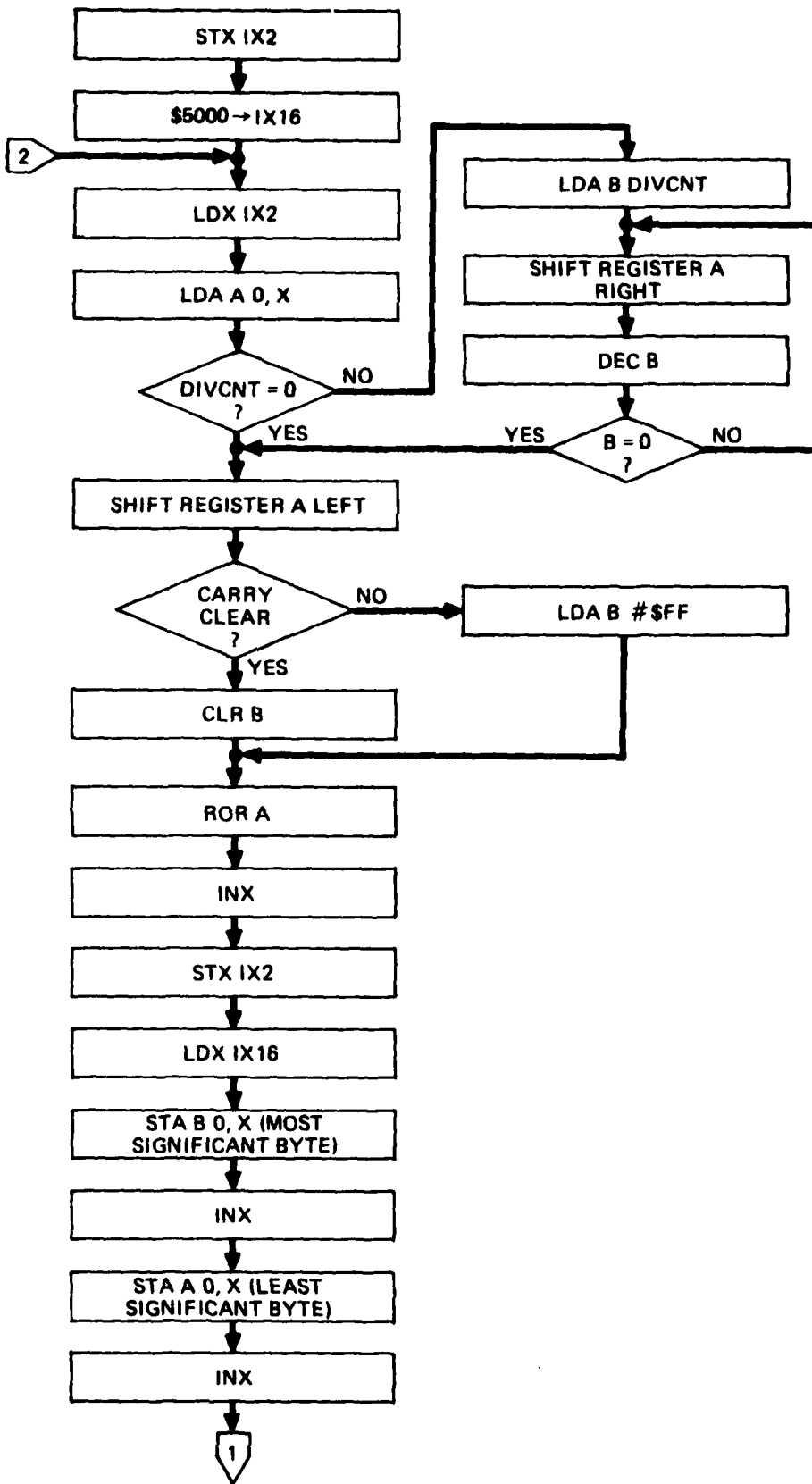


SUBROUTINE AVG



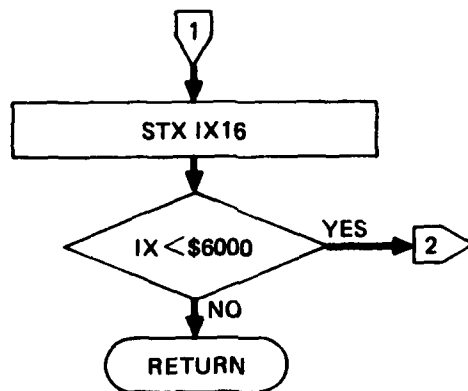
SUBROUTINE NORM

ARL:UT
AS-81-982
RTT - GA
8-3-81

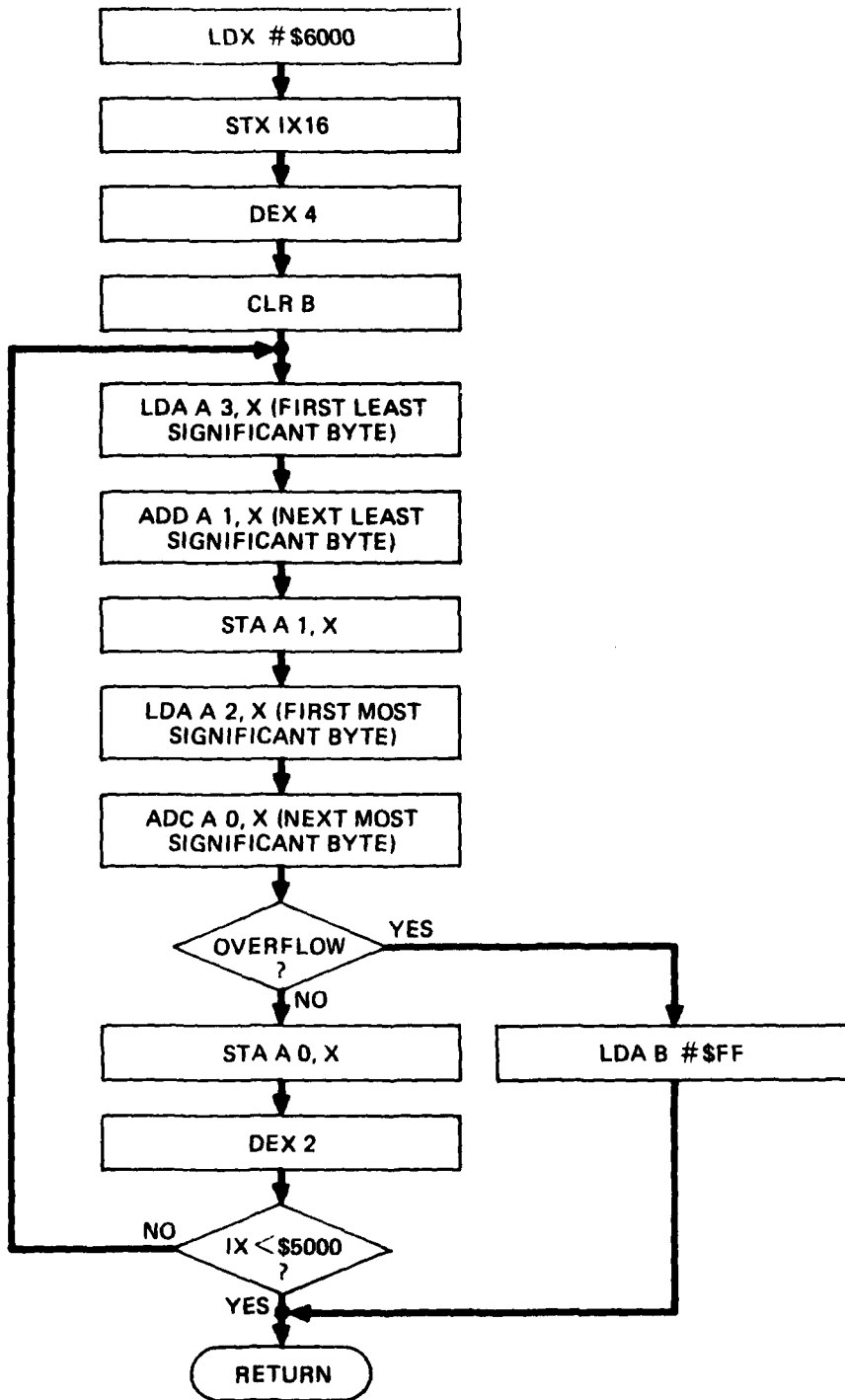


SUBROUTINE MOV16

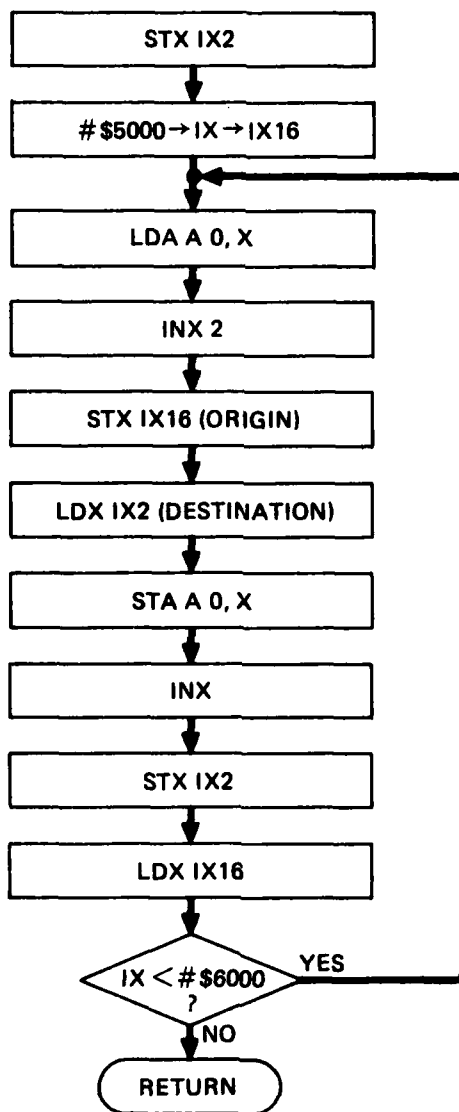
ARL:UT
AS-81-883
RTT - GA
8-3-81



SUBROUTINE MOV16 (Cont'd)

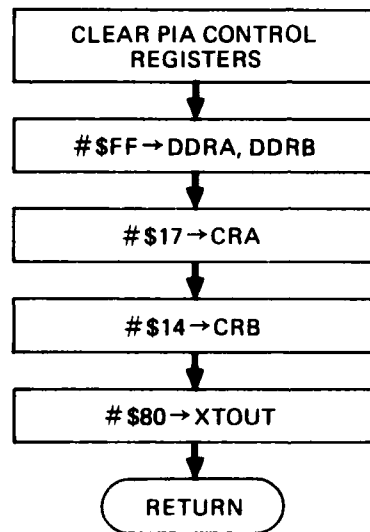


SUBROUTINE INTGRT

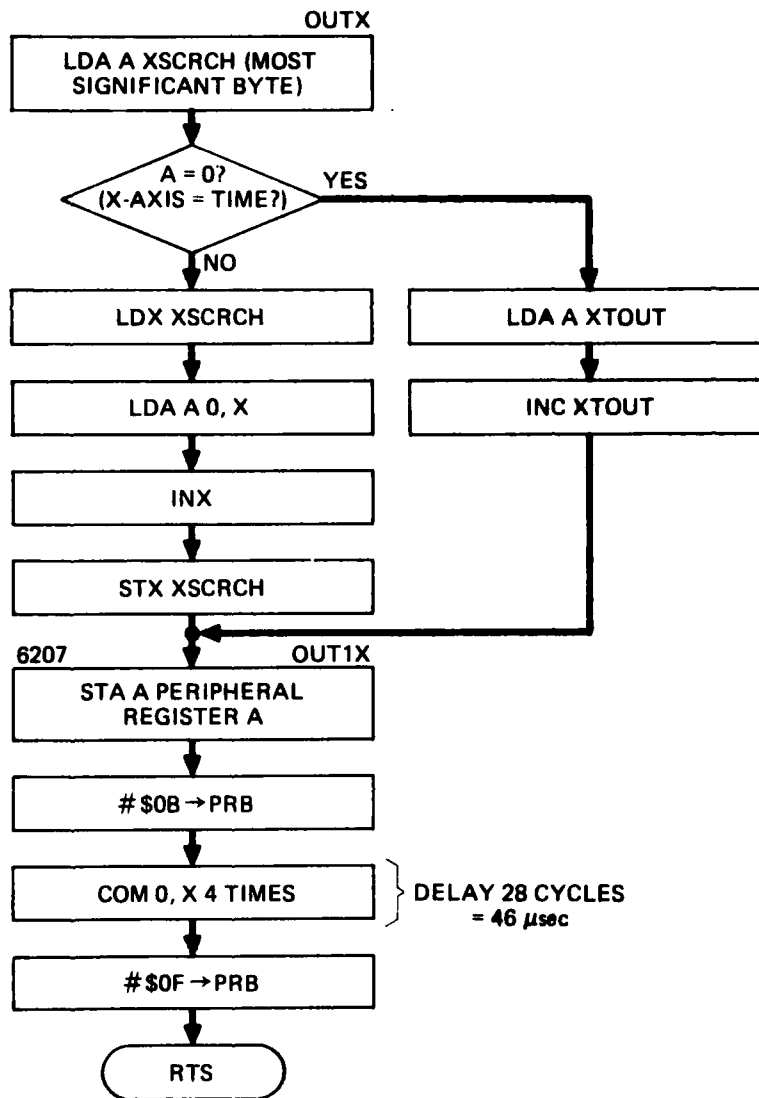


SUBROUTINE MOV16 B

ARL:UT
 AS-81-866
 RTT - GA
 8-3-81

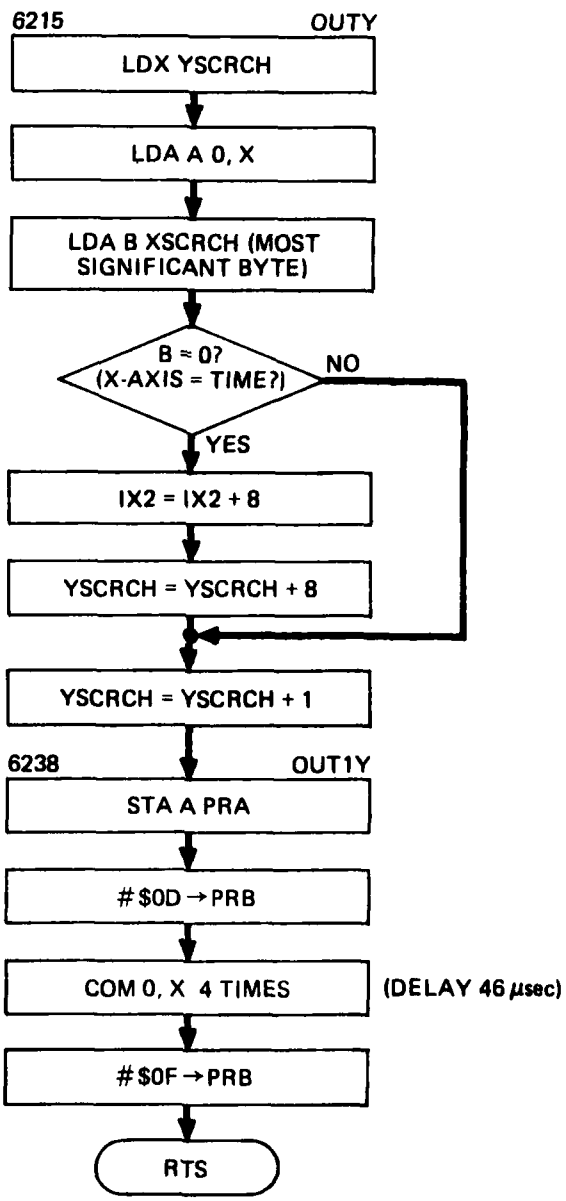


SUBROUTINE OUTSET



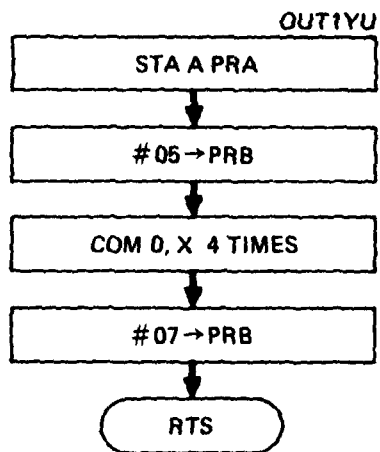
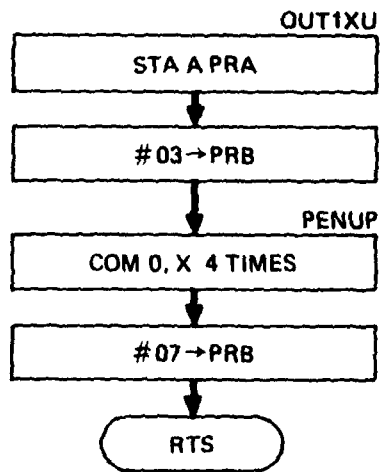
SUBROUTINES OUTX, OUT1X

ARL:UT
AS-81-868
RTT - GA
8 - 3 - 81

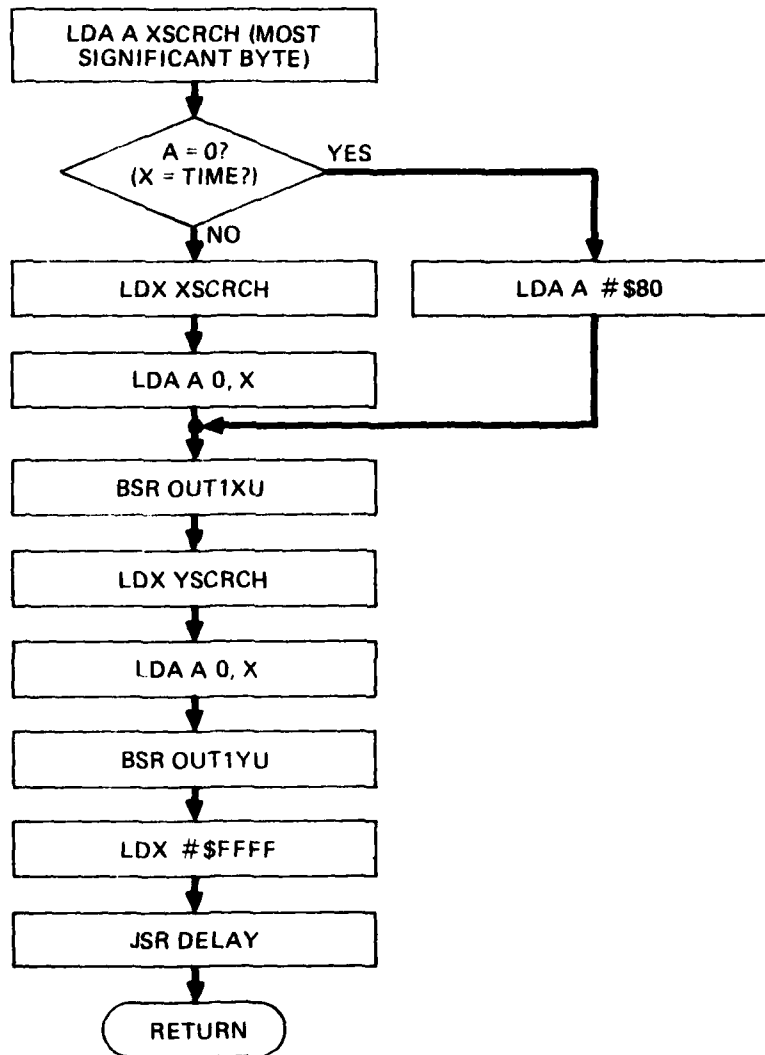


SUBROUTINES OUTY, OUT1Y

ARL:UT
AS-81-869
RTT - GA
8 - 3 - 81

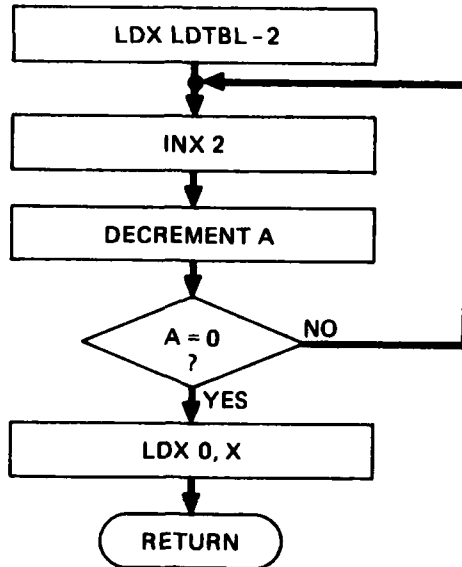


SUBROUTINES OUT1XU, PENUP, OUT1YU



SUBROUTINE PNSTRT

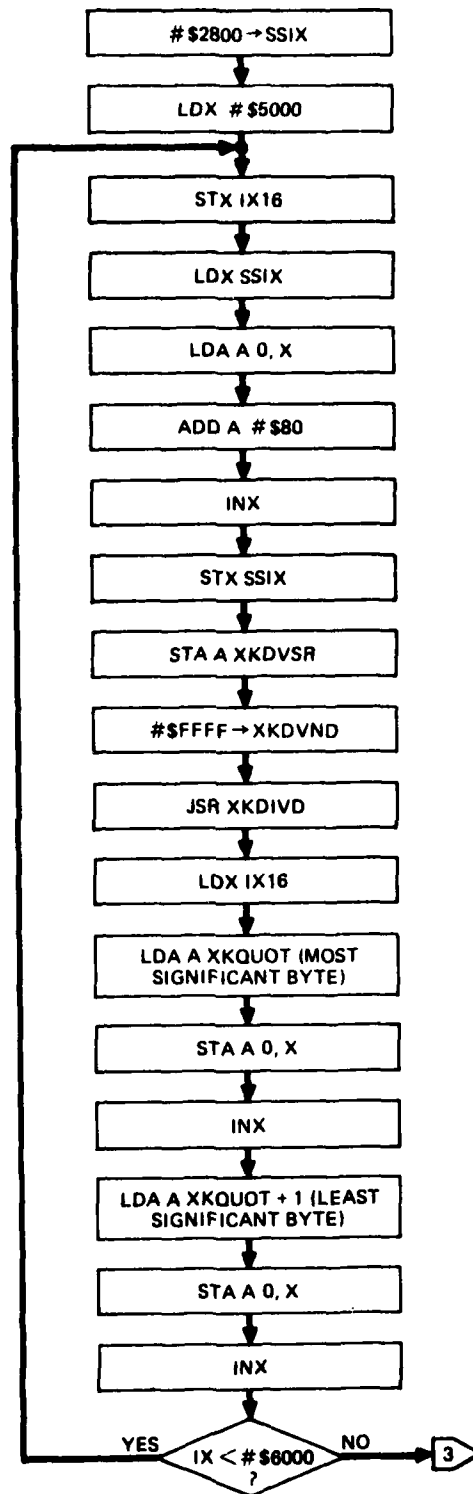
ARL:UT
AS-81-871
RTT - GA
8-3-81



FOR XKDIVD
FLOWCHARTS,
SEE MOTOROLA
APPLICATIONS
MANUAL

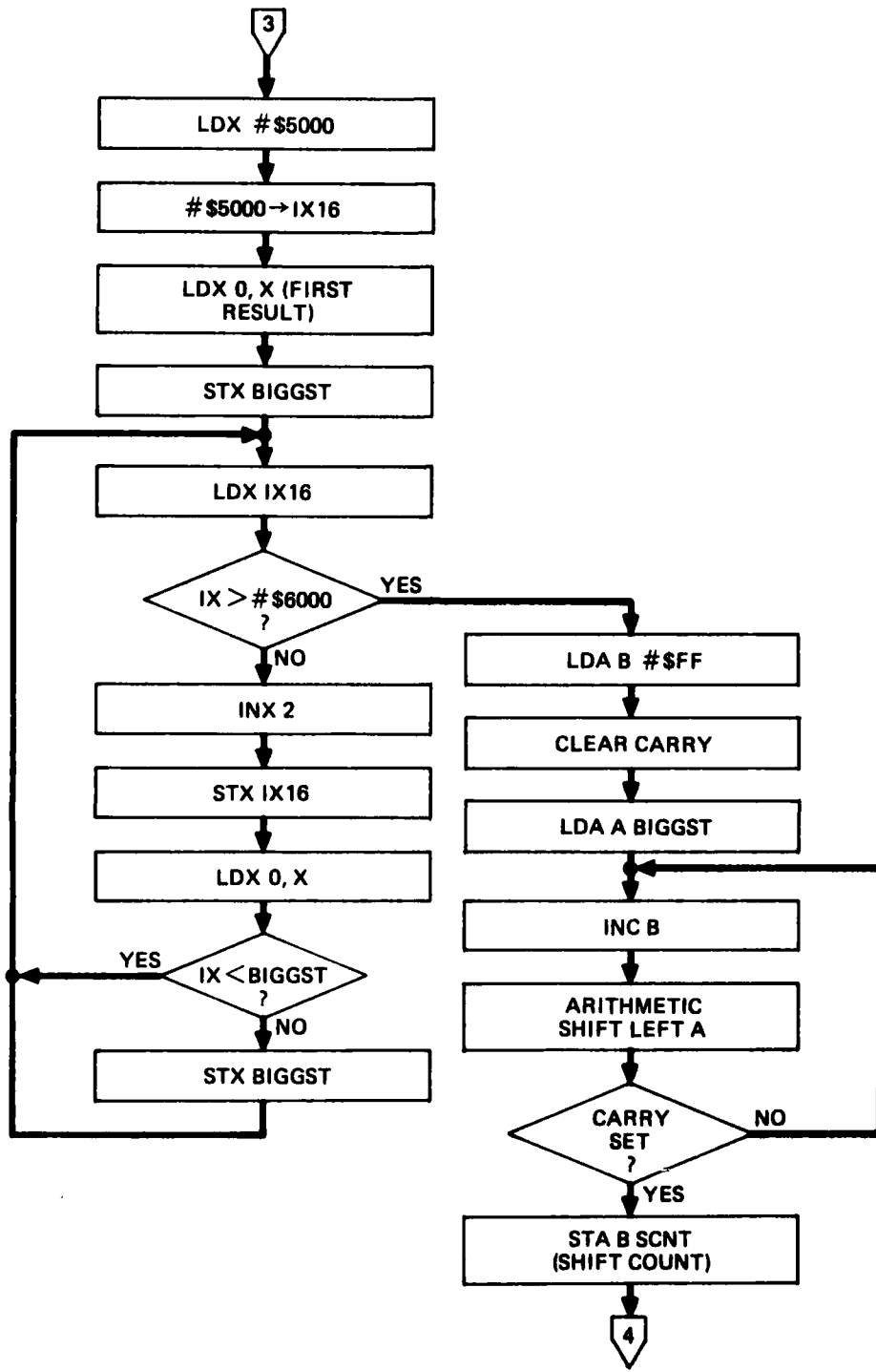
LDTBL	2000
	2800
	3000
	3800
	4000
	0000
	4800

SUBROUTINE SELBLK

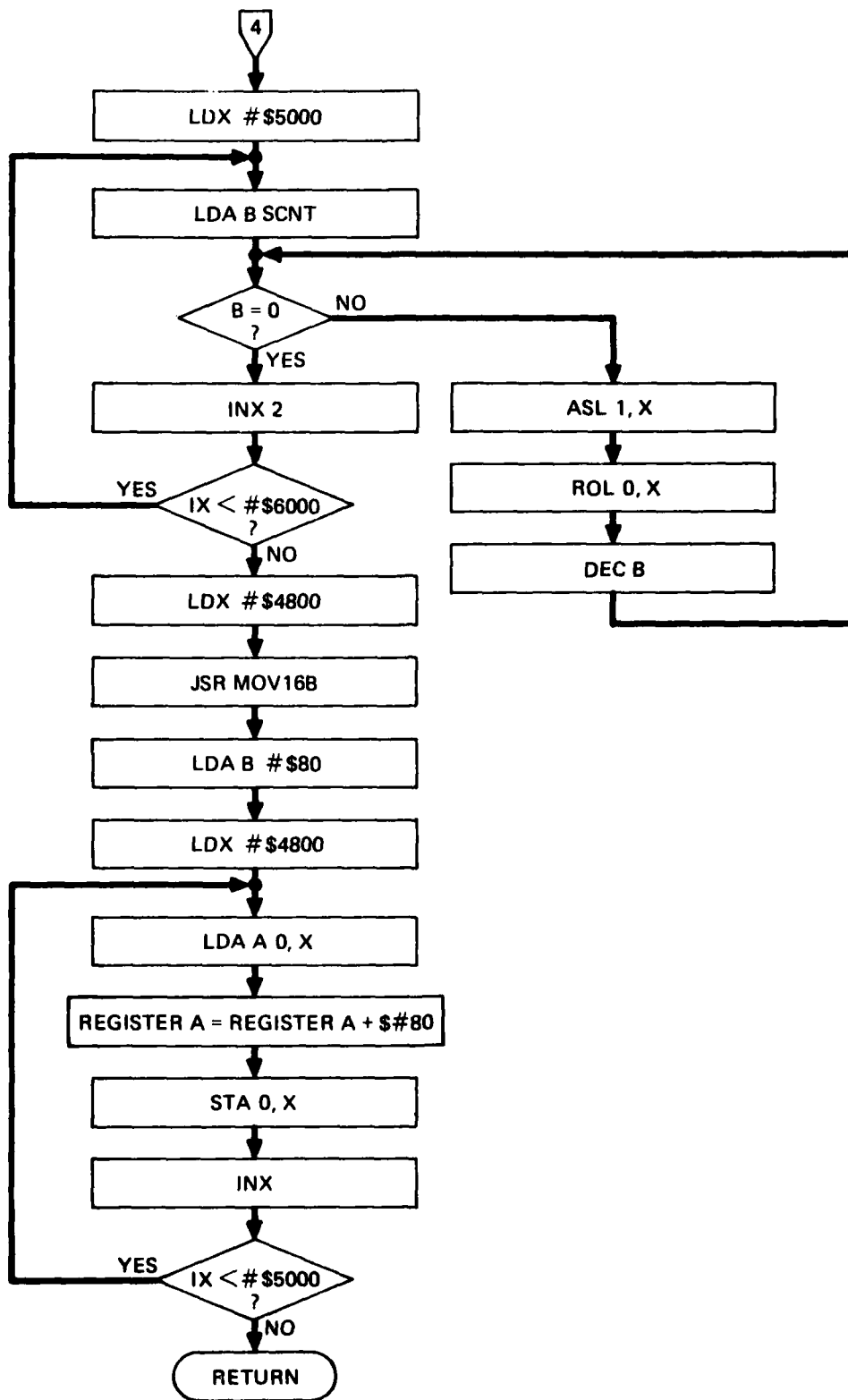


SUBROUTINE INVERT

ARL:UT
AS-81-873
RTT-GA
8-3-81

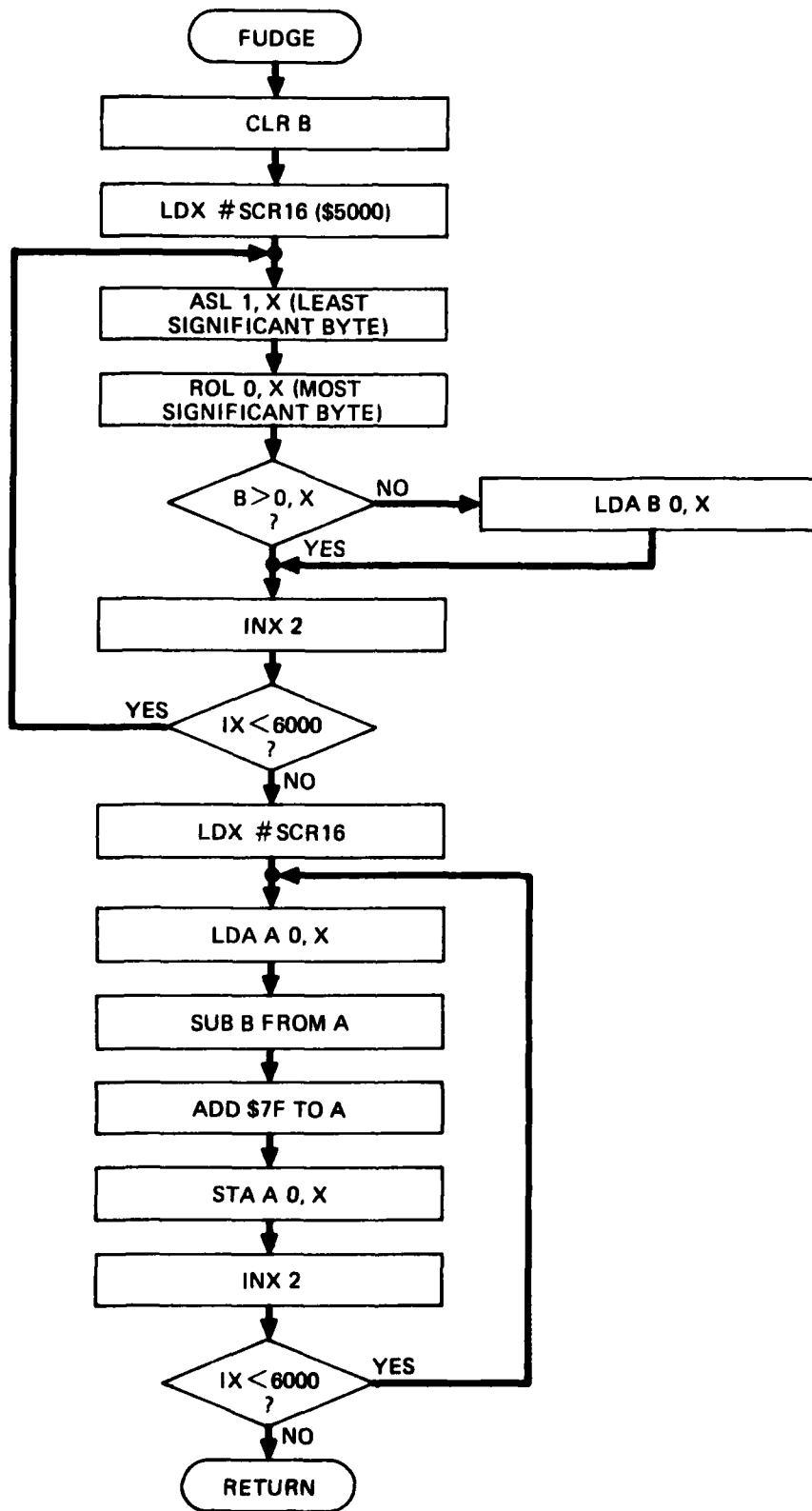


SUBROUTINE INVERT (Cont'd)



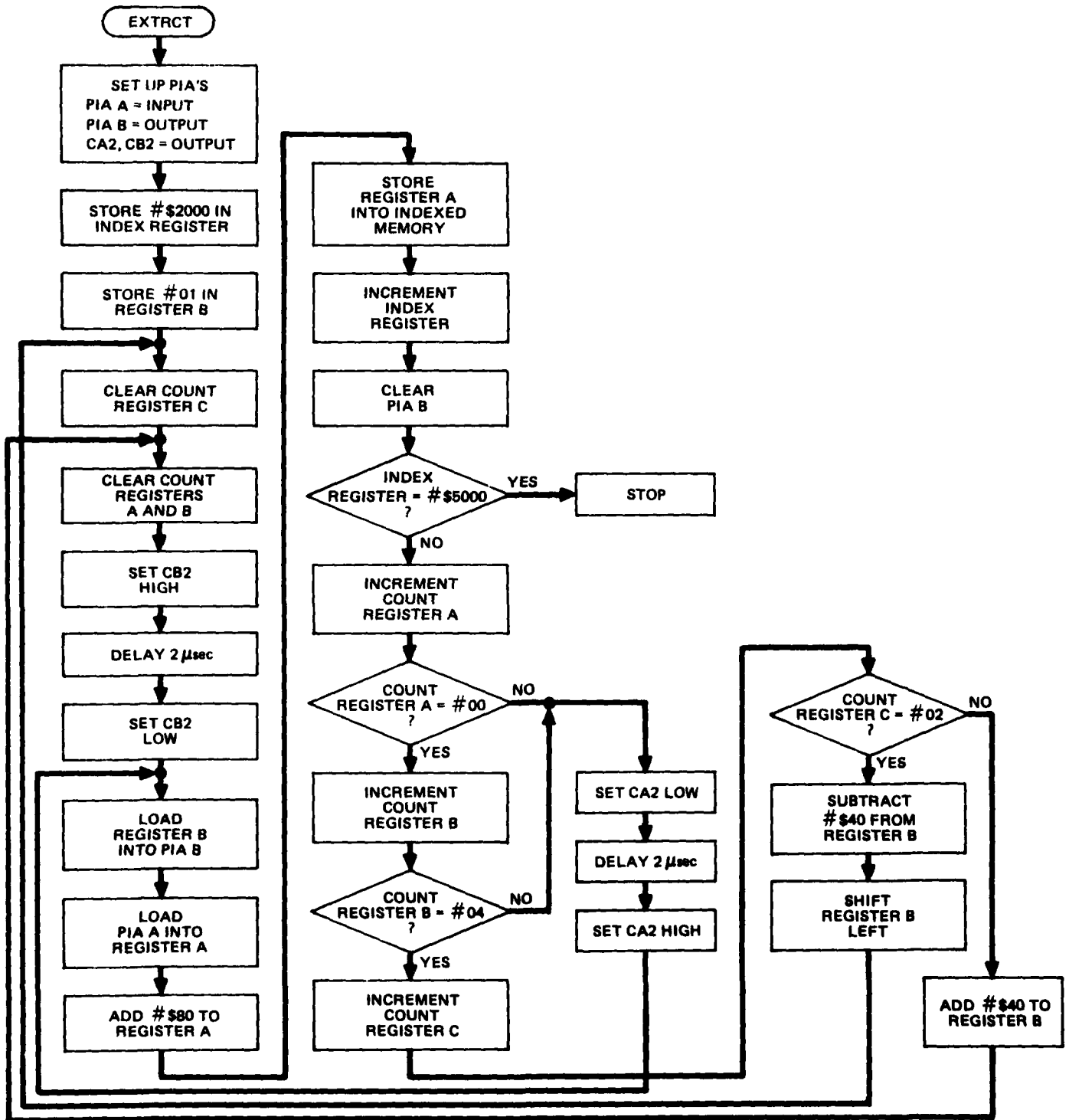
ARL:UT
 AS-81-875
 RTT - GA
 8-3-81

SUBROUTINE INVERT (Cont'd)

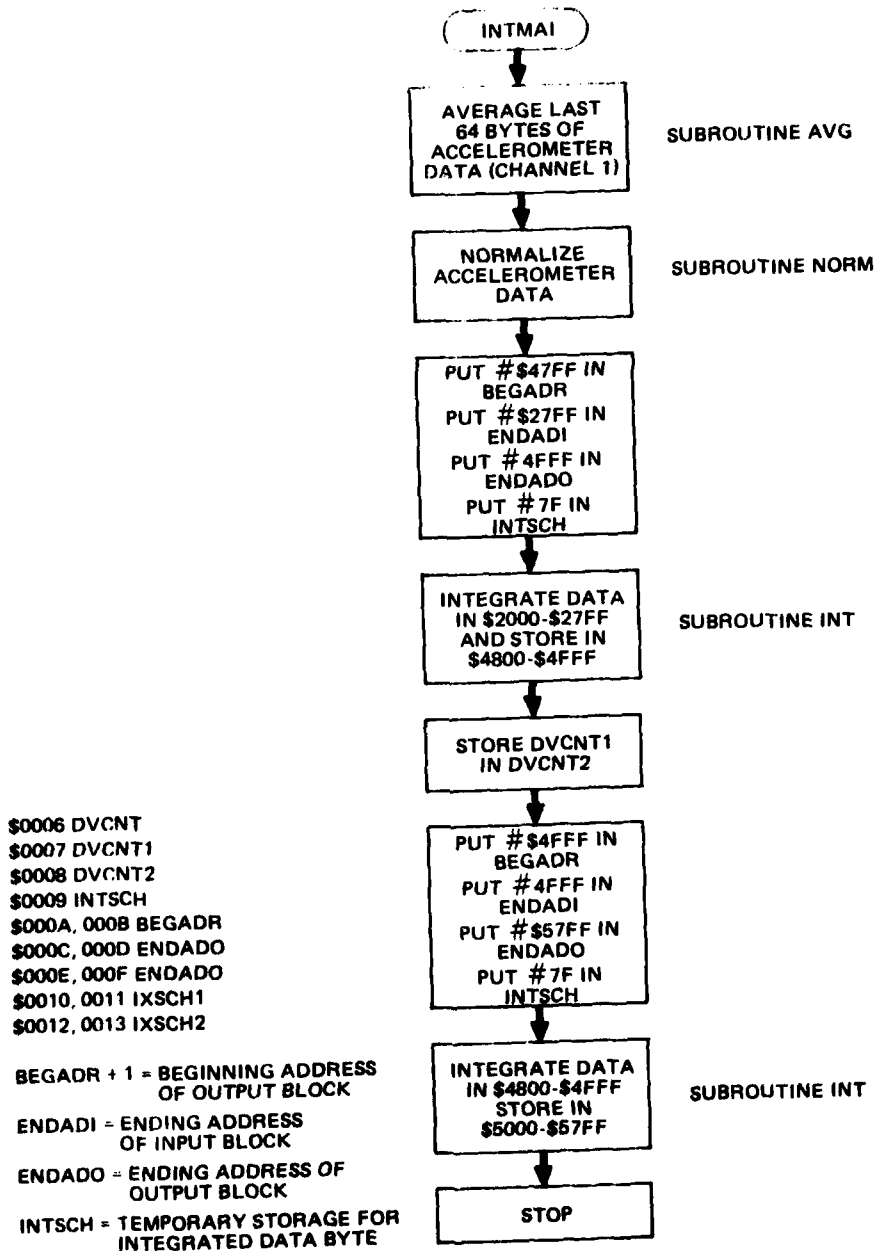


ARL:UT
AS-81-876
RTT - GA
8-3-81

SUBROUTINE FUDGE

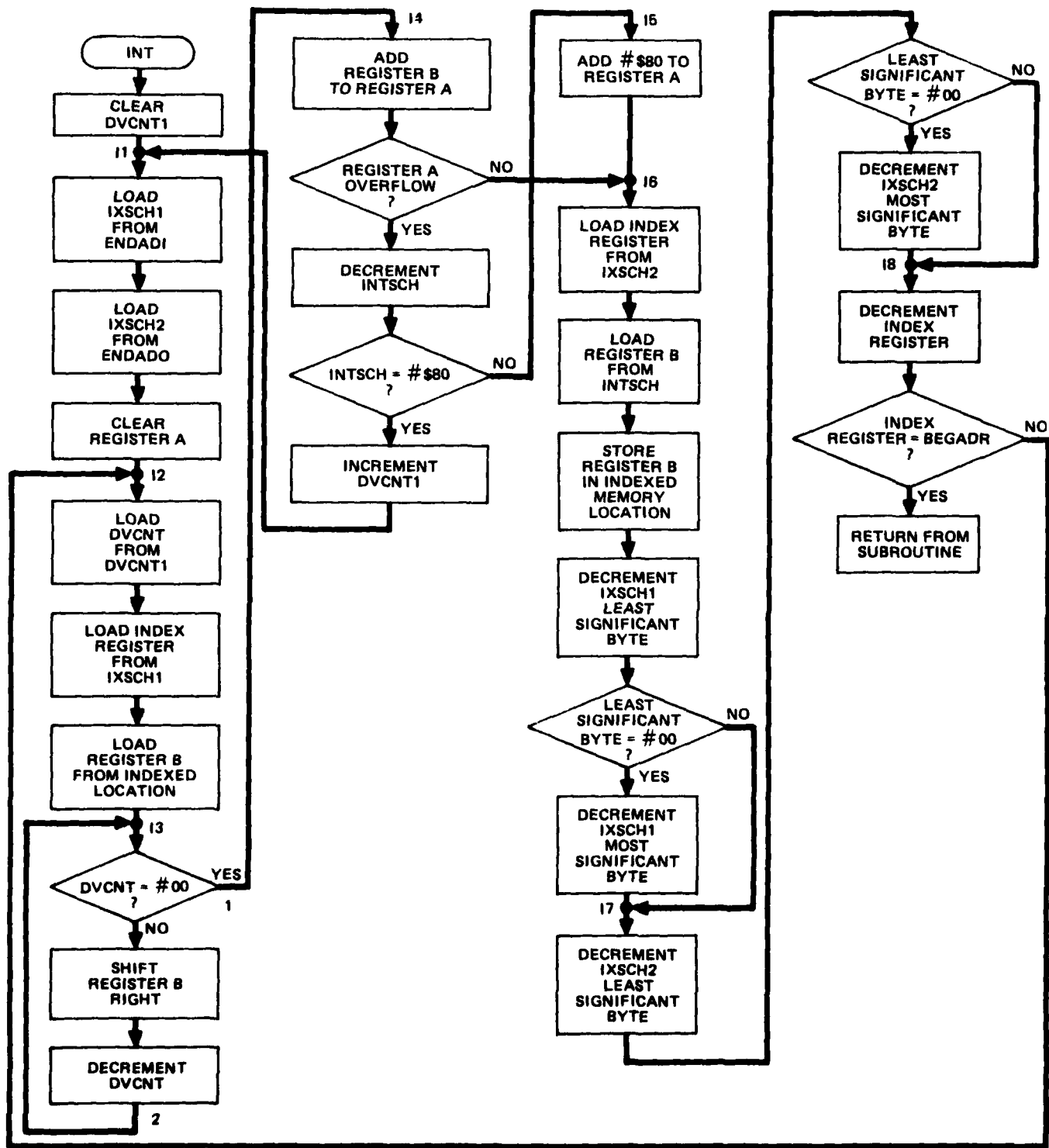


ROUTINE EXTRCT



ROUTINE INTMAI

ARL:UT
 AS-81-878
 RTT - GA
 8-3-81



SUBROUTINE INT

APPENDIX D

ONR CODE 480 PROGRAM

DOCUMENTATION

S. R. Addy, E. W. Behrens, T. R. Haines, D. J. Shirley and J. L. Worzel, "Correlation of Some Lithologic and Physical Characteristics of Sediments with High Frequency Subbottom Reflection Types," Proceedings of the 11th Annual Offshore Technology Conference, Houston, Texas, 30 April - 3 May 1979.

A. L. Anderson, "Acoustics of Gas-Bearing Sediments," Applied Research Laboratories Technical Report No. 74-19 (ARL-TR-74-19), Applied Research Laboratories, The University of Texas at Austin, May 1974.

A. L. Anderson and L. D. Hampton, "In Situ Measurement of Sediment Acoustic Properties During Coring," presented at the ONR Symposium on Physical and Engineering Properties of Deep-Sea Sediments, Airlie House, Airlie, Virginia, 24-27 April 1973.

A. L. Anderson and L. D. Hampton, "Measurement of In Situ Acoustic Properties During Sediment Coring," presented at the ONR Symposium on the Physics of Sound in Marine Sediments, Lakeway Inn, Austin, Texas, 8-10 May 1973.

A. L. Anderson and L. D. Hampton, "A Method for Measuring In Situ Acoustic Properties During Sediment Coring," in Physics of Sound in Marine Sediments, edited by Loyd Hampton (Plenum Press, New York, 1974).

A. L. Anderson and L. D. Hampton, "In Situ Measurements of Sediment Acoustic Properties During Coring," in Deep-Sea Sediments, Physical and Mechanical Properties, edited by A. L. Inderbitzen (Plenum Press, New York, 1974).

A. L. Anderson and L. D. Hampton, "Acoustics of Gas-Bearing Sediments. Part I: Background," J. Acoust. Soc. Am. 67, 1865-1889 (1980).

A. L. Anderson and L. D. Hampton, "Acoustics of Gas-Bearing Sediments. Part II: Measurements and Models," J. Acoust. Soc. Am. 67, 1890-1903 (1980).

A. L. Anderson and L. D. Hampton, "Use of Tubes for Measurement of Acoustical Properties of Materials," presented at the 89th Meeting of the Acoustical Society of America, Austin, Texas, April 1975.

A. L. Anderson, R. J. Harwood, and L. D. Hampton, "Temperature Studies on Lake Travis Stratification in a Warm Monomictic Reservoir," The Texas Journal of Science XXVI, Nos. 3 and 4, 353-371 (1975).

D. W. Bell, "Shear Wave Propagation in Unconsolidated Fluid Saturated Porous Media," Ph.D. Dissertation, The University of Texas at Austin, May 1979. (ARL-TR-79-31, May 1979)

D. W. Bell and D. J. Shirley, "Temperature Variation of the Acoustical Properties of Laboratory Sediments," J. Acoust. Soc. Am. 68, 227-231 (1980). (ARL-TP-80-1, January 1980)

L. D. Hampton, "ARL Experience with Acoustics and Gas in Sediments," presented at Symposium on Natural Gases in Marine Sediments and Their Mode of Distribution, The University of California Lake Arrowhead Conference Center, Lake Arrowhead, California, 28-30 November 1972.

L. D. Hampton and A. L. Anderson, "Acoustics and Gas in Sediments: Applied Research Laboratories (ARL) Experience," in Natural Gases in Marine Sediments, Marine Science Vol. III, edited by Isaac R. Kaplan (Plenum Press, New York, 1974).

J. M. Hovem, "Some Aspects of Sound Propagation in Saturated Sand," presented at the Seminar on Bottom Effects in Underwater Sound Propagation, Miami, Florida, 26-28 April 1979.

J. M. Hovem, "Finite Amplitude Effects in Marine Sediments," presented at the Conference on Underwater Applications of Nonlinear Acoustics, University of Bath, Bath, England, September 1979. (ARL-TP-79-41, June 1979) (ARL-TO-79-7, September 1979)

J. M. Hovem, "Viscous Attenuation of Sound in Suspensions and High Porosity Marine Sediments," J. Acoust. Soc. Am., 67, No. 5, 1559-1563 (1980). (ARL-TP-79-62, September 1979)

J. M. Hovem, "The Nonlinearity Parameter of Saturated Marine Sediments," J. Acoust. Soc. Am. 66, 1463-1467 (1979). (ARL-TP-79-17, rev., May 1979)

J. M. Hovem and G. D. Ingram, "Viscous Attenuation of Sound in Saturated Sand," J. Acoust. Soc. Am. 66, 1807-1812 (1979). (ARL-TP-79-35, April 1979)

A. C. Kibblewhite, "Attenuation of Underwater Sound of Low Frequencies," Applied Research Laboratories Technical Report No. 76-1 (ARL-TR-76-1), Applied Research Laboratories, The University of Texas at Austin, December 1975.

D. J. Shirley, "Final Report under Contract N00014-70-A-0166, Task 0005," Applied Research Laboratories Technical Report No. 72-6 (ARL-TR-72-6), Applied Research Laboratories, The University of Texas at Austin, January 1972.

D. J. Shirley, "Interim Technical Description of the ARL Compressional Wave In Situ Core Profilometer," Applied Research Laboratories Technical Memorandum No. 74-9 (ARL-TM-74-9), Applied Research Laboratories, The University of Texas at Austin, March 1974.

D. J. Shirley, "Calibration Manual for ARL Profilometer," Informal Memorandum, July 1974.

D. J. Shirley, "Fine Structure of the Sound Speed Profile in Ocean Bottom Sediments from In Situ Measurements," presented at the 89th Meeting of the Acoustical Society of America, Austin, Texas, 8-11 April 1975.

D. J. Shirley, "Transducer for Generation and Detection of Shear Waves," ARL Invention Disclosure, September 1975.

D. J. Shirley, "Determination of the Acoustic Properties of Deep Ocean Sediments from In Situ Profiles," presented at the 92nd Meeting of the Acoustical Society of America, San Diego, California, 16-19 November 1976.

D. J. Shirley, "Acoustic Impedance Measuring Device for Marine Sediments," presented at the 93rd Meeting of the Acoustical Society of America, University Park, Pennsylvania, 6-10 June 1977.

D. J. Shirley, "Laboratory and In Situ Sediment Acoustics," Applied Research Laboratories Technical Report No. 77-46 (ARL-TR-77-46), Applied Research Laboratories, The University of Texas at Austin, August 1977.

D. J. Shirley, "Method for Measuring In Situ Acoustic Impedance of Marine Sediments," J. Acoust. Soc. Am. 62, 1028-1032 (1977). (ARL-TP-77-19, May 1977)

D. J. Shirley, "An Improved Shear Wave Transducer," J. Acoust. Soc. Am. 63, 1643-1645 (1978). (ARL-TP-77-39, December 1977)

D. J. Shirley, "The ARL:UT Subseafloor Environmental Simulator," Applied Research Laboratories Technical Report No. 79-53 (ARL-TR-79-53), Applied Research Laboratories, The University of Texas at Austin, November 1979.

D. J. Shirley and A. L. Anderson, "Compressional Wave Profilometer for Deep Water Measurements," Applied Research Laboratories Technical Report No. 74-51 (ARL-TR-74-51), Applied Research Laboratories, The University of Texas at Austin, December 1974.

D. J. Shirley, and A. L. Anderson, "Studies of Sediment Shear Waves, Acoustical Impedance, and Engineering Properties," Applied Research Laboratories Technical Report No. 75-23 (ARL-TR-75-23), Applied Research Laboratories, the University of Texas at Austin, May 1975.

D. J. Shirley and A. L. Anderson, "Acoustic and Engineering Properties of Sediments," Applied Research Laboratories Technical Report No. 75-58 (ARL-TR-75-58), Applied Research Laboratories, The University of Texas at Austin, October 1975.

D. J. Shirley and A. L. Anderson, "In Situ Measurement of Marine Sediment Acoustical Properties During Coring in Deep Water," IEEE Trans. on Geoscience Electronics GE-13, No. 4, 163-169 (1975). (ARL-TP-75-3, 1975)

D. J. Shirley and A. L. Anderson, "Experimental Investigation of Shear Waves in Laboratory Sediments," presented at the 90th Meeting of the Acoustical Society of America, San Francisco, California, 3-7 November 1975.

D. J. Shirley and A. L. Anderson, "Shear Waves in Unconsolidated Sediments," presented at the 92nd Meeting of the Acoustical Society of America, San Diego, California, 16-19 November 1976.

D. J. Shirley, A. L. Anderson, and L. D. Hampton, "In Situ Measurement of Sediment Sound Speed During Coring," Applied Research Laboratories Technical Report No. 73-1 (ARL-TR-73-1), Applied Research Laboratories, The University of Texas at Austin, March 1973.

D. J. Shirley, A. L. Anderson, and L. D. Hampton, "Measurement of In Situ Speed During Sediment Coring," OCEAN '73, Record of the International Conference on Engineering in the Ocean Environment, Seattle, Washington, 25-28 September 1973.

D. J. Shirley and D. W. Bell, "Acoustics of In Situ and Laboratory Sediments," Applied Research Laboratories Technical Report No. 78-36 (ARL-TR-78-36), Applied Research Laboratories, The University of Texas at Austin, August 1978.

D. J. Shirley and D. W. Bell, "Temperature Variation of the Acoustic Properties of Laboratory Sediments," presented at the 98th Meeting of the Acoustical Society of America, Salt Lake City, Utah, November 1979.

D. J. Shirley, D. W. Bell, and J. M. Hovem, "Laboratory and Field Studies of Sediment Acoustics," Applied Research Laboratories Technical Report No. 79-26 (ARL-TR-79-26), Applied Research Laboratories, The University of Texas at Austin, June 1979.

D. J. Shirley and L. D. Hampton, "Acoustic Velocity Profilometer for Sediment Cores," OCEAN '72, Record of the International Conference on Engineering in the Ocean Environment, Newport, Rhode Island, 13-15 September 1972.

D. J. Shirley and L. D. Hampton, "Determination of Sound Speed in Cored Sediments," Applied Research Laboratories Technical Report No. 72-44 (ARL-TR-72-44), Applied Research Laboratories, The University of Texas At Austin, December 1972.

D. J. Shirley and L. D. Hampton, "Acoustic Velocimeter for Ocean Bottoms Coring Apparatus," ARL Invention Disclosure, November 1973.

D. J. Shirley and L. D. Hampton, "Shear Wave Measurements in Laboratory Sediments," *J. Acoust. Soc. Am.* 63, 607-613 (1978). (ARL-TP-77-31, August 1977)

D. J. Shirley, J. M. Hovem, G. D. Ingram, and D. W. Bell, "Sediment Acoustics," Applied Research Laboratories Technical Report No. 80-17 (ARL-TR-80-17), Applied Research Laboratories, The University of Texas at Austin, April 1980.

K. H. Stokoe (UT Austin), D. G. Anderson (Fugro, Inc.), E. J. Arnold (UT Austin), R. J. Hoar (UT Austin), and D. J. Shirley, "Development of a Bottom Hole Device for Offshore Shear Wave Velocity Measurement," *Proceedings of the 10th Annual Offshore Technology Conference*, Houston, Texas, 8-11 May 1978.

B. E. Tucholke (Lamont-Doherty Geological Observatory, Columbia University) and D. J. Shirley, "Comparison of Laboratory and In Situ Compressional-Wave Velocity Measurements on Sediment Cores from the Western North Atlantic," *J. Geophys. Res.* 84, 697-695 (1979).

11 May 1981

DISTRIBUTION LIST FOR
ARL-TR-81-20
UNDER CONTRACT N00014-76-C-0117
UNCLASSIFIED

Copy No.

Commanding Officer
Naval Ocean Research and Development Activity
NSTL Station, MS 39529

1 Attn: R. R. Goodman (Code 110)
2 A. L. Anderson (Code 320)
3 S. Marshall (Code 340)
4 L. Solomon (Code 500)
5 R. Gardner (Code 520)
6 E. Choaka, (Code 530)
7 H. Eppert (Code 360)

Commanding Officer
Office of Naval Research
Arlington, VA 22217

8 Attn: CAPT A. Gilmore (Code 200)
9 J. McKisic (Code 486)
10 M. Odegard (Code 483)
11 R. Obrochta (Code 464)

Commander
Naval Electronic Systems Command
Department of the Navy
Washington, DC 20360

12 Attn: J. Sinsky (Code 612)
13 J. Reeves (Code PME 124-30)
14 H. Ford (Code PME 124-60)
15 S. Hollis (Code 6125)

Commander
Naval Sea Systems Command
Department of the Navy
Washington, DC 20362

16 Attn: R. Farwell (Code 63R)

Chief of Naval Material
Office of Naval Technology
Department of the Navy
Washington, DC 20360

17 Attn: CAPT E. Young

Distribution List for ARL-TR-81-20 under Contract N00014-76-C-0117

Copy No.

	Commanding Officer Naval Oceanographic Office NSTL Station, Bay St. Louis, MS 39529
18	Attn: W. Geddes
19	W. Jobst
20	M. G. Lewis
	Commander Naval Ocean Systems Center Department of the Navy San Diego, CA 92132
21	Attn: Library
22	M. A. Pedersen
23	N. O. Booth
24	E. L. Hamilton
25	H. P. Bucker
	Director Naval Research Laboratory Department of the Navy Washington, DC 20375
26	Attn: B. Adams
27	R. Mosley
4 copies	Code 2627
	Chief of Naval Operations Department of the Navy Washington, DC 20350
28	Attn: CAPT J. Harlette (OP-952D1)
	Commander Naval Air Development Center Department of the Navy Warminster, PA 18974
29	Attn: C. L. Bartberger
	Commander New London Laboratory Naval Underwater Systems Center Department of the Navy New London, CT 06320
30	Attn: B. Cole (Code 24)
	Commander Naval Coastal Systems Center Panama City, FL 32401
31	Attn: E. G. McLeroy, Jr.
32	B. Tolbert

Distribution List for ARL-TR-81-20 under Contract N00014-76-C-0117 (Cont'd)

Copy No.

	Superintendent Naval Postgraduate School Monterey, CA 93940
33	Attn: H. Medwin, Physics Dept.
34	C. Dunlap, Oceanography Dept.
35	Library
	Woods Hole Oceanographic Institution Woods Hole, MA 02543
36	Attn: C. Hollister
37	B. Tucholke
38	E. Hayes
	Hawaii Institute of Geophysics The University of Hawaii 2525 Correa Road Honolulu, HI 96822
39	Attn: G. Sutton
40	M. Manghani
	The Scripps Institution of Oceanography The University of California/San Diego San Diego, CA 92152
41	Attn: P. Lonsdale
42	R. Tyce
43	F. Fisher
	Department of Geological Oceanography Texas A&M University College Station, TX 77840
44	Attn: W. R. Bryant
	Geophysics Laboratory Marine Science Institute The University of Texas 700 The Strand Galveston, TX 77550
45	Attn: E. W. Beherns
	The Catholic University of America 6220 Michigan Avenue, NE Washington, DC 20017
46	Attn: H. M. Überall

Distribution List for ARL-TR-81-20 under Contract N00014-76-C-0117 (Cont'd)

Copy No.

	Lamont-Doherty Geological Observatory
	Palisades, NY 10964
47	Attn: G. Bryan
48	W. J. Ludwig
49	R. D. Stoll
	Department of Civil and Ocean Engineering
	The University of Rhode Island
	Kingston, RI 02881
50	Attn: A. J. Silva
	University College of North Wales
	Marine Science Laboratories
	Menai Bridge
	Anglesey, NORTH WALES
51	Attn: D. Taylor Smith
52	P. Schultheiss
	Director
	SACLANT ASW Research Centre
	La Spezia, ITALY
53	Attn: T. Akal
	The University of Auckland
	Auckland, NEW ZEALAND
54	Attn: A. Kibblewhite, Department of Physics
	Defence Research Establishment Atlantic
	9 Grove Street
	Dartmouth, N.S., CANADA
55	Attn: Library
	Department of Civil Engineering
	The University of Texas at Austin
	Austin, TX 78712
56	Attn: K. Stokoe
	Southwest Research Institute
	P.O. Drawer 28510
	San Antonio, TX 78284
57	Attn: T. Owen
58	D. J. Shirley

Distribution List for ARI-TR-81-20 under Contract N00014-76-C-0117 (Cont'd)

Copy No.

- 59 Western Electric Company
 Department 7426
 P.O. Box 20046
 Greensboro, NC 27420
 Attn: T. F. Clark
- 60 Electronics Research Laboratory
 The University of Trondheim
 The Norwegian Institute of Technology
 O. S. Bragstad Plass 6
 N-7034 Trondheim, NTH, NORWAY
 Attn: J. Hovem
- 61 Applied Physics Laboratory
 The Johns Hopkins University
 Johns Hopkins Road
 Laurel, MD 20812
 Attn: J. Lombardo
- 62 Applied Research Laboratory
 The Pennsylvania State University
 P.O. Box 30
 State College, PA 16801
- 63 Department of Geology
 The University of Texas at Austin
 Austin, TX 78712
 Attn: M. Backus
- 64 - 75 Commanding Officer and Director
 Defense Technical Information Center
 Cameron Station, Building 5
 5010 Duke Street
 Alexandria, VA 22314
- 76 Commanding Officer
 Naval Facilities Engineering Command
 Department of the Navy, 200 Stovall Street
 Alexandria, VA 22332
 Attn: R. A. Peloquin, Code 0320
- 77 Office of Naval Research
 Branch Office Chicago
 Department of the Navy
 536 S. Clark, Room 286
 Chicago, IL 60605

Distribution List for ARL-TR-81-20 under Contract N00014-76-C-0117 (Cont'd)

Copy No.

78	Office of Naval Research Resident Representative Room 582, Federal Building Austin, TX 78701
79	Environmental Sciences Division, ARL:UT
80	David T. Blackstock, ARL:UT
81	Harlan G. Frey, ARL:UT
82	Stephen K. Mitchell, ARL:UT
93	Thomas G. Muir, ARL:UT
94	Library, ARL:UT
95	Reserve, ARL:UT

DATE
ILME